UNIVERSITÀ DI BOLOGNA

Dipartimento di Scienze della Terra
e Geologico-Ambientali

DOTTORATO IN SCIENZE DELLA TERRA
XIX° CICLO

GEO/02 GEOLOGIA STRATIGRAFICA E SEDIMENTOLOGICA

Dinamica sedimentaria torbiditica in bacini confinati: margine orientale della Sardegna.

Coordinatore: Prof. William Cavazza

Relatori: Dott**. Fabiano Gamberi**
Dott. **Michael Marani**

Dottorando: **Dott. Giacomo Dalla Valle**

Bologna, 15 marzo 2007

Index

Chapter 1

Introduction and aims of thesis 15

Geological setting

Data and methods

Chapter 2

This chapter is presented in form of an article of Fabiano Gamberi and mine "The impact of margin-shaping processes on the architecture of the Sardinian and Sicilian margin deep sea depositional systems (Tyrrhenian Sea)" submitted to Society of Economic Paleontologist and Mineralogists Special Pubblication: "External control on deep water depositional systems".

Chapter 3

The Olbia basin

Chapter 4

The Baronie basin: the Posada Turbidite system

Chapter 5

The nothern Ogliastra basin and the Arbatax turbidite system 157

ABSTRACT

Deep-water sedimentation is currently a major focus of both academic research and industrial interest. Recent studies have emphasized the fundamental influence of seafloor topography on the growth and morphology of submarine fans; in many turbidite systems, depositional system development has been moderately to strong controlled by pre-existing bounding slopes.

The aim of this work is to study the effect of the basin confinement on the main deep water turbidite systems of the eastern Sardinian margin, that represent a passive margin with intraslope basin, bounded seaward by structural highs. The turbidite system have been imaged through high-resolution multibeam bathymetric dataset acquired by ISMAR (Institute for Marine Science) of Bologna during cruise Tir99. The multibeam data has been integrated with seismic analysis, in order to understand the shape, the morphology and internal organization of the deep water system and of both their large and small scale architectural elements.

Three intraslope basin (Olbia, Baronie, nothern Ogliastra basin) have been investigated. The Olbia basin is the northernmost intraslope basin of the eastern Sardinian margin, and is bounded seaward by the Etruschi and Baronie seamounts. The Caprera fan is the main turbidite system and is composed of feeding canyons incised in the continental slope and of a long, wide leveed channel at the base of the slope that is a unique case in the entire eastern Sardinian margin. The Caprera fan faces a wide shelf sector, and this could explain the peculiar sedimentary architecture of its deep sea fan. The effect of the basin confinement on the shape and on the evolution of the deep sea fans is evident on the asymmetry of the levees and on the migration of the fan channel. The Olbia intraslope basin is completely filled, and has developed a bypass sector to a new base level in the distal rim of the margin where bounding seamounts die out. The effects of this lowering of the base level is evident in the distal part of the system with the development of distributary channels and of wide, low relief V-shaped erosional features that represent the upslope portions of the bypass canyon.

The Baronie intraslope basin is the central basin of the eastern Sardinian , and is bounded seaward by the Baronie seamount, with a lateral escape pathways represented by the Gonone-Orosei canyon systems. The Posada is the main turbidite system of the Baronie basin, consisting of a deeply incised canyon in the shelf and

in the slope, a small, radial fan at the base of slope and a distal distibutary channel system. The morphology of the turbidite system is the result of the complex interplay between the topography of the receiving basin, and the behaviour of the sedimentary flows. The topography of the basin has forced the system to change the pathways of the Posada fan, from an eastward to a southward trend. Large scale mass wasting processes affect the Posada deep sea fan, that contributing to the reorganization of the turbidite system. The Ogliastra basin is located to the south with respect the Baronie basin, and is bounded seaward by the Quirra High. The nothern continental slope of the Ogliastra basin is characterized by slope canyons that evidence hybrid depositional characters, with multiple stage of incision and abandonment. The Arbatax is the main turbidite system of the nothern Ogliastra basin, showing an active souther sector, dominated by a fan channel, and by an abandoned nothern sector that is the loci of intense seafloor instability and mass wasting processes.

In general the results of the study highlight the importance of the external factors controls and of the pre-existing topography in controlling the sedimentary processes of the architectural elements and the depositional evolution of turbidite systems. In particular, appear evident as the depositional style of confined turbidite systems, do not conform to the simple deep sea fan models still used as facies prediction tools for hydrocarbon exploration and exploitation.

RIASSUNTO

La sedimentazione clastica di mare profondo è attualmente uno dei principali argomenti della ricerca sedimentologica sia in ambito puramente accademico che in ambito petrolifero-industriale. Gli studi recenti hanno enfatizzato l'influenza fondamentale della topografia preesistente del fondo marino sulla crescita e la morfologia sui fan di mare profondo; si è visto come, in molti systemi torbiditici, l'evoluzione dei processi deposizionali sia stata da moderatamente a fortemente controllata dall' effetto di confinamento di scarpate tettoniche, ridge strutturali e seamounts. Scopo di questo lavoro è studiare l'effetto del confinamento alla scala di bacino sui principali sistemi torbiditici del margine orientale della Sardegna che rappresenta un margine passivo articolato di bacini di intraslope confinati verso mare da seamounts. Lo studio dei sistemi deposizionali è stato eseguito attraverso l interpretazione di dati di batimetria multibeam ad alto dettaglio acquisiti dall' ISMAR di Bologna durante la crociera Tir99. L' interpretazione multibeam è stata integrata con l' analisi di profili sismici a riflessione per comprendere la morfologia l'organizzazione interna e l'evoluzione nel tempo dei principali elementi deposizionali dei sistemi torbiditici. Tre bacini di intraslope (Olbia, Baronie e il settore settentrionale del bacino Ogliastra) sono stati investigati. Il bacino di Olbia è il bacino piu settentrionale del margine orientale della Sardegna ed è limitato verso mare dai seamount Etruschi e Baronie. Il principale sistema torbiditico del bacino di Olbia è costituito dal Caprera, articolato in un sistema di canyon alimentatori nella piattaforma e nella scarpata continentale e da un ampio canale con argini alla base della scarpata. Il Caprera è fiancheggiato da un ampia piattaforma continentale, e questa, fungendo da "magazzino" per il materiale piu grossolando, può spiegare la peculiare architettura sedimentaria del suo fan. L' effetto di confinamento

L'effetto di confinamento del bacino sulla forma e sull'evoluzione del fan del Caprera è evidente soprattutto sull'asimmetria dei levee e su fenomeni di avulsione che hanno coinvolto il canale. Il bacino di intraslope di Olbia appare completamente riempito, e, nel bordo orientale, è presente il canyon di intrabcino verso il bacino sottostante. Gli effetti dell abbassanto del livello di base sono visibili nel settore distale del sistema, dove si ha lo sviluppo di canali distributari e di valli erosive a basso rilievo, che rappresentano le porzioni *upslope* dei canyon di *bypass*.

Il bacino di intraslope del Baronie è il bacino centrale del margine, confinato verso mare dal seamount delle Baronie, e presenta una via di fuga laterale rappresentato dal sistema di canyon di Gonone-Orosei. Il Posada è il sistema torbiditico principale, consiste di un canyon profondamente inciso nella piattaforma e nella scarpata, e sviluppa alla base della scarpata un piccolo fa radiale. La morfologia del è il risultato dell'interazione complessa tra la geoemtria del bacino ricevente ed il comportamento dei flussi sedimentari. La forma del bacino ha costretto il sistema torbiditico a cambiare la direzione di sviluppo, da est verso sud. Processi di framanento in massa a grande scala hanno inoltre contribuito alla riorganizzazione del sistema torbiditico.

Il bacino dell' Ogliastra è localizzato nel settore meridionale del margine, limitato verso mare dal seamount Quirra. Il settore settentrionale della scarpata continentale del bacino Ogliastra è caratterizzato da canyon e incisioni di carattere ibrido, con tratti deposizionali ed erosivi. L'Arbatax è il principale sistema torbiditico del bacino di Ogliastra caratterizzato da un settore meridionale dominato da un canale alimentatore e da un settore settentrionale abbandonato, caratterizzato da fenomeni di smantellamento e instabilità gravitativa.

In generale i risultati dello studio evidenziano l'importanza della combinazione dei fattori di controllo esterni, e della topografia preesistente, nello sviluppo dei processi sedimentari e degli elementi deposizionali dei sistemi torbiditici In particolare, appare evidente come lo stile deposizionale dei sistemi torbiditici in ambiente confinato diverga sostanzialmente da quello previsto dai modelli di fan sottomarini usati come strumenti predittivi nella esplorazione e sfruttamento dei giacimenti di idrocarburi.

Chapter 1

Introduction and aims of thesis

The study of deep water turbidite systems has generated an abundant literature in the last thirty years, with very detailed high-quality data sets from both modern and ancient systems giving new insights into the processes and deposits occurring within thie deep sea environment. High resolution multibeam echosounder and side scan sonar equipment, together with the development of 3D/4D seismic technology and petroleum company exploration wells, has revealed the complex morphology of deep sea channels and related fans in unprecedent detail. Summaries of the recent advancements on the knowledge of deep water systems can be found in Bouma *et al.,* (1985a), Weimer & Link (1991), Pickering *et al.,* (1995), Lomas & Joseph (2004), Hodgson & Flint (2005).

If the structure and the mode of development of the deep water systems appear to be generally well understood, some turbidite fields recently developed appear fairly substantially different from the fan models described and used as predictional tools for the hydrocarbon exploration. A clear understanding of the geometry, facies relationship and reservoir quality is therefore critical for exploring and exploiting these deposit effectively.

The first models classifying the processes, deposits and the anatomy of the deep water clastic emerged in the 1960's and early 70's (*historic review in*: Shanmungam, 2000). In the 70's two approaches were developed: i) ancient fan models elaborated through pure sedimentological observations in ancient thrust-fold belts turbidite basin-fill (Mutti & Ricci Lucchi, 1972) and ii) models based on the study of modern submarine fan systems (Normark, 1970). Both approach were successively combined in a simple, all purpose fan model by Walker (1978), the extended suprafan model where the system is divided in distinct sector (feeder channel, upper fan, mid-fan/suprafan lobe and lower fan) through the purely sedimentological approach of the facies analysis. The conceives currents in past years to place all know submarine fan and turbidite systems in few, detaliled models is however still not possible at this time, and probably never will be (Bouma, 2004). In natural systems there are too many factors controlling and influencing the final deposition characteristics (Weimer, 2005). Conceptual and experimental models of

turbidity current deposition and submarine fan development envisaged essentilally unconfined radial development of lobe and fan-shaped depositional bodies. However, a wealth of case studies now avaible from many contrasting turbidite system worldwide, makes it clear that, in many basin, both sediment dispersal patterns and the geometries of the depositional lobes have been profounldly affected by pre-existing or developing basin-floor relief (Lomas & Jospeh, 2004). It seems that perhaps most large natural turbidity currents, particularly in intracontinental basins, are not free to spread radially across a uniform basin floor (Lomas & Joseph, 2004).

The aim of my work is to furnish a detailed description of modern, small turbidite systems located in sub-confined envirorment in order to understand the variability of overall architercture (size, morphologies and geometry) and the architectural elements (e.g. feeder canyons, channel-levee systems, lobe etc.), where pre-existing tectonic related topography is the main controlling factors on deep sea systems. In addition, the work is estabilished the purpose to underlines differences and similes of confined turbidite systems with the current fan models elaborated for unconfined, small deep sea systems. With these intensions, I have begun a collaboration with the ISMAR (Institute for the marine sciences) of Bologna that has made me available their high quality data set on the seafloor morphology and on the subsurface of the southern Tyrrhenian sea. The area chosen for the study is the eastern Sardinian margin, that, in the upper sector consist of sub-confined intraslope basins, where at the base of slope, canyons and system of canyons develops small deep sea fans.

1.1 Controlling factors on deep sea clastic sedimentation.

In frontier hydrocarbon exploration, knowledge of reservoir architecture will constraints risk assessments and help the development of appropriate drilling strategies (Richard & Bowman, 1998). Models for deep water systems are still too simple and incomplete and need to be greatly improved (Damuth, 2002). Three major factors, and combinations of these, control the deposition of these systems (Mutti & Normark, 1991; Normark, Posamentier & Mutti, 1993, Reading and Richards, 1994).

Geodynamic setting and tectonics, sea level variations, and climate (Fig. 1) commonly interact with each other and finally control deep-sea sedimentation (Stow *et al.,* 1985; Weimer, 2005). Sea level variations, through eustatic and tectonically induced fluctuations, can affect deepwater systems by varying the supply of clastic input (Posamentier, 1991; Bouma, 2004). Hinterland geology and climate control the shape, type and nature of both the source area and the nearshore and the shelf environment affect the rate and type of sediment supply to the deep-sea environment (Fig. 2) (Weimer, 2005). The triggering mechanism for sedimentary gravity flows, (large, catastrophic, earthquake-driven flows, moderate episodic flows from major floods, or continuous hyperpicnal flows) controls the rheology and the behaviour of the flows and finally have a large impact on the geometry and internal organization of deep-sea depositional bodies (Reading, 1998; Weimer, 2005).

Tectonics influences almost all aspects of submarine fan architecture, affecting the processes occurring from source to sink (Bouma, 2004). Tectonics can have in fact a major influence on:

(1) The type of continental margins (i.e. passive or active margins);

(2) The relief of the source areas and the pattern and width of on-land drainage basins;

(3) The locations and spacing of the entry points to the coastal areas;

(4) The rate of sediment supply;

(5) The width and morphology of the shelf and continental slope, that affect the capacity of the shelf to store shallow-marine sediments prior to their discharge into the deep-water realm;

(6) The type, size and morphology of the receiving basin

All the factors that are controlled by the tectonics have a large impact on the resultant architecture and constituents of deep-sea depositional systems.

However, the recent investigations on many continental margins have highlight that the size and morphology of the receiving basin has the ultimate fundamental control on the architecture of deep-sea depositional systems. In the following a review is presented on confined turbidite systems.

Topographically complex slopes or even gently dipping continental slopes flanking deep-sea basin plain, can be segmented by faults, resulting in a set of tectonically shaped basins (Fig. 3). The term confined turbidite systems have been coined for those deepwater depositional system whose evolution has been constrained by basin floor topography (Lomas & Joseph, 2004). The origin of confining topography is mainly tectonic: from the large-scale structural features, to local fault scarps, folds, or subtle perturbation of basin floor topography with associated tilting and faulting (Lomas & Joseph, 2004). Nevertheless basin floor relief may be also the result of slope collapses masses, mud diapirism, and halokinesis (Lomas & Joseph, 2004; Bouma, 2004). Syn- and post- depositional changes are common and depend on tectonic style and activity. Unconfined basins normally are large, and their sediment source is far from the coastal zone; confined basins commonly are coarse-grained and may have significant amounts of gravel, as well as a low percentage of fine grained mud (Bouma, 2004).

1.2 Basin geometry and effects on large scale depositional architecture

The geometry and the dimension of the receiving basin, play a fundamental role on deep sea depositional systems, controlling the shape and the development at the big scale (Bouma, 2004). Nevertheless, is important to remember that the dimensions and the form of the basin are not fixed, but can be modified by the tectonic activity during the phases of infilling (Sinclair, 2000). Besides, it also able to control the distribution of the sediments after its cessation (Pickering *et al.,* 1989). The recent researches has furnished the evidence for complex submarine slope setting around the continental margins. The types of structurally induced topography that can be found on complex subaqueous slope can be divided into three broad classes (Smith, 2004):

1. Silled sub-basin (i.e. a closed depression);
2. Partially silled basin with lateral escape paths;

3. Tectonically induced bounding slopes that guide, but do not block, flows paths.

A silled sub-basin is a closed topographic depression on a slope that has a topographic barrier at its downdip margin (Smith, 2004). Ponding occurs when the flows are large in volume relative to the scale of the basin and can spread over the whole basin being reflected by the seaward bounding high. Deposition from smaller volume non-ponded flows results in downflow tapering beds, that terminate without reaching the bounding slopes (Smith, 2004). The most studied silled sub-basin is the complex of salt-withdraw minibasin of the Gulf of Mexico slope (Diegel *et. al.* 1995; Liu & Bryant 2000). Examples of partially silled basins with lateral escape paths include those associated with the Chumash fracture zone in Monterey fan (Normark *et al.,* 1984), and the present-day Brunei slope (Demyttenaere *et al.,* 2000). For the third case, the present day Borneo Slope and the Campos slope are the most famous examples. Different types of complex slope topography may co-exist laterally on a given slope (Bieggert *et al.* in review.)

1.3 Early studies on confined turbidite system

The researches on the effects of topographic structures on sediment gravity flows, have initially been conducted in small tectonic basins located on the Middle-Atlantic Ridge (Van Andel & Komar, 1969). The two authors described turbidite successions with characters of sedimentation from density currents repeatedly reflected by fault scarps (Van Andel & Komar, 1969). They used the term *ponding* to refer a situation in which turbidity currents are fully contained by an area of enclosed bathymetry. Evidences of topographical control on the flows during the deposition, have been described subsequently by Pickering & Hiscott, (1985) on the Middle Ordovician sequence of the Cloridorme Formation in Canada. The authors used the term *contained* turbidites to describe beds deposited from turbidity currents that were confined within a basin too small to permit sustained unidirectional flow (Pickering & Hischott, 1985). Terms as *ponding* and *containment*, are now generally used to indicate a situation in which sediment gravity flows fill an enclosed depression and are unable to surmount the sills, which create a mini-basin or a ponded depocentre (Lomas & Jospeh, 2004). Evidence of deflection and reflection of large volume

turbidity currents revealed by the reversal of paleocurrents indicators, has subsequently been recognized at outcrop in various other successions such as, the Eocene-Oligocene Grès d' Annot (Sinclair, 2000; Kneller, 1991) the Eocenic flysch of Jugoslavia (Marjanac, 1990), the Ordovician Welsh Basin in the United Kingdom (Smith, 1987), and the Tortonian Tabernas Basin in Spain (Houghton, 1994). Divergent paleocurrent indicators are thought to represent depositional system where turbidity currents have interacted with basin-bounding slope or intrabasinal slope (Kneller *et al.,* 1991; Smith, 2004).

Regarding the modern systems, early published examples documenting the influence of topography on patterns of deposition and erosion include: the California Borderland *fill and spill* models (Douglas & Heitman, 1979); the Monterey Fan (Normark *et al.,* 1984) where channels cut headward into the Ascension Valley when fan extended south of the Chumash Fracture Zone; forearc slope basins (Stevenson & Moore, 1985).

1.4 The fill and spill model for the salt-withdrawal intraslope basins

Intensive study of the Gulf of Mexico slope (Fig. 4), which is affected by numerous salt-withdrawal sub-basin, resulted in detailed models for the fill and downslope spilling of such mini-basin. Satterfield & Behrens (1990) were the first to propose processes of "*spill-and-fill*" for the northern Gulf of Mexico slope. The term was introduced by the authors to describe the complex iterative processes of intraslope basins filling from updip to downdip. Many authors have expanded on the fill and spill concept for modern intraslope basin of the Gulf of Mexico (Winker, 1996; Pirmez *et al*., 2000) and for the subsurface (Prather *et al*., 1998; Weimer *et al*., 1998, Booth *et al*., 2000; Meckel *et al.*, 2002).

In the fill-and-spill models developed for the intraslope basin of the Gulf of Mexico, the concept of accommodation along the irregular slope profile play a very important role. Prather *et al.,* 1998 has defined three kinds of accommodation: (1) ponded-basin accommodation develops in association with salt withdrawal and minibasin formation. (2) Slope accommodation is the space between a graded slope profile pinned at the shelf break, and the steeped-equilibrium profile at the top of the ponded basin accommodation. (3) Healed slope accommodation is the space between a lower gradient profile and the deep surface at the top of the combined

ponded and slope accommodation (Prather *et al.,* 1998). Each kind of accommodation is associated with specific deposit and their corresponding seismic facies (Prather *et al.,* 1998). The timing of fill between to sub intraslope basin has been interpreted differently by authors, both as being autocyclic and allocyclic. Booth *et al*., 2000 is convinced that spilling from an updip basin to a lower minibasin can occour only during a transgression. By contrary, Beauboeuf & Friedmann (2000) describing four connected Late Pleistocene intraslope basins, affirm that timing has to be controlled by eustatic controls, with spilling occurring during Late Pleistocene low stand level. The style of sediment dispersal following the fill and spill model has also been interpreted from the Paleocene of the United Kingdom Atlantic margin (Lamers & Carmicheal, 1999) and the Lower Cretaceous of the North Sea (Argent *et al.,* 2000).

1.5 The fill and spill model for tectonically controlled intraslope basins

On the basis of the observation conducted both in modern and ancient system, Sinclair & Tomasso (2002) proposed a simplified spill and fill model also for intraslope basins, not affected by halokinesys. The model infact foresees a static intrabasinal high that divide the two subsbasin (in Gulf of Mexico, as example, the bounding slope may growth as fast as 10 mm/yr, Prather *et al.,* 1998), with a single point source of surge type, mixed grain size turbidity currents and regardless of other important controlling factors such as tectonic activity, and sea-level changes. The resulting depositional model can be divided into four main phases, that record the dominant response of the incoming currents to the basin morphology as it being progressively fills (Fig. 5).

Phase 1: Flow ponding

In this phase, the kinetic energy of the gravity flows is insufficient to surmount the topographic barriers of the intraslope basin and the ponding of the flows take place (Sinclair & Tomasso, 2002). Flow thickness is as a primary control for the run up distance of a single flow (Muck & Underwood, 1990). For a subcritical, uniform density currents, run up distance is approximately 1.5 times the thickness of the flow head (Muck & Underwood, 1990). Once the turbidity current runs up on the

opposing slope, the transformation of kinetic energy into potential energy take place, resulting in reflected component of the flows. The interference between incident and reflected flow generate an internal bore located at the base of the slope (Edwards, 1993). Kneller & McCaffrey, (1999) explain the abrupt transition from massive coarse sandstones up into structured fine sandstone with variable paleocurrent direction, in the Gres d' Annot Sandstone, as a consequence of density stratification within ponded turbidity currents. In their interpretation the upper higher-density portion of the flow decelerates rapidly, resulting in rapid sediment fall out, whereas the lower density portion is reflected by the bounding topography (Kneller & McCaffrey, 1999).

Phase 2: Flow stripping

The process of flow stripping happens when the turbidity currents are partially able to surmount the barrier with their lower-density fraction (Sinclair, 2000). Recognized as potentially important process in meandering submarine channels (Piper & Normark, 1983), the flow stripping in this case, has the potential to transfer the finer-grained, lower density component of the flow over a barrier, while confining the coarser-grained, higher density portion of the flow upstream from the barrier (Sinclair & Tomasso, 2002). This implicates that, during the infilling of the upper basin, the effective barrier height will be less than the potential run up of the incoming flows. The model foresees that the coarser fraction will be deposited in the upper confined basin, whereas the finer component will be stripped off and carried into the lower basin (Sinclair & Tomasso, 2002).

Phase 3: Flow bypass

When the upper basin is completely filled, the break in slope that defined the margin of the updip basin becomes healed (Prather *et al.,* 1998). With no topography able to trap the incoming currents, the bulk of the sediment is bypassed (Sinclair & Tomasso, 2002). This leads to the formation of an incision with bypass over the confined basin, or to the abandonment and redirection of the incoming flows away from the confined basin (Sinclair & Tomasso, 2002). The transition from phase 2 to phase 3 is associated with a progressive increase in sediment texture, volume and

velocity of the currents able to travel over the confinement, until the threshold for erosion is reached, with the incision of an intrabasinal canyon (Satterfield & Behrens, 1990). The progressive downcutting of the canyon will create a new base level for the updip basin, lower than the previous in phase 1 and 2. This result in a rejuvenation of the erosion on the updip basin sediments (Ci in fig. 5) The erosional scour in the upper deposit in the Annot Sandstone upper sub-basin is interpreted as a record of canyon incision during spilling and bypass (Sinclair & Tomasso, 2002). Another possible scenario is the switching of the sediment away form the upper basin after the end of Phase 2 (Cii in fig. 5). In this case, the upper basin will be abandoned, resulting in fine-grained overbank deposit: this is interpreted for the thick accumulation of mudstones on the top of the Inner Basin of Taveyannaz sandstone (Sinclair, 2000). During phase 3, the depositional processes at the proximal parts of the lower basin are very similar to those seen at the base of the continental slope of the "classic basin" with an hydraulic jump from supercritical to subcritical flow due to the abrupt break in slope at the base on intrabasinal high. In the Annot sandstone this process is recorded by the amalgamated and dewatered toe-of-slope deposits that onlap southward of the interbasinal Covey Canyon. Similarity, the high degree of erosional amalgamated in the sand packages of the Outer Basin of the Taveyannaz Sandstones are interpreted as a result of this processes (Fig. 6) (Sinclair, 2000; Sinclair & Tomasso, 2002).

Phase 4: Blanketing

By the time the lower basin is filled, the depositional gradient of the system is reduced. Where bypass has occurred by incision, the interbasinal canyon will become backfilled by sediment accumulation in the lower basin, and so the local base level for the upper basin will rise, leading to renewed sediment accumulation (Sinclair & Tomasso, 2002). This situation is seen in the filled basins of the upper slope of the Gulf of Mexico, where channel–levee systems aggrade over the basins and link with interbasinal canyons that incise into uplifting interbasinal highs (Satterfield & Behrens 1990). It is also recorded in the infill of the Coyer Canyon in the Annot Sandstones; the depositional setting for these deposits are channel–sheet complexes. It is proposed that this records the reduction in gradient, and the

associated development of meandering channel systems, with condensed overbank fines (Sinclair & Tomasso, 2002).

1.6 The connected tourtuos corridor model

Whereas structurally induced bathymetry may form closed depression on slopes, as seen for the Gulf of Mexco, in many other cases (Biegert *et al.,* in press) flows paths extend in connected, variably tortuous route down complex slopes.

Petroleum companies well penetrations and the arrival of the 3D seismic analysis demonstrate that apparently separate silled sub-basin are in fact connected in the third dimension (Smith, 2004). This type of sediment-receving depression on a topographically complex slope is termed connected tortuous corridor (Fig. 7) (Smith, 2004). Changes in gradient occurs along this connected pathways, with expected segments of substrate erosion alternate with sectors of enhanced deposition (Demyttenaere *et al.,* 2000). Such flows paths have been documented on slopes in West Africa (Fig. 8) and Brazil (Fig. 9), and have been inferred for the Brunei Slope (Demyttenaere *et al*., 2000). In the Brunei case, the seismic show fan lobes deposited in subtle depression or at local break in slope. Erosional cutting across shale ridge contain mud-rich channel-levee complexes (Demyttenaere *et al*., 2000). Moraes *et al.,* (2000) discussing on the reservoir development of the Cretaceous Carapeba system in the Campos Basin, interpreted amalgamated sand-rich turbidite channels occur in erosionally modified fault-controlled troughs, comparable in form and dimensions with those of the Annot Sandstone system (Smith, 2004). Other examples coming from Lower Congo Basin, offshore Angola. In connected tortuous corridor case, fills of the channels guided by topography may contain high-quality reservoir if the source sediment is poor in mud and contains coarse-grade sand and fine gravel that enable deposition rather than bypass on the steeper slopes (Moraes *et al.,* 2000). Coarser size and the presence of gradient reductions will enhanced deposition on reservoir-forming sands (Moraes et al., 2000). More mud-rich supply result in turn in channelized sandstone bodies enclosed in a mudstone background phase with consequent reservoir connectivity problems (Reading & Richards, 1994). Criteria for distinguish a series of cascades of silled sub-basin from connected tortuous corridors have been resumed by Smith (2004): (1) Fills of successive basins will tend to young in the down-paleoflow direction (Prather, 2000); (2)

Proximal to distal facies trends should be reset in each successive sub-basin (Winker, 1996); (3) the tendencies for spill-phase incision in updip basin-fills to be mudstone-filled rather than backfilled with sandstone; (4) the presence of thick mudstone caps to individual turbidites can indicate full ponding of the flows. A schematic diagram showing the differences between the silled sub basin case and the connected tortuous case is showed in fig. 10.

1.7 Modern turbidite system

Gervais *et al.,* 2004 described the modern sandy Golo turbidite system, developed in a partly confined setting on the eastern margin of Corsica. The turbidite system consist of four non coalescent fans characterized by stacked depositional bodies. Each of these fan appears to have fed by separate canyons, ultimately linked up-dip to a single fluvio-deltaic point-source. Structural confinement of the system as a whole has led to a predominance of aggradation, and smaller-scale slope variations have constrained the specific morphology and architecture of depositional lobes (Gervais *et al.,* 2004). Notwithstanding the setting adiacent to a tectonically active, uplifting margin, the dominant influences on depositional pattern appear to have been the pre-existing morphology, sediment source characteristic and eustaic sea level variations (Gervais *et al.,* 2004).

Babonneau *et al.,* (2004) described a very different confined system from the deeply incised Zaire submarine valley. The authors focus on striking array of multiple terrace imaged along the inner flanks of the upper-fan valley, adiacent to the deeply incised sinuous thalweg. The morphology analisys coupled with seismic characters has lead to interpret these features as levees, confined within the incised valley (Babonneau *et al.,* 2004). Many terraces correspond to the infill of abandoned meander loops, and are believed to record aggradation of relatively dilute turbidite currents deposit associated with spillover and flow-stripping processes (Babboneau *et al.,* 2004).

1.8 Effects of basin confinement on turbidity currents

The factors determining the efficiency of turbidity currents to carry sands in basinward direction have been largely discussed in the past by many authors

(Normark, 1978; Mutti & Normark, 1987; Laval *et al.,* 1988; Gladstone *et al.,* 1998; Bouma, 2000). On the basis of field observation, Mutti (1979; 1992) concluded that the final geometry of individual beds or groups of beds, is determinated not only by the slope and basin configuration but also by the flow efficiency, as controlled by the grain-size composition of the suspended sediment load and the flow volume. He suggested that relatively thick, large volume flows are less affected by the relief of the basin floor than are thinner ones (Mutti, 1992).

The bathymetry controls depositional patterns principally by inducing spatial variations in flow properties, i.e. flow non-uniformity, flow unsteadiness and hence depositional processes (Kneller, 1995; Kneller & McCaffrey, 1999). Flow velocity non-uniformity is determined principally by topography; the spatial changes in current velocity are described by the term non-uniformity: flows that become more rapid downstream are described as *accumulative,* whereas flows which becomes slower are called *depletive* (Kneller & Branney, 1995). The flow non-uniformity arise when flows experience changes in slope or degree confinement (Fig. 11a). The related effects can occur at different scales from: 1) scales greater than the flow thickness, affecting the entire flow (e. g. change from slope to basin floor); 2) scales of the same order of the flows (e.g channelization); and 3) scales less than the flow thickness (e.g. erosional scours or flutes, or aggradational bedforms) (McCaffrey & Kneller, 2004).

Another key variable is the flow unsteadiness, which describes the flow's temporal evolution. Unsteadiness is thought largely to be determined by the flow triggering mechanism (Normark & Piper, 1991). Turbidity currents initiated by seismogenic slumping or major storms typically generate surge-type currents (Kneller & Branney, 1995), whereas hyperpycnal flows directly fed by fluvial system have the potential to generate sustained currents (Mulder *et al.,* 1998). Steady flow is defined as a succession of fluid particles having identical velocity vectors (Allen, 1985); waning flow describes a situation where current passing a given point gets slower, and a waxing flow where it becomes faster (Fig. 11b) (Kneller & Branney, 1995).

The suspended-load fall out rate (SLFR) is dependent on the flow velocity and on the flow concentration (Amy *et al.,* 2004). It controls depositional facies in several ways, controlling the rate of aggradation of the bed: thicker beds occurring in area of more depletive flow and therefore high SLFR. It also affects bed form development, and thus the formations of sedimentary structures (Lowe, 1988).

At the flow scale, topography exert a potential major controlling factor on the deposition, by controlling the non-uniformity of the currents or by confining and "ponding" them, either partially, as in a valley, or completely (e.g. Wilson & Walker, 1985; Branney & Kokelaar, 1992; Rothwell *et al.,* 1992). The behaviour of turbidity currents around an obstructing topography varies with the forward velocity of the current, the obstacle height, the current density and, most significantly, the density stratification within the current (Muck & Anderwood, 1990; Alexander & Morris, 1994). The topography interaction has strongimplications for the spatial distribution of sediments in the deep sea, for the interaction of unconfined currents with intrabasinal highs and basin margins, and for channelized currents with channel margin and levees (Kneller & Buckee, 2000).

To date, relatively very few experimental work have been carried on studies regarding the influence of topography on turbidity flows (Al Jaidi *et al.,* 2004; Amy et al., 2004; Muck & Underwood, 1990). However, in the recent, few important fieldwork, regarding the effects of the topography on the flows has been reported by Haughton, 1994; Kneller & McCaffrey, 1999; Haughton, 2001 and Mutti *et al.,* 2002.

In particular, the experiment lead by Al Jaidi *et al.,* (2004) has investigated the effects of partial blocking on flows of different efficiency. The authors noted that as well as introducing more sediment that was able to surmount the obstacle and escape into the downstream sub-basin also increased with the proportion of the fines in the initial flow (Al Jaidi *et al.,* 2004). Follow the authors interpretation, this indicates a flow efficiency control on the effectiveness turbidity currents, with more efficient currents better able to surmount obstructing bathymetry (Al Jaidi *et al.,* 2004).

Tank experiments, coupled with outcrop observations in the Gres d'Annot lead by Amy *et al.,* 2004, attempt to quantify the impact of a lateral basin floor slope on the velocity field of incoming flows and the resulting deposits. The results suggest that lateral confinement reduces the spreading of the flow, and induces thicker deposits along the slope compared with the basin if the flow velocity is low, and bypass if flow velocity is high (Fig. 12). However, the authors has specified that it also necessary to take in account the spatial non-uniformity of the flow concentration to make reasonable prediction of the lateral evolution of the sediment thickness (Amy *et al.,* 2004).

1.9 The run up height of a turbidity currents on a bounding slope

Oceanographic data suggests that if the obstacles are much larger that the incoming current, the run-up distance may be many hundreds of meters (Dolan *et al.,* 1989, Lucchi & Camerlenghi, 1993). Numerical and laboratory experiments lead by Muck & Underwwod, (1990) show that a finite volume of fluid related to the head may surmount the obstacles if the relief is less than 1.5 times the height of the head of the currents. The bulk of the remaining mass should rebound into adjacent basin and deposit a reflected turbidite. However, additional experiments are required, the authors conclude that direct upslope bypassing of relatively small barriers (less than 500 m of relief) may be commonplace (Muck & Underwood, 1990). Turbidite deposition on a bathymetric high can occur through any combination of flow thickness, tilting of the cross-flow surface, and a vertical shift in the flow's centre of gravity (Muck & Underwood, 1990).

1.10 The blocking of turbidity current by topography

The complete blocking happens when none of the current gets over the top of the topography: for 2D system, i.e., where the obstacles axis is perpendicular to flow and effectively infinite in extent. Woods *et al.* (1998) provide an analysis of the criteria for full and partial blocking of unstratified currents by two dimensional topography, based on the concept of critical flow velocity, and critical flow thickness. The minimum height for complete blocking is equal to the thickness of the bore generated upstream (Woods *et al.,* 1998), which is around 2.2 times the critical flow thickness (Woods *et al.,* 1998). In the 3D world, things are more complex and flow probably goes around the obstacle when the densiometric Froude number is much less than 1, but also the stratification plays an important role (Kneller, 2000).

The effect of blocking is to generate a disturbance upstream of the obstacle, which consist of internal bore, that migrate upstream (Kneller, 2000). Where the current is completely blocked, the fluid velocities within the bore may be negative (i.e. upstream) and it therefore constitutes a current reflection (Edwards, 1993). Kneller *et al.,* (1991), Edwards (1993) and Kneller (1995) have shown that in 3D situations, these reflections propagate perpendicular to the reflecting surface.

Multiple paleocurrent direction within single beds have been reported from many both recent and ancient turbidite system. These multiple-paleocurrent directions have been interepreted as reflections of the turbidity current from topography at the basin margin (Kneller & McCaffrey, 1999). In some cases, the reflections are more or less diametrically opposed to the forward currents (Pickering & Hiscott, 1985), while in many cases, the reflections are roughly perpendicular. Often the changes in current direction occur in association with abrupt reversal in grading (Pickering & Hiscott, 1985), and these reversal or repetition have been used to imply current reflection.

1.11 Implications for sedimentation at the flow scale

Where turbidity currents interact with large obstacles and are partially blocked, the flows experience a massive and a rapid decrease in both competence and capacity associated with the upstream jump, and sedimentation is likely to occur (Kneller & Buckee, 2000). Kneller (1995) and Kneller & McCaffrey, (2000) show marked localization of deposition associated with base of slope jump, despite the sudden increase in the turbulence that should be expected there. In rapidly waning currents, the jump must remain almost stationary where the currents strikes the obstacle at high angle. Rapidly waning currents may also produce higher energy jumps since they propagate through the thinning tail of the forward current and so the ratio of jump height to forward current thickness progressively increase (Kneller & Buckee, 2000). Deposition may similarly be concentrated in the lee of the obstacles in association with the downstream hydraulic jump, possibly producing an abrupt downstream thickening in the deposit. Deposition beneath supercritical flow on the lee side of obstacles may produce antidune stratification, whose preservation in the sediment thus need not imply that the currents was supercritical except on the downstream facing slope of the obstacles (Kneller & Buckee, 2000).

The vertical velocity and turbulence structure of turbidity currents is fundamental to the manner in which sediments are distributed within the current, and thus affects many aspects of deposition, especially in the currents that are in contact with the bed (Kneller & Buckee, 2000). This includes depositional topography such as the levees of submarine channels. The stratification of currents flowing down leveed channel is instrumental in partitioning different grain-sizes of sediments between the channel

axis and the levee (Peakall *et al.,* 2000). The degree of overspilling on the channel bends is determinated by the Froude internal number, (generally defined as the ratio between the current velocity with the height of the obstacle and the buoyancy frequency, (Baines, 1995) controlling the height of dividing streamlines inside the flows respect to the levee crest (Fig. 13a) and the behaviour of the portion of the currents overtop the levee (Fig. 13b).

Geologic Setting

1.12 The Tyrrhenian sea

The Tyrrhenian basin (Fig. 14) formed as a result of lithospheric stretching and thinning during the Late Tortonian-Early Pliocene, of the areas previously occupied by Alpine-Apenninic orogens (Dewey *et al.,* 1989, Patacca *et al.,* 1990). Extensional tectonics in the rear of the orogen went on concomitantly with continued thickening of the external portion of the Appenninc-Maghrebid chain (Elter *et al.,* 1975; Patacca *et al*., 1990). This evolution, characterized by extensional tectonics at the rear of a migrating orogen, has been interpreted as the result of back-arc opening driven by the sinking, and passive rollback of the Ionian lithosphere beneath the Calabrian arc (Fig. 15) (Malinverno & Ryan, 1986; Sartori, 1990). The opening of the Tyrrhenian basin lead to the formation of oceanic domains in the central and southern Tyrrhenian. First production of oceanic crust occurred westward, during the Pliocene spreading of the Vavilov basin (4.3-2.6 Myr), (Kastens & Mascle *et al.,* 1990) accompanied by the thermal subsidence of the thinned western margin crust. A subsequent change to ESE-directed extensional stress in Late Pliocene-Quaternary resulted in the emplacement of basaltic crust southwestward, generating the Marsili back-arc basin (2 Myr) (Kastens & Mascle *et al.,* 1990).

The deep-water oceanic-like crust, that floor the central and southern Tyrrhenian sea is surrounded by different geodynamic setting of the margin. The western Tyrrhenian margin represent a typical passive continental margin, while the Calabrian and Sicilian margin to the east and south are associated with high seismicity, active volcanism and elevated rates of uplift of land areas represented by the Appennic-Maghrebid mountain chain (Marani & Gamberi, 2004).

1.13 The Tyrrhenian passive margin province: the eastern Sardinian margin

The Eastern Sardinian margin represents the passive margin of the Tyrrhenian basin, is delimited to the north by the Etruschi seamount, at 41°30N and to the south by the Ichnusa Seamount, at 39°N, covering the marine area westward from 11°30E (Fig. 16). Based on the results of the deep sea drillings in the frame of the ODP leg 107,

the initiation of the tectonic activity, estabilished from the data of the hole 654, in this sector is dated as Tortonian (10 Myr), (Kastens & Mascle, *et al.,* 1990).

During ODP Leg 107 a NW-SE transect of seven sites across the Tyrrhenian basin was drilled. It shows a migration of the zone of maximum extension from the upper Sardinian margin (UM) to the lower Sardinian margin (LM) represent by the Cornaglia terrace (Fig. 3) (Kastens & Mascle *et al.,* 1990). When normal faulting and crustal thinning started in the late Tortonian, it was concentrated along the present UM (Sartori *et al.,* 1990). During the Messinian (6.5-4.8 Myr) the locus of the maximum extensional shifted toward the southeast (Kastens & Mascle, 1990). The lower margin (LM), represented by the Cornaglia Terrace, became the depositional axis of evaporitic sedimentation (Spadini *et al.,* 1995). The synrift sediments on the LM are Messinian to Pliocene in age (Kastens & Mascle, 1990), indicating that this sector was the most active rift system during early Pliocene (4.8-3.5 Myr), (Trincardi & Zitellini, 1987). The latter rifting phase caused the formation of the oceanic crust in the Vavilov basin, where the oldest sediments lying on the basalts flows have been dated at around 3.5 Ma (Sartori, 1990).

The eastern Sardinian margin consist of broadly of two distinct physiographic belts parallel to the Sardinia coastline and with increasing water depth (Fig. 16).

At regional depth of 1000-1700 m, an upper slope belt, about 50 km wide, of sediment filled, flat lying intraslope basins (the Olbia basin, the Baronie Basin, the Ogliastra and the Sarrabus basin) develops, bounded seaward by a series of structural highs Etruschi, the Baronie and the Quirra High (Fig. 16). The Baronie seamount is the largest structural high in the Tyrrhenian with a length of over 120 km and is an up to 1200 m high tectonic horst that completely confined seaward the Baronie basin. The other structural highs that bound the intraslope basins display subdue topography (Fig. 16). These highs, infact, are actually uplifted footwall leading edges of large tilted blocks, formed by the development of rotational faults generally dipping eastwards, with the half grabens formed by block tilting and now practically filled (Gamberi & Marani, 2004). The intralsope basins are generally delimited landwards by the outer continental shelf and slope dissected by numerous canyons (Fig. 16). This promote the intraslope basin filling but also contribute to the development of the larger scale Gonone-Orosei and Sarrabus canyon systems that merge at a breach in the bounding structural highs, in the proximity to the southern Baronie seamount, to continue to the deeper ocean as the Valley of Sardinia (Fig.

14, 16). The Valley of Sardinia cross the Cornaglia Terrace (CT), consisting of a relatively flat lying deep water plain (2500-2800 m of water depth), extending about 70 km seaward (Fig. 14). The plain is bounded eastwards by a NE-SW trending fault scarp, the Selli Line that separates the Sardinian margin form the Vavilov abyssal plain (Fig.14).

Data and Methods.

This study is based on the interpretation of multibeam bathymetry and single channel reflections seismic data collected by ISMAR (Istituto Scienze Marine-Bologna, Italy) during the cruise Tir-99 in 1999. The cruise TIR 1999 was designed to accomplish the full coverage swath bathymetry mapping of the Tyrrhenian Basin (Figs. 17), downslope the isobaths of 500-1800 m (Fig. 18), after a previous cruise lead during september-october 1996 (Tir 96) that mapped the Central and Southeastern portions of the basin. In addition, a series of old, Sparker 30Kj single channel seismic profiles, acquired by the IGM during 70' s cruise has been used to implement the multibeam bathymetry interpretation.

1.14 Multibeam bathymetry: elaboration and data processing

During the Tir-99 cruise a Kongsberg-Simrad (KS) EM12-120S hull-mounted multibeam was used as primary source during the campaign; some small areas were investigated with the available hull-mounted KS EM-950. The swath coverage of the KS multibeam can reach as much as 7 times the water depth. Analysis of backscatter information from the sonar data also provides reflectivity data from the sea bottom. The survey was planned and performed at the speed of 10.5 Kn, and the data logging and survey control were done by the KS MERMAID and MERLIN software.

The initial processing, controlling and cleaning of the bathymetric data along the study area was performed through the following guidelines:

- creation of blocks (with NEPTUNE software package), with an average number of 500000 points (Fig. 19)

- line positioning processing (smoothing with cutoff frequency 0.07 and filter length 20), with NEPTUNE's POSPROC Module;

 depth processing with the appropriate sound velocity profiles (generated upon the XBT and statistical data) and additional local processing if necessary, with NEPTUNE's DEPTHCORR Module;

 block processing with Statistical or hand filtering, with NEPTUNE's BINSTAT Module (cell size ranging from 100 to 200 m, according to the cross-track resolution of the data, noise 3%, local rules to get rid of macroscopic depth errors); a lot of effort was applied in order to keep as much of valid data as possible. This was not always sufficient to eliminate some of the errors that were present on the ovelapping swaths on deepest areas.

 export of the block data in NEPTUNE binary xyz format (geographical);

1.15 Elaboration and production of the bathymetric maps

After the processing of the multibeam bathymetric data, i proceeded to the elaboration and production of bathymetric data of the eastern Sardinian margin. The data were preliminarily prepared through the following procedures:

 division of the eastern Sardinian area in 1 x 2 Degrees Latitude and Longitude sheets at the scale 1:250000 according to the Join Operation Group (JOG) cuts, to be produced with the UTM and Mercator projections.

 division of each JOG sheet in 4 working maps at the scale of 1:100000 (Direct Mercator on 40N), extending 2 km WSEN of the geographical limits.

The gridding and DTM production by cartographic software underwent the following guidelines:

1. preparation of all previuos data (including grids and single beam) for the input to chartographic software and datum transformation to WGS84 if necessary.

2. reading and storing of the xyz NEPTUNE files in the SIMRAD proprietary STB format (Direct Mercator on 40N), and straight conversion to UTM 32 or 33 of the STB file if necessary

3. production of the DTM 100x100 m for each of the above 1:100000 working maps (Direct Mercator on 40N) (search radius 1000m, number of quadrant 4, number of point per quadrant 8);

4. production of the DTM 250x250 m 1:250000 (Direct Mercator on 40N) by regridding the 4 1:100000 DTMs (search radius 1250 m, number of quadrant 4, number of point per quadrant 8).

5. straightforward production of GMT (Generic Mapping Tool) software *netcdf* grids from the cartographic softward grids

The final passage has been the production of detailed vectorial bathymetric maps of scales ranging from 1:50000 to 1:100000 of the eastern Sardinian margin (Fig. 20), with different contours interval ranging between 5m to 50 m. The vectorial maps has been saved on Post-Script format and elaborated with commercial graphic software (Corel and Adobe) and printed in various format with high-resolution ink-jet Hewelett-Packard plotter. For some selected areas, to envisage morphological elements that are under the resolution of the multimeam the bathymetry, multibeam reflectivity map, and shaded relief map has also been produced through the same processes.

1.16 Single channel reflection seismic

During the Tir-99 cruise, together with the multibeam data acquisition for bathymetric mapping, which normally provides the pattern of navigation lines, a single channel Air Gun seismic was acquired. The raw data was processed directly

on board, and digitized and recorded in standard formats, such as SEG-D and SEG-Y. Finally each seismic lines was printed on A4 rolls paper using a Oyo-Geospace thermal plotter.

1.17 Sparker single channel seismic

Single channel Sparker 30 Kj seismic profiles acquired by the IGM (Institute for Marine Geology- Bologna) during oceanographic survey lead in 1970, 1977 and 1978 along the eastern Sardinian margin, has been used to improve the interpretation of the multibeam bathymetric data. The equivalent seismic profile are available only in paper format and heliographic copy, so the profiles has been digitalized at 600dPi and elaborated through commercial graphic software (Corel Draw X and Corel Photo Paint X).

1.18 Data interpretation

The interpretation of the high resolution multibeam bathymetry allows to recognize the shape and the geometry of the intraslope basin of the eastern Sardinian margin, and to describe the morphological features of the small scale architectural elements of the main turbidite systems.

The analysis of the seismic lines has been focused on the control of topography on the deep water depositional system at the basin scale, only for the post-rift sequences. The seismic analysis integrate the multibeam bathymetric interpretation, furnishing the internal architecture of the sedimentary bodies and allows to recognize their facies, geometries and to infer the evolution of the sedimentary processes.

In the study area 4 main types of seismic facies have been recognized:

1. Continuous bedded well reflective facies
2. Continuous bedded faintly reflective facies
3. Chaotic, irregular facies
4. Transparent facies

The well reflective facies is characterized by numerous parallel reflections or by convergent reflections. The continuous, bedded faintly reflective facies is characterized by numerous low amplitude reflections. The chaotic facies is characterized by short, discontinuous reflection segments of variable dip and generally high amplitude.

This facies kinds have been referred to specific depositional processes and related sedimentary environment, following the consolidated models as summarized in Weimer & Link (1991).

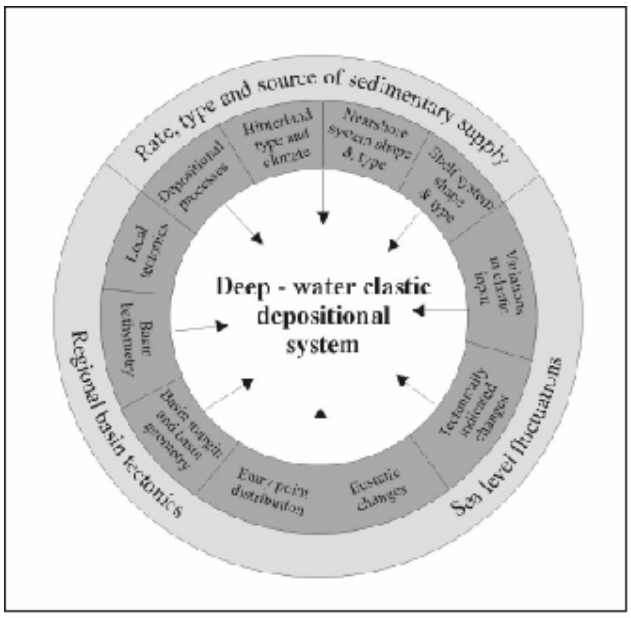

Fig. 1 Schematic diagram illustrating the wide range of controls influencing the deep water sedimentation. fom Richards, 1998

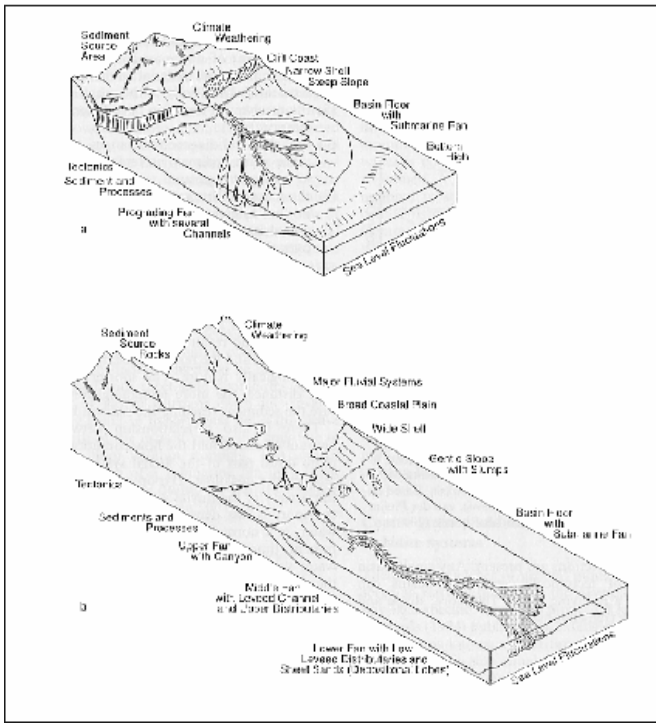

Fig. 2 Schematic block diagrams showing two end models with different relative distances from sediment-producing mountains, to the coast, the relative width of the shelf, and the shape and location of the submarine fan. The major actors controlling the transport and the deposition are mentioned. (A) Coarse-grained sand rich fans; (b) fine gained-mud rich fans. From Bouma, (2004).

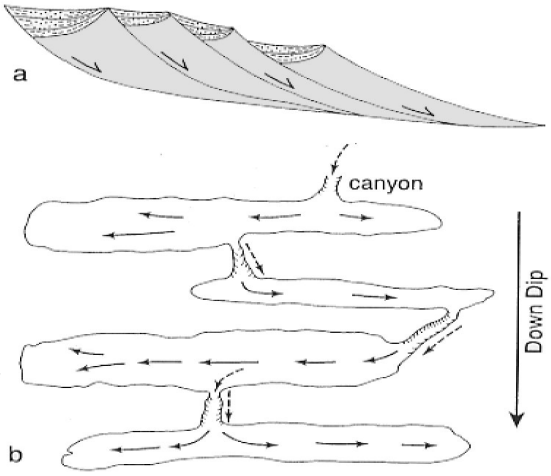

Fig. 3 Schematic dip section (a) and plain view (b) of faulted blocks, resulting in individual tilting of adjacent turbidite ub basin. The spilling over occurs only when the up dip basin is filled. The location of the lowest spot in the outside wall f an individual sub-basin, and the gradients in each sub-basin can result in one or two transport and filling directions in the next sub basin. From Bouma, 2004.

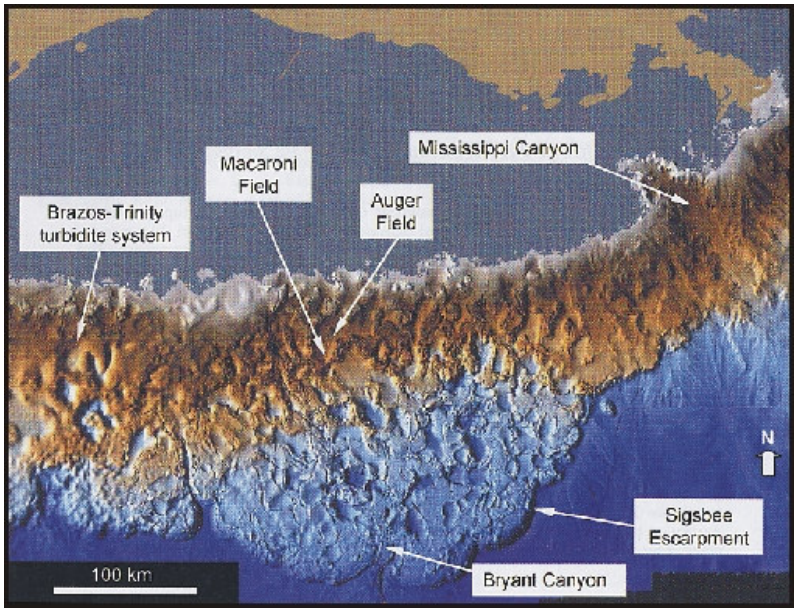

Fig. 4 Seloor image of the Gulf of Mexico salt-based slope. This represent the archetipal example of a silled sub basins. The small, circular to eliptical salt-withdrawal intraslope basins have diameters ranging between aproximately 5 and 20 km. The main morphological elements are indicated. From Smith, 2004.

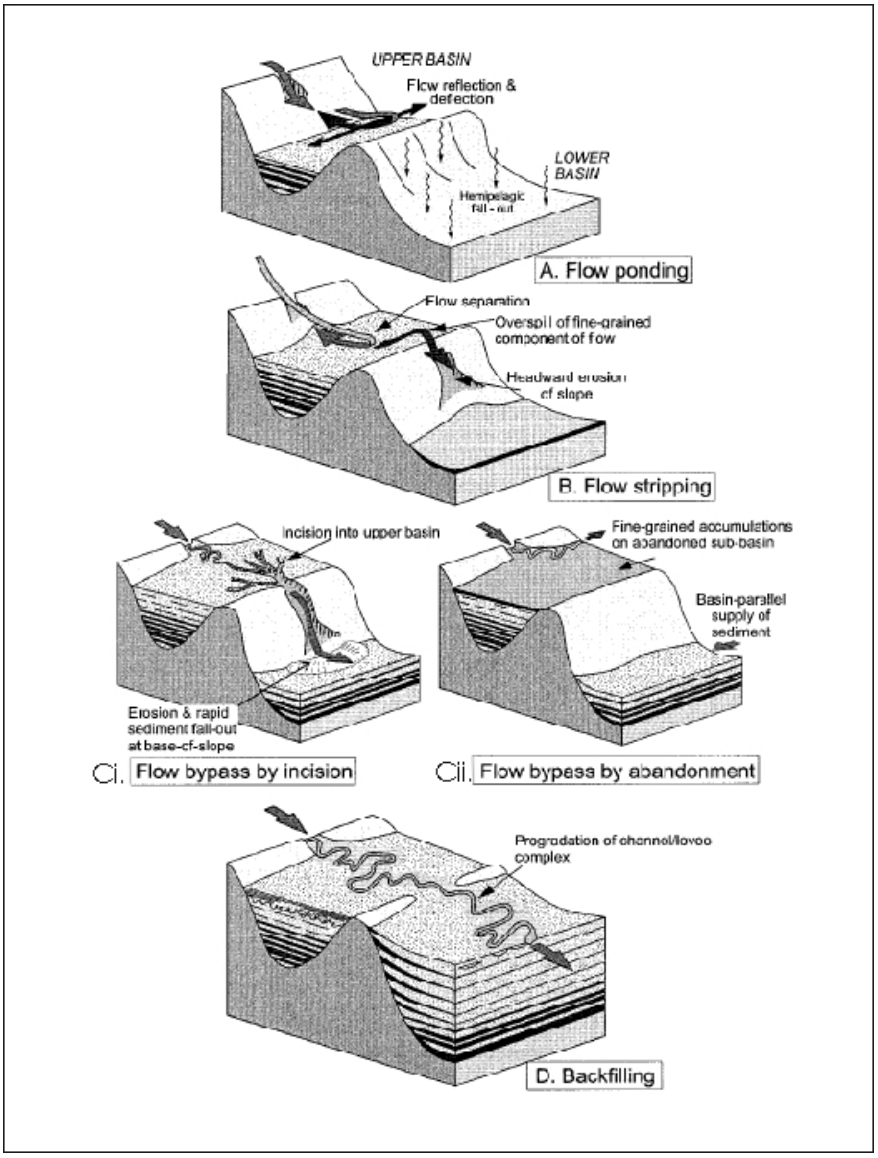

Fig. 5 Depositional model for the progressive infill of a confined turbidite basin and associated deposits at the base oFthe slope of a lower basin. See text for descriptions of the each stages of the model. From Sinclair & Tomasso, 2000

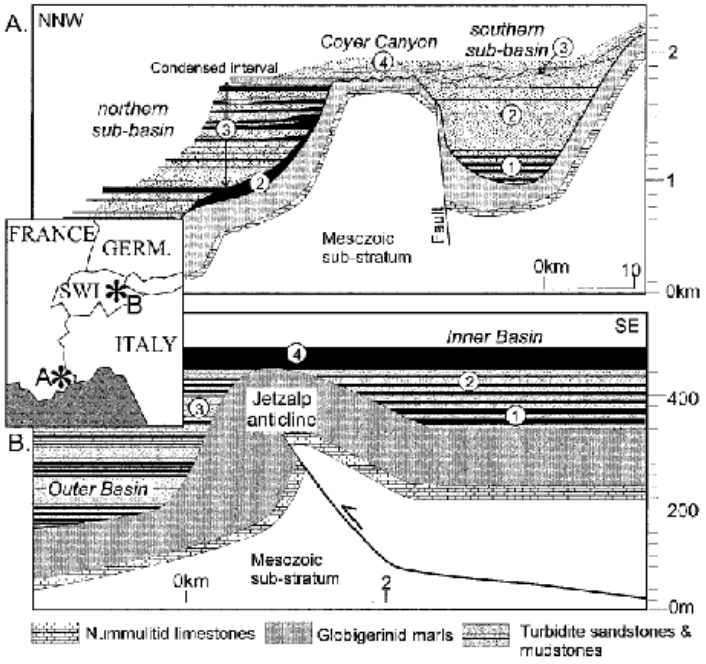

Fig. 6 (A) Reconstructed stratigraphy through the Annot Sandstones of the southern and northern sub-basins, and the intervening Coyer Canyon; (B) Reconstructed stratigraphy through the Taveyannaz Sandstones of the Inner and Outer basins, separated by the Jetzalp Anticline. The circled numbers refer to the four phases in a typical confined-basin sequence described by the fill and spill model proposed by Sinclair & Tomasso (2000). From Sinclair & Tomasso, 2000.

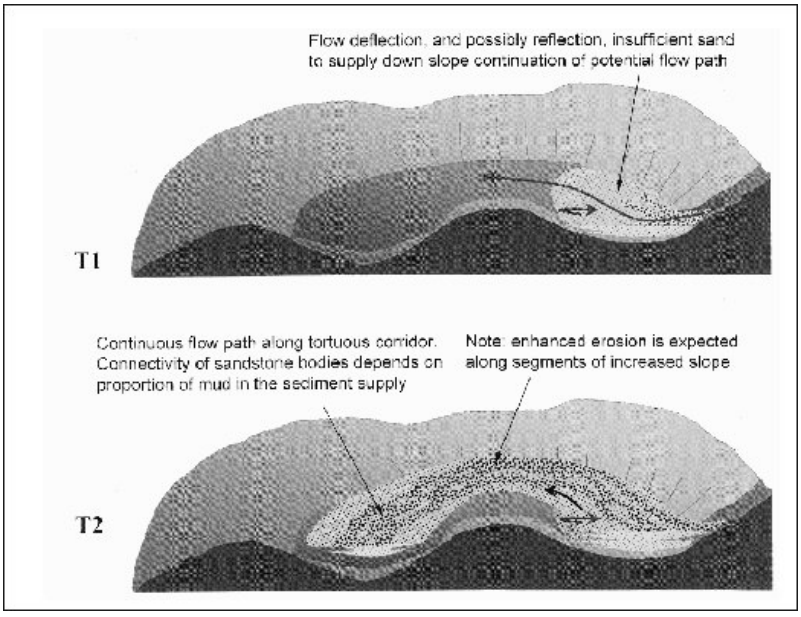

Fig. 7 Summary cartoon of the conncted tortuous corridor model showing a case with small volume sand-transporting flows and large volume sand transporting flows. From Smith, 2004.

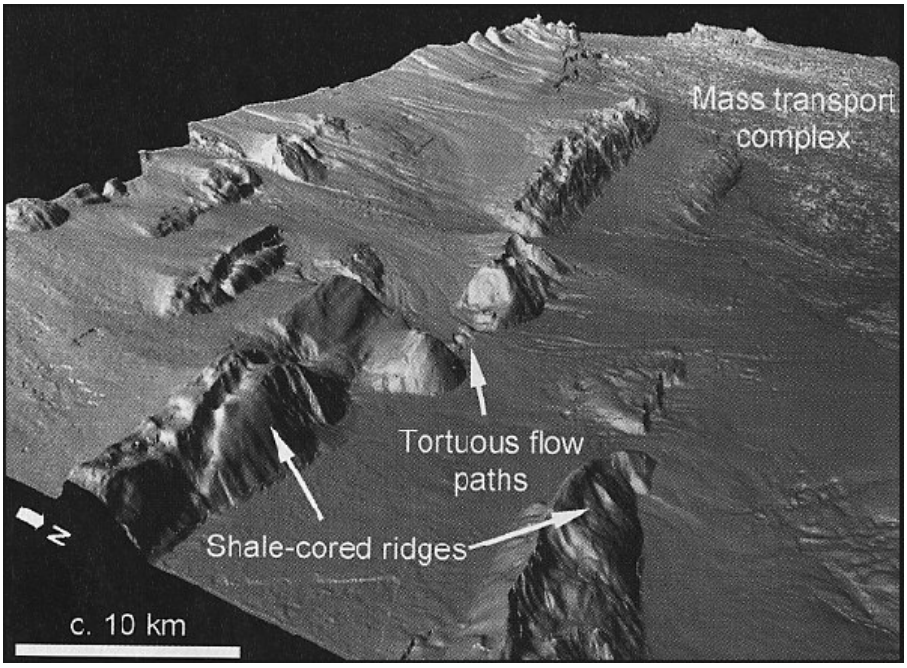

Fig. 8 Stepped topography of the northwestern Borneo slope, with tortuous lateral escape paths, betweens hale-core ridges The flows descendig fromone step to the next. From Smith, 2000.

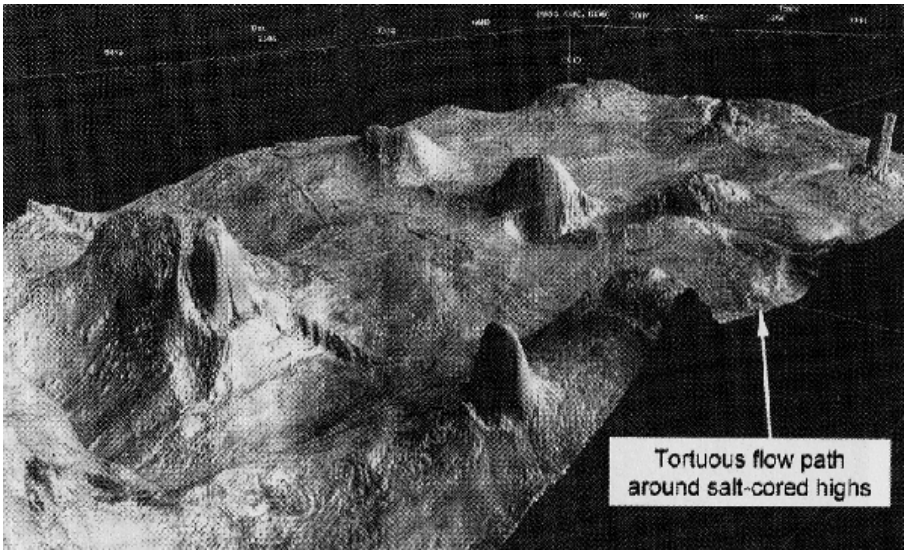

Fig. 9 3D seismic image showing continuity of sediment distribution paths around salt highs. Tortuous flow paths arounds salt.core highs are indicates. From Smith, 2004

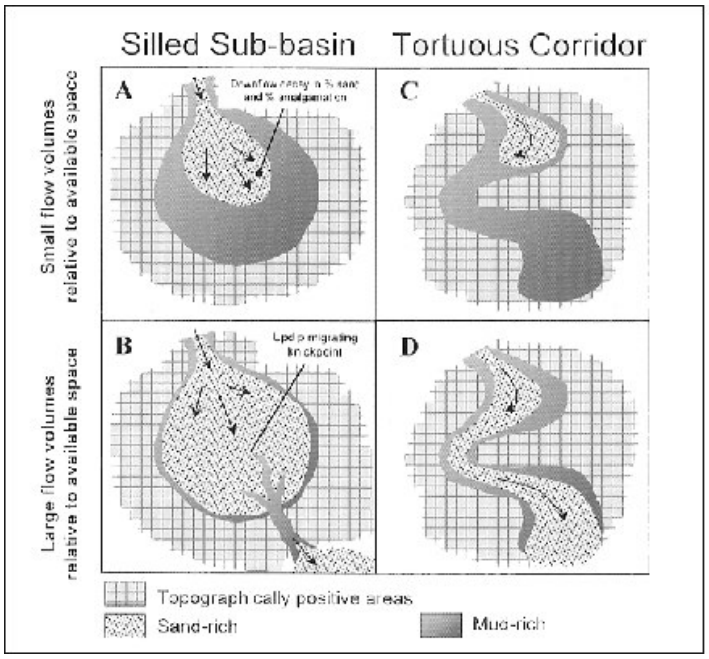

Fig. 10 Schematic diagram showing the silled sub basin case and the connected tortuos corridor case, evidencing the importance of the areal extent of sediment gravity flow relative to the areas of receving basin. A. Silled sub basin with small volme sand-flows relative to the receiving basin. B. Flows large in volume relative to the scale of receiving space. The diagram show the spill to the lower sub-basin with associated incision and bypass sector on the upper slope. C. Connected tortuous corridor in which sand-trasporting flows are small in volume relative to the potential flow path. D. Connected tortuous corridor with large volume flows relative to the potential flow path From Smith, 2004.

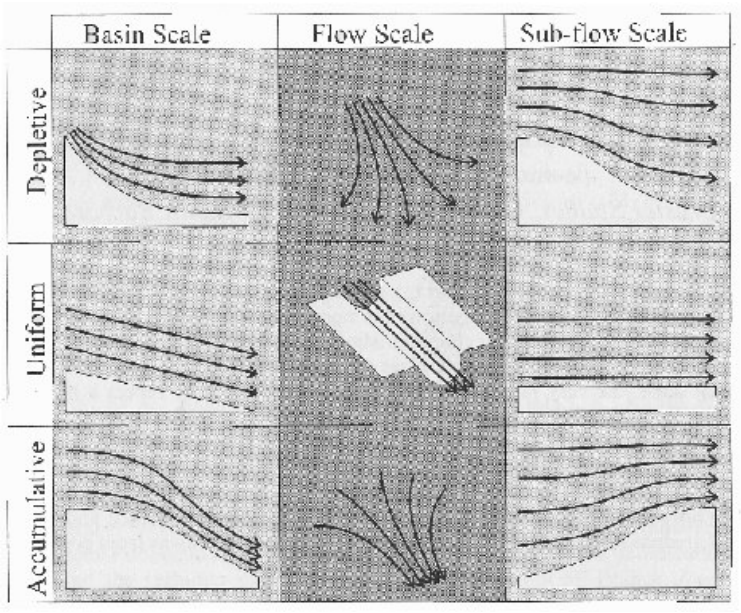

Fig. 11a Situationss producing uniform and non-uniform flow at basinal, flow and sub-flow scales. The diagrams are not to scale, and do not incorporate the effects of entrainment or detrainment of sediment or fluid. From McCaffrey & Kneller, 2004.

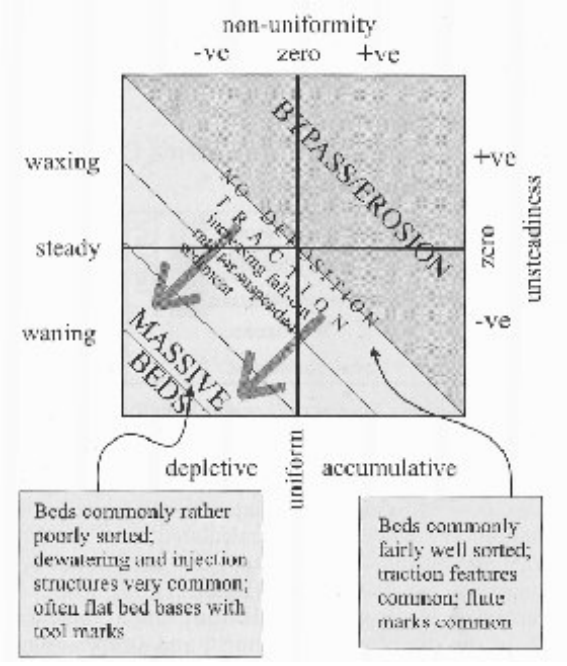

Fig. 11b Schematic graph of flow unsteadiness versus flow non-uniformity. The graph is countured for increasing rates of suspended load fall out rate, with characteristic textures and structures developed at high and low fallout rates detailed. (From Kneller & McCaffrey, 1995).

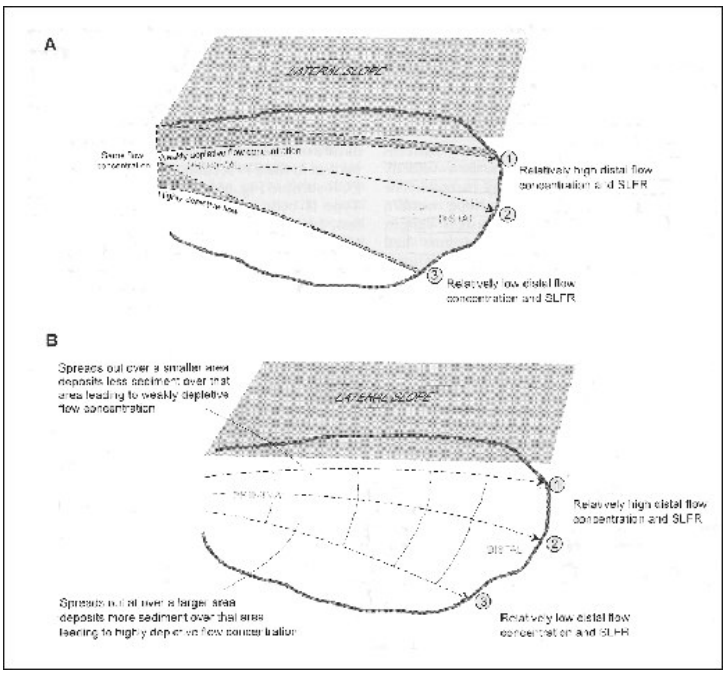

Fig. 12 Diagram showing how a particular flow concentration non-uniformity pattern could lead to relatively high SLFR in medial and distal location. (a) Pattern of variability depletive flow (illustrated by changes in sediment concentration along streamlines 1 and 3); (b) summary of how this pattern may be produces by differences in lateral spreading rates rates within the flow (illustrated by differences in area covered by the flow between streamlines 1-2 and 2-3 as the flow proceeds). From Amy *et.al.,* (2004).

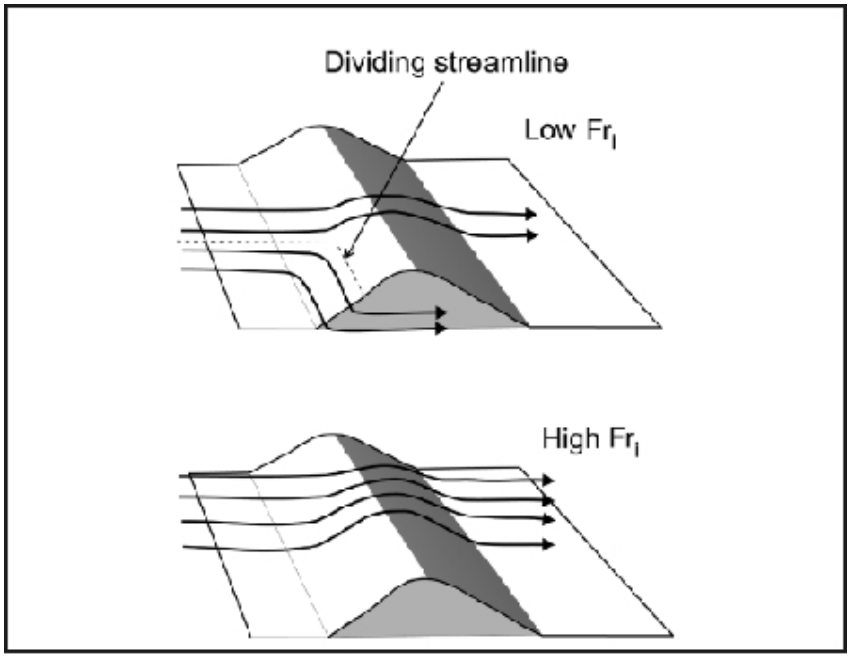

Fig. 13a Effects of internal Froude number (Fri) on behaviour of flows upstream of 3D topography; dividing streamlines forms at low Fr. From Kneller & Buckee, 2000.

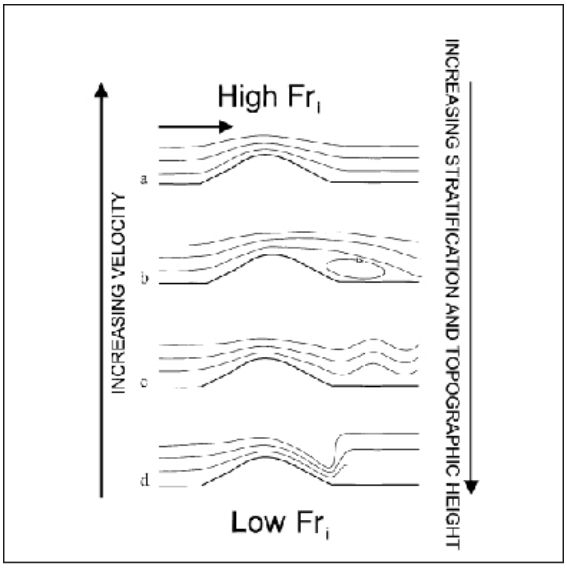

Fig. 13b The effect of the Fri on the behaviour of flows downstream of topography. From Kneller & Buckee, 2000.

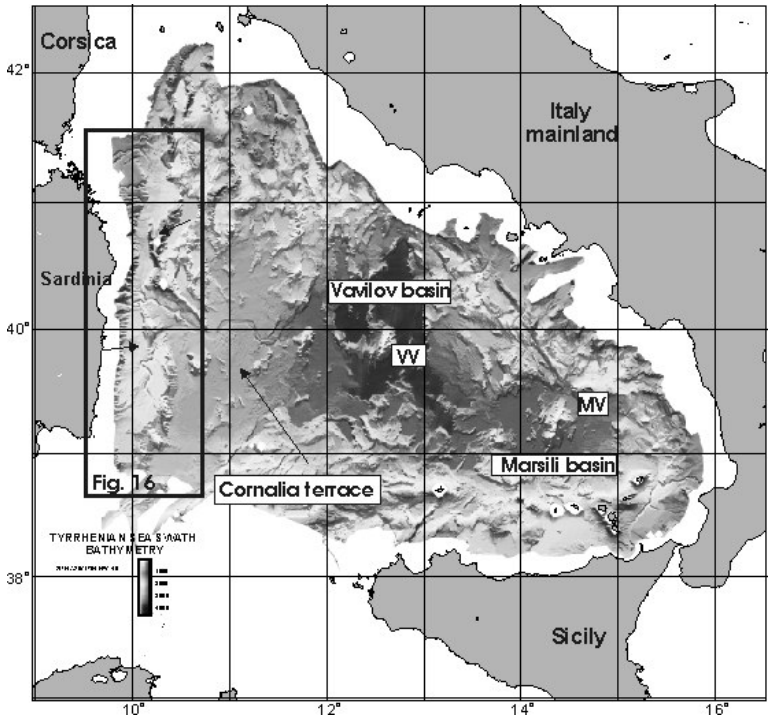

Fig. 14 Shaded relief bathymetric map of the Tyrrhenian sea. Depthes are colour coded, illumination from the NW. The box cover the eastern Sardinian margin, illustrated more in details in fig.163. VV=Vavilov volcano, MV=Marsili Volcano.

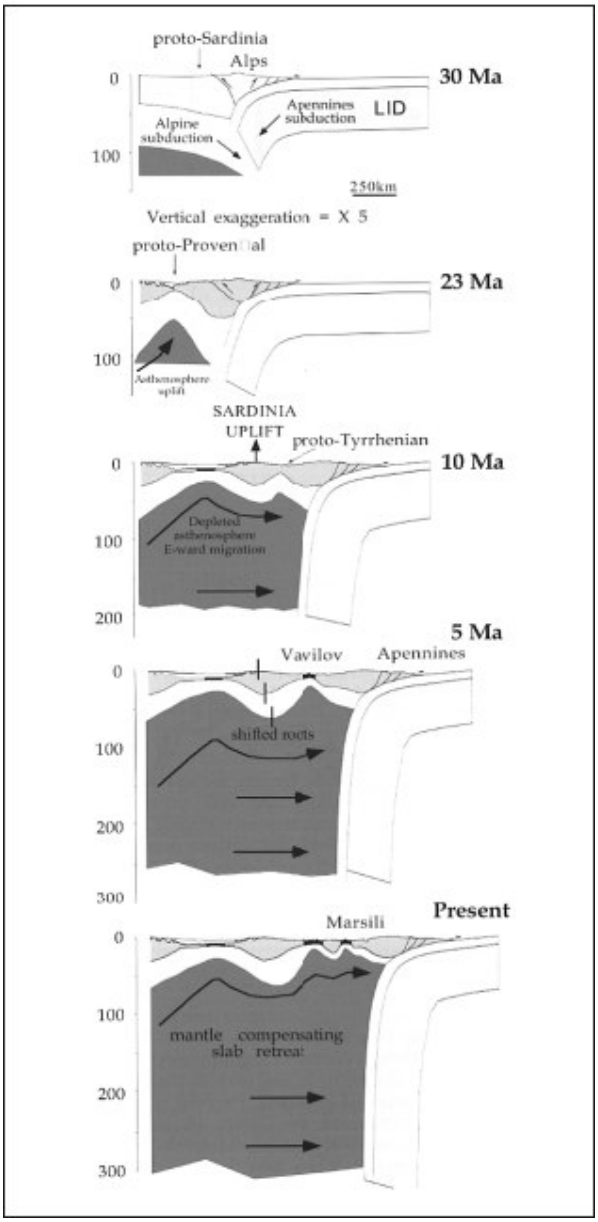

Fig. 15 Slab retreatment and boudinage of the back arc basin in the hangingwall of the Appennine subduction during the last 30 Ma. From Doglioni *et al.,* 2004.

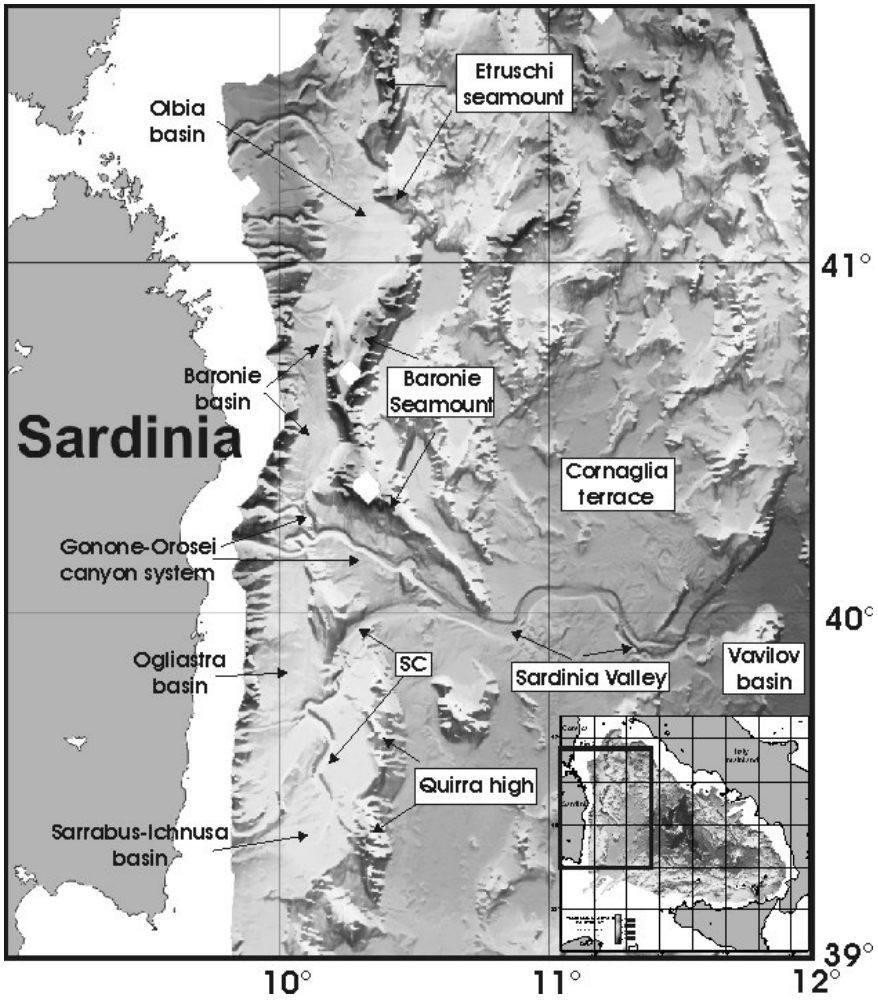

Fig. 16 Shaded reflief map of the eastern Sardinian margin. The main physiographic elements described in the text are indicated. SC= Sarrabus Canyon

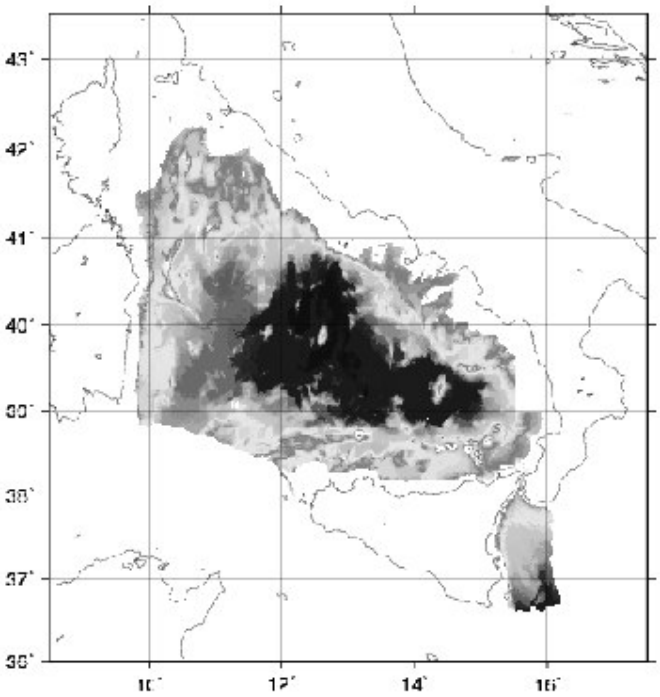

Fig. 17 Shaded relief map of the southern Tyrrhenian basin seafloor.

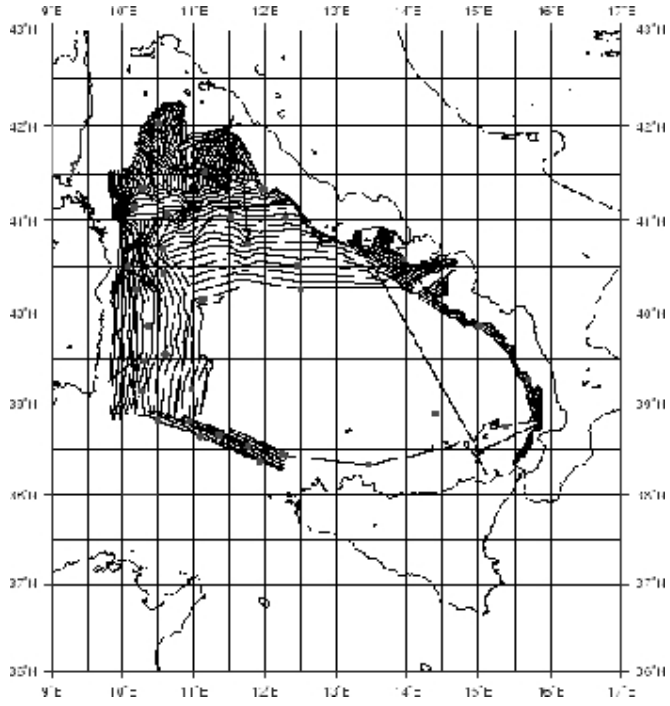

Fig. 18 Navigation lines acquired during cruise TIR99

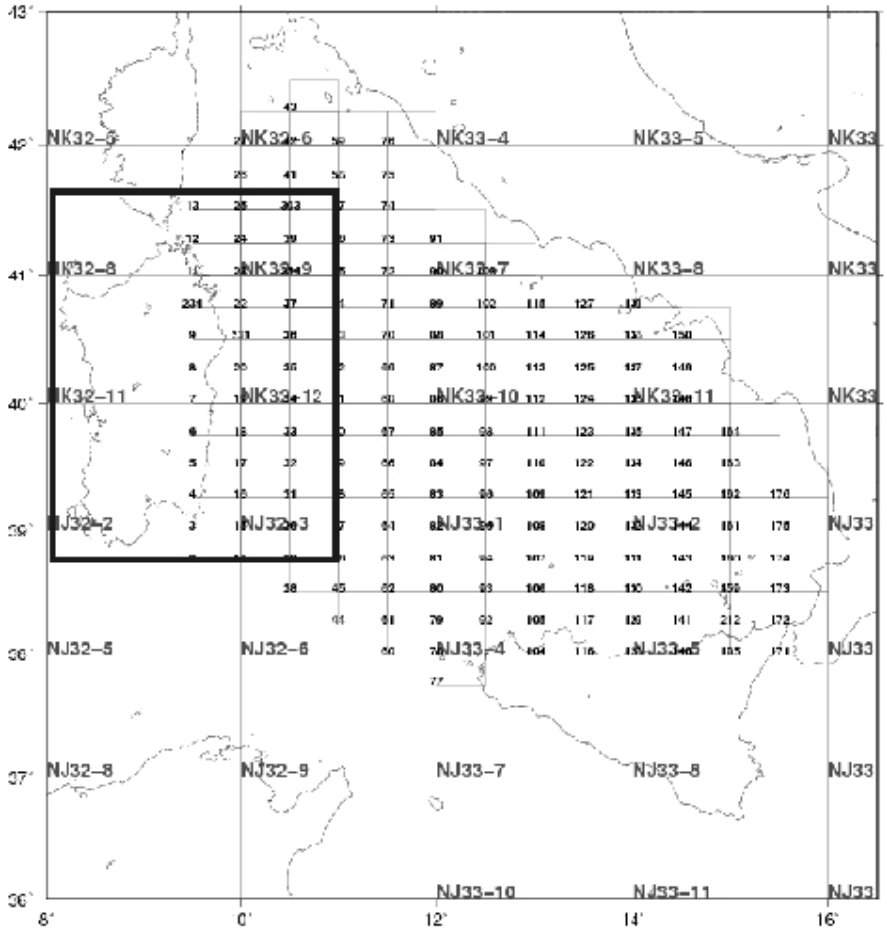

Fig. 19 Subdivision on the survey area for the compilation of the bathymetric maps. The black numbers corresponds to the Kongsberg-Simrad's Neptune blocks. The box represent the sector of the eastern Sardinian margin.

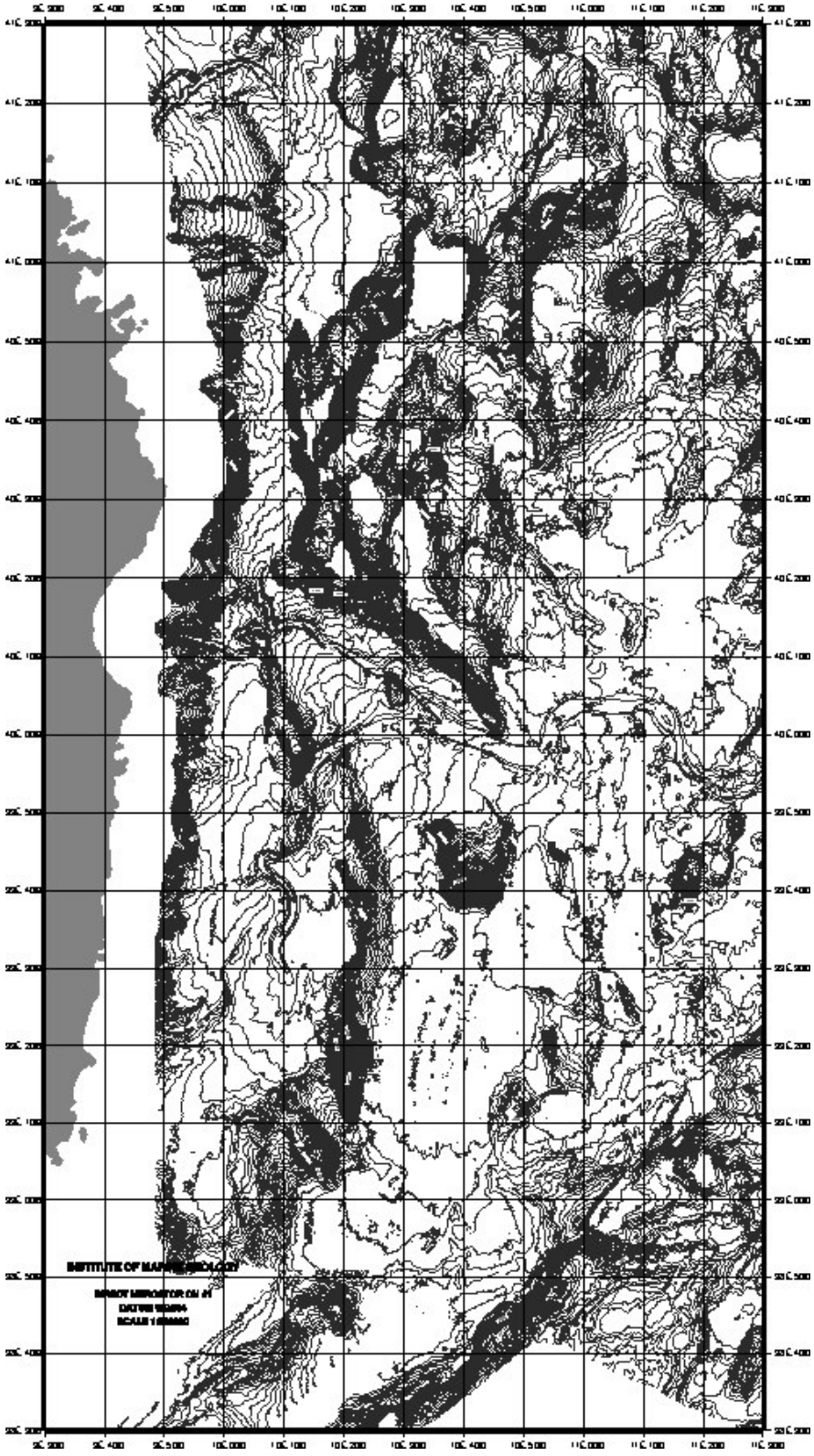

Fig. 20 Multibeam bathymetic map of the eastern Sardinian margin. Contours interval 50 m

Chapter 2

This chapter is presented in form of an article of Fabiano Gamberi and mine **"**The impact of margin-shaping processes on the architecture of the Sardinian and Sicilian margin deep sea depositional systems (Tyrrhenian Sea)" submitted to Society of Economic Paleontologist and Mineralogists Special Pubblication: "External control on deep water depositional systems"

The impact of margin-shaping processes on the architecture of the Sardinian and Sicilian margin deep sea depositional systems (Tyrrhenian Sea)

Fabiano Gamberi[1] and Giacomo Dalla Valle[1,2]
1) Istituto di Scienze Marine, Sezione Geologia Marina di Bologna, Italy
2) Dipartimento di Scienze della Terra, Università di Bologna, Italy

ABSTRACT

The Tyrrhenian Sea was formed through rifting and back-arc extension above the subducting Ionian oceanic slab. Within the basin and in the surrounding regions, extensional processes were diachronous, first affecting the Sardinian margin and then migrating toward the SE in the Sicilian and Calabrian margins and on the western side of the Italian peninsula. Thus, in the Sardinia passive margin the tectonic activity has been quiescent since Early Pliocene whereas, in the Sicilian active margin extensional processes are on going. The resulting different geological setting of the hinterland areas have a large impact on the present-day depositional systems along the two margins. In the Sardinian margin, a relatively large spacing of river entry points to the coastal areas, results in widely spaced slope canyons that thus feed isolated deep sea fans in the intraslope basins. In the Sicilian margin, as a consequence of smaller river drainage basins, canyons are very close in the slope and feed base of slope coalescing sedimentary bodies, thus creating an apron consisting of channel levee deposits. The hinterland geology also influences the nature of the deep sea depositional systems along the single margins. Generally, the small, radial fans of the Sardinian margin face narrow shelf regions and a direct input of coarse grained sediments to the canyon heads can be inferred. The large elongated Caprera fan, on the contrary, forms where the shelf is larger and can efficiently trap much of the coarse grained sediments. In the Sicilian apron, in the areas facing the depressed regions, with smaller uplift rates on land, the Gioia basin channel levee system is actively upbuilding. On the other hand, destructive processes are affecting the Sicilian apron where high uplift rates are affecting the adjacent land areas.

INTRODUCTION

Since the 1970s, the demand of predicting subsurface lithology distribution has driven the formulation of various models linking the architecture of deep-sea depositional systems to the character of the source area (Normark 1974; 1978; Mutti and Johns 1978; Walker 1978). Successively, a completely different perspective was developed with the sequence stratigraphy approach that tied up the development of different facies tracts in deep sea depositional systems with sea level variations (Mitchum, 1977; Vail et al., 1977; Mitchum and Van Wagoner, 1991). A more thorough classification linking deep sea depositional systems to external controls, such as rate, type and source of sediment supply, regional tectonics and sea level fluctuations was presented by Reading, (1991) and successively slightly modified (Reading and Richards, 1994; Richards et al., 1998; Galloway, 1998). In this classification, deep sea fans are single point-source turbidite systems, whereas submarine ramps and aprons are related multiple point-source ones (Richards et al., 1998). Within this large subdivision, the constituent elements and the architecture of the different depositional systems are then further controlled by the sediment caliber that depends on the tectonics, the lithology and the processes that feed sediments to the deep sea (Richards et al., 1998). Nowadays, with the extensive use of 3-D seismic surveys and the onset of seismic geomorphology the complexities of deep sea depositional systems in terms of processes, geomorphic elements, stratigraphic architecture, lithology distribution can be further evaluated (Posamentier and Kolla, 2003; Posamantier, 2005). In turn, the role of external controls in determining the resulting style of deep sea depositional systems can be better defined. Notwithstanding, the seismic geomorphology approach still relies on the scheme of Richards et al., (1998) in linking the style of deep sea depositional systems to external forcing controls (Posamentier and Kolla 2003).

In this paper, we describe how the different geology of the Sardinia and Sicily Islands influences the deep sea depositional style along the corresponding margins leading respectively to base of slope fan and apron development. In addition, we highlight how variations of the geological setting along the single margins can lead to variable processes and architecture within the basic fan and apron depositional styles.

GEOLOGICAL SETTING

The Tyrrhenian Sea was formed through rifting and back-arc extension of the Alpine/Apennine suture above the northwesterly subducting Ionian oceanic slab (Kastens and Mascle, 1990). E-W directed rifting in the northern Tyrrhenian and along the western margin of Sardinia marked the initial opening of the Tyrrhenian sea in the Miocene. During this phase, the Sardinian margin fault-bounded intraslope basins and the oceanic domain of the Vavilov basin were formed (Fig. 1). The subsequent retreat of the subducting slab to its present-day position below the Calabrian arc caused the rifting of the rear of the chain in the southeastern Tyrrhenian Sea and along the Sicilian and Calabrian margins; concomitantly, the Marsili back-arc basin was formed (Fig. 1). Therefore, the Sardinia Island is a passive margin where tectonics has been inactive since Early Pliocene, whereas the Sicily island is an active margin where extensional processes are on going on the rear of the still deforming Appeninic-Maghrebian chain (Sartori, 1990).

EASTERN SARDINIAN MARGIN DEEP SEA DEPOSITIONAL SYSTEMS

Four intraslope basins parallel to the margin and lying at water depth ranging between 1300 m and 1800 m are present in the upper part of eastern Sardinia margin (Fig. 1). To the north, the Olbia and Baronie intraslope basins are bounded seaward by the Etruschi and Baronie seamounts (Fig. 2a). To the south, the Quirra tectonic lineament marks the limit between the Ogliastra and Sarrabus intraslope Basins and the Cornaglia terrace (Figs. 1, 2b). The Gonone-Orosei Canyon system separates the southern from the northern intraslope basins (Fig. 1, 2a, 2b). It is a large submarine valley that cuts the entire upper Sardinian margin with a NW-SE trend and, joining the Sarrabus Canyon at a depth of about 2600 m, gives rise to the Sardinia valley that reaches the Vavilov basin plain (Fig. 1).

The Olbia intraslope basin

The Olbia intraslope basin is the northernmost basin of the Sardinian margin and is bounded seaward by the Etruschi and Baronie seamounts (Fig. 2a). It is flanked by a 25 km large shelf, narrowing southward, and by a 20 km wide continental slope with an average dip of around 2° (Fig. 2a). A detailed bathymetric map of the Caprera,

the largest turbidite system of the Olbia basin, is shown in Fig. 3. It is fed by two tributary canyons that join in a single canyon further downslope (Fig. 3). At the base of slope, the canyon evolves into an elongated fan centred by a 2 km wide leveed channel (Figs. 3, 4). The levee asymmetry (Fig. 3), reflects the flow confinement due to the basin geometry. Besides deposition within the Caprera deep sea fan, channelized bodies are also present in the slope (Fig. 5). To the south of the Caprera system, the low sinuosity, E-W trending Mortorio, Tavolara, and Molara canyons dissect the slope of the Olbia basin (Fig. 2a). Small, unconfined, radial, base of slope fans are developed at the mouth of the canyons, with low relief channels running on the upper fan sectors (Fig. 6).

The Baronie intraslope basin

The Baronie Basin is around 10 km wide and 55 km long, and is bounded seaward by the up to 1300 m high Baronie seamount (Figs. 1; 2a). The shelf is around 13 km wide, with minimum values in correspondence with the Posada canyons (Fig. 2a). The continental slope is steep, averaging a dip of around 13° (Figs. 2a, 7). With the exception of the Posada canyon and the Gonone-Orosei canyon system, located respectively at the northern and southern limit of the basin, the Baronie slope is completely devoid of canyons (fig. 2a).

The Posada turbidite system is the main system of the Baronie basin (Figs. 2a, 7). It is fed by the homonymous river that develops a small submarine delta in front of the Posada canyon (Fig. 2a). The Posada canyon is deeply incised both in the shelf and the slope, with steep walls scoured by linear chutes and slumps scars (Fig. 7). At the base of slope, the Posada canyon results in a 10 km radius fan, confined by the Baronie seamount to the east. A low sinuosity, single channel runs in the south-western sector of the fan (Fig. 7). Further downslope, beyond 1400 m in depth, the single channel evolves into a series of straight, low relief channels spanning the entire width of the basin plain (Fig. 7). A seismic line (Fig. 8) shows that the depositional style of this portion of the basin consists of a network of distributary channels, and mass transport deposit.

The Gonone-Orosei canyon system

The submarine sector in the front of the Gulf of Orosei, is dominated by the Gonone-Orosei canyon system (Figs. 1, 2b, 9) . In this area the shelf is almost absent, with the heads of the canyon system, located only 1 km from the coastline (Figs. 2b). The continental slope is steep, with an upper sector dipping at around 5° and a lower sector dipping at about 13°. In the upper slope, the canyon system consists of the Ginepro, the Gonone and the Orosei canyons that span a 20 km wide margin sector (Fig. 9). At the base of slope, a 9 km long levee is developed on the right side of the Gonone canyon; in addition, depositional features also form sideways from the Ginepro and Orosei canyons (Fig. 9). At around 2000 m depth, the canyons join into one single element, the Orosei-Gonone Canyon, that runs parallel to the flank of the Baronie seamount for a length of around 50 km (Figs. 1, 2b).

*The Ogliastra and the Sarrabus intraslope basin***.**

The Ogliastra and the Sarrabus intraslope basins are located south of the Gonone-Orosei canyon system and are separated by the S.Lorenzo high and the Sarrabus canyon (Fig. 2b). The shelf has an average width of only 7 km, with minimum values of 3.5 km (Fig. 2b). The continental slope of the basin narrows southward, with an increase of the steepness, from 4° in the northern sector, to an average degree of 17° south of the Arbatax fan (Fig. 2b).

The Arbatax and the Pelau canyons develop radial, base of slope fans (Fig. 2b). The Arbatax fan occupies much of the Ogliastra basin with its distal portions adjacent to the Quirra high. The proximal part of the fan is scoured by a single, up to 100 m deep meandering channel that converges downslope in the Sarrabus canyon (Fig. 2b). A similar morphology characterizes the Pelau fan that is distinctive only in having a rectilinear planform of the channel that reaches the Sarrabus canyon (Fig. 2b). The Sarrabus canyon is the main erosive feature of the Ogliastra-Sarrabus basin, that runs along the axis of the basin, crosses the Quirra high in a relay ramp zone, and joins with the Gonone-Orosei to form the Valley of Sardinia (Fig.1).

NORTHEASTERN SICILIAN MARGIN

The northeastern Sicilian margin consists of the Capo d'Orlando and Gioia intraslope basins. They are separated by a structural ridge that connects the Sicilian margin to the volcanic high of the Aeolian Island arc (Fig.10). The Capo d'Orlando basin is completely silled seaward by the Aeolian Island arc, whereas the Gioia Basin is connected through the Stromboli axial valley to a deeper base level. The Gioia Basin spans the easternmost part of the Sicilian margin and part of the Calabrian one. A description of the geology of the whole Gioia Basin has been presented by Gamberi and Marani, (in press); here we focus exclusively on the Sicilian portion of the basin.

Gioia Basin

In the western part of the Gioia Basin a channel levee system is present spanning a 20 km long stretch of the margin (Figs. 11, 12). It consists of the channel fill and overbank deposits of the Milazzo, Niceto and Mele channels with the thickness diminishing eastwards (Fig. 12). The channels develop at the base of slope and are fed by deeply incised slope canyons. The Milazzo and the Niceto channels join at a depth of about 1100 m in the upper reach of the Stromboli valley (Fig. 11); on the contrary, the Mele channel dies out at a depth of about 1100 m giving way downslope to unconfined flow deposits (Figs 11, 13). Sediment waves are present in the crest of the right levee of the Niceto channel (Fig. 11) that is the major site of recent sediment deposition (Fig. 12). Deformation and mass wasting processes in the levee are infrequent and only evident as slump scars in the distal outer flank of the right levee of the Niceto channel and in the inner side of the right levee of the Milazzo channel (Fig. 11).

In the eastern portion of the Gioia Basin, 500 m wide gullies with relief in the order of 20-30 m are spaced at 2-3 km (Fig. 11). The main salient features of this portion of the Gioia basin are multiple scars that with different shapes, relief and lateral extents cut the slope and the base of slope seafloor particularly close to the Acquarone structural high (Fig. 11). They correspond with the failure surfaces of the Villafranca mass transport deposit that has a lateral width of about 10 km and occupies the entire basin down to the axial Stromboli valley (Fig. 11). The crosscutting relationships of the scars point to multiple failure events eventually

leading to a 300 m thick chaotic body (Figs. 12, 14). As a matter of fact, in the central part of the Villafranca mass transport deposit, a surficial mound with a positive relief of about 20 m that corresponds with the deposit of a single failure event is present (Fig. 11).

Capo d'Orlando Basin

The Capo d'Orlando basin is about 70 km long and 50 km wide being bounded to the east and to the north by the Aeolian Island arc volcanoes and to the west by a fault-bounded basement high (Figs. 11, 15). In the eastern part of the basin the slope is cut by 1 km large canyons spaced at intervals varying between 2 and 3 km. They die out at the base of slope without forming any sedimentary body with enough relief to be recognized in the bathymetric data (Fig. 10). A different setting characterizes the base of slope in the central part of the Capo d'Orlando Basin where two distinct bulges of channel levee deposits are evident (Fig. 11). A detailed bathymetric map of the western channel levee system is shown in Fig. 15; three main channels are responsible for deposition in the area. The westernmost channel is about 3 km wide and runs with a westward trend at the base of slope, thus developing a levee only in its right side away from the slope. Two smaller channels are developed further east and they are free to run in a NW direction until they die out at a depth of about 1400 m at the transition with the flat basin plain (Fig. 15). The main characteristic of the Capo D'Orlando depositional system is the high degree of deformation and mass wasting processes that affect the channel levee deposits. Scars with elongated or amphitheater planform are in fact ubiquitous on the channel flanks and on the levees (Fig. 15). The scars are as high as 100 m and correspond with the boundary of displaced levee blocks with a lateral size of about 6 km^2. The fill of the channel often consists of chaotic seismic units that can represent the product of levee degradation; a similar seismic facies is also developed on the surface of the levees (Fig. 16). In some cases the removal areas of the outer levees are faced downslope by lobe-shaped features with positive relief that are the depositional bodies associated with levee destruction (Fig. 15). A transition to more continuous seismic reflections, indicative of basin-wide depositional units is present further downslope in the flat portion of the basin plain (Fig. 17).

DISCUSSION

The eastern Sardinian margin is a passive margin where extensional tectonics has been quiescent since Early Pliocene and is in general characterized by minor rates of vertical movements (Antonioli, 1999, Ferranti et al., 2006). In the northern and southern part of the Sardinia Island, rivers have relatively large drainage basins; smaller drainage basins characterize, on the contrary, the central region of the Island (Figs., 2a, 2b). Furthermore, a wide shelf is present along much of the eastern Sardinian margin and in the northern area reaches a width of about 20 km (Fig. 2a). As a consequence of the wide spacing of the river entry points, the depositional systems of the Sardinia margin consist of deep sea fans fed by canyons (Figs 1, 2a, 2b). In the northern slope, not all of the major canyons of the Caprera, Mortorio, Tavolara and Molara systems are however directly linked, at the present-time, to the two major river entry points (Liscia and Padrogiano rivers in Fig. 2a). The considerable width of the shelf in this portion of the margin (around 20 km) could be responsible for the shifting of the direct river sediment discharge in the upper slope during different eustatic sea level low stands; consequently the formation of new canyons can be promoted. Actually, the Caprera and the Tavolara canyon systems are made up of upper slope tributaries that join into single conduits in the lower slope (Figs., 2a, 3).

The largest fan of the Sardinia margin is the Caprera one that is the unique system characterized by an elongated fan with a 20 km long leveed channel sector (Figs. 3, 4). The Mortorio, Tavolara, Posada, Arbatax and Pelau fans, are on the contrary, characterized by a radial planform and by a very short leveed valley sector if any (Figs, 2b, 6, 7). The morphology of the Caprera system, similar to mud-rich elongated fans (Richards et al., 1998) can be controlled by the width of the surrounding shelf that can act as a trap for the coarser grained sediments. In the remaining deep sea fans a direct connection of the systems with short, small drainage basin streams results in morphologies akin to coarse grained systems (Richards et al., 1998).

As wells as the external controls, the steepness of the slope is also important in controlling the evolution of the Sardinian margin deep sea depositional systems. In fact, where mass wasting processes affect the steeper slope sectors they also have

impact on the depositional processes of the Posada fan with mass transport deposits that interfinger with the general pattern of channelized deposits. (Fig. 7).

The large Gonone-Orosei canyon system is present in the central part of the Sardinia margin, where no large rivers are present (Figs, 2a, 2b, 9). Its origin is probably connected with instability processes following the uplift of the region because of recent volcanic activity (Carobene, 1978; Lustrino *et al.,* 2002). The width of the system that is composed of three tributaries can be further controlled by the important modification on the morphology and the hydrography on the costal sector of the Gulf of Orosei (Carobene, 1978; Borsetti et al., 1979). The large sediment input to the canyon system due to slope instability processes can in addition be responsible for the development, at the base of slope, of leveed tracts of the system in the absence of large external sediment supply (Fig. 9).

The Calabrian and the Sicilian margins lie above the Ionian subducting plate and as a consequence of the evolution of the convergent zone, the whole area is affected by very high uplift rates. Hence, for the last 0.6 m.y. an uplift in the order of 1m/1000years has been documented for the coastal area of Sicily and southern Calabria (Westaway, 1993). Uplift is also affecting regions that before the middle Pleistocene were sites of subsidence and coastal basin filling resulting in the exhumation of recent sedimentary units along the coastal areas of Sicily and Calabria (Fig. 10) (Ciaranfi et al. 1983).

On land, in the Castanea, Naso and S'Agata structural ridges, the high uplift rate has resulted in the exposure of the Calabride rocks following the erosion of their clastic coverage (Stilo, Capo d'Orlando flysch) that it is still preserved in the surrounding depressed areas. Miocene, Pliocene and Quaternary deposits are present in the extensional Barcellona depression. A network of parallel, intermittent discharge, mountainous rivers run perpendicular to the margin in the tectonically depressed areas and enter the coastal region at intervals of less than 10 km (Fig 10). In addition, along the entire northeastern Sicilian margin the shelf is very narrow (Fig. 10). On the slope, canyon face most of the river entry points; in general, the canyons are followed downslope by leveed channels (Figs., 10, 11, 15). At the base of slope, an apron consisting of laterally coalescing deposits of leveed channels is formed (Figs., 10, 11, 15). However, in the eastern part of the margin, where the rivers have very small drainage basins and the rate of uplift is high, a destructional apron consisting of the Villafranca mass transport deposit is present (Figs., 11, 12, 14).

In more detail, different present-day processes characterize the channel levee deposits along the different reaches of the margin. Active levee construction characterizes the Gioia basin system that faces the depressed area of the Barcellona depression (Figs. 11, 12, 13). Destructional processes are on the contrary affecting the channel levee system in the Capo d'Orlando basin (Figs. 15,16, 17). They can be related to the recent reorganization of the margin and a consequent change in the sedimentary regime connected with the recent uplift of the Naso ridge where Late Pleistocene marine deposits are presently found at an elevation of around 500 m (Fig. 10).

CONCLUSIONS

1) The geology of the hinterland is the main control on the basic characteristics of the Sicilian and Sardinian margin depositional systems. In the tectonically dormant Sardinian passive margin, relatively large river drainage basins result in a wide spacing of the major river entry points to the coastal areas. As a consequence, in the upper slope, widely spaced canyons form and feed isolated deep sea fans at the base of slope. In the tectonically active Sicilian margin, rivers have small drainage basins; accordingly, closely spaced canyons form in the slope and evolve downslope into channels that originate an apron consisting of interfingering channel levee deposits.
2) The width, shape and the constituent elements of the deep sea fans of the Sardinian margin are controlled by the nature of the canyon feeding systems. The Caprera turbidite system with an elongated shape and a long leveed channel sector faces a wide shelf area that can store much of the coarse grained sediments. On the contrary, where the shelf is narrow, due to the possibility of a more direct input of coarse grained material from the coastal area to the proximal part of the canyons, radial fans with short leveed channels form.
3) In the areas with the largest shelf of the Sardinian margin, a shift from deep sea fan to upper slope deposition is recognized. A possible influence of eustatic variations in controlling the main site of deposition during different sea level stands can be envisaged.

4) In general, the canyons that are not connected with major river entry points do not feed large depositional bodies at the base of slope. However, leveed channels ensue from the Gonone-Orosei canyon system that is not fed by major rivers. In this case, a large amount of sediments is available to the system due to slope instability processes and mass wasting caused by the recent uplift of the area connected with recent volcanism.
5) Vertical movements influence the development of the Sicilian margin apron. The eastern part of the Gioia basin, facing an area with large uplift rates, is in fact the site of a destructional apron consisting of the Villafranca mass transport deposits.
6) Vertical movements and the possible reorganization of onland drainage basins control the evolution of the channel levee system in the Sicilian apron. The Gioia basin upbuilding channel levee system faces a depressed area with a relatively low uplift rate. On the contrary, the Capo d'Orlando channel levee system faces an area with large uplift rates and is mainly affected by destructional processes.

FIGURE CAPTIONS

Fig. 1. Shaded relief map of the Tyrrhenian Sea from multibeam bathymetric data. The Sardinian margin is composed of intraslope basins lying at water depth between 1300 and 1800 m that are separated by structural highs from the Cornaglia terrace at a depth of 3000 m. The Gonone-Orosei canyon system separates the northern from the southern intraslope basins of the Sardinian margin. The Capo d'Orlando and the Gioia Basins straddle the northeastern Sicilian margin. The Capo D'Orlando basin is completely silled seaward by the Aeolian Island Arc, whereas the Gioia Basin is connected through the Stromboli valley to the Marsili deep sea fan. The boxes correspond with the detailed bathymetric map of Figs. 2a, 2b and 10.

Fig. 2. Multibeam bathymetric maps of the northern (a) and the southern (b) sectors of the eastern Sardinian margin (contour interval 50 m; location in Fig. 1). The intraslope basins, seamounts and the main turbidite systems are indicated. The shelf break (dashed line) is taken from Bellagamba *et al.,* (1979), whereas the location of the submarine deltas is from Ulzega et al., (1987). The map of the Sardinia Island with a schematic lithological subdivision has been simplified from Ulzega et al., (1987). The river drainage basins are also indicated with a solid black line.

Fig. 3. Multibeam bathymetric map of the Caprera turbidite system in the Olbia basin (contour interval 20 m; location in Fig. 2a). Two tributary canyons with a length of around 16 km, join into the Caprera canyon that is around 9 km long, and has initially a SW-NE trend and subsequently turns toward the SE. The Caprera fan leveed channel is around 20 km long, with levees that span almost the entire width of the basin. A low relief overbanking channel run on the left levee, forming a small lobe at its mouth. In the distal sector of the slope, scars and headless chutes are present evidencing seafloor instability. The dashed lines are the traces of the seismic profiles of Figs. 4 and 5.

Fig. 4. Strike airgun seismic profile of the leveed channel sector of the Caprera turbidite system (location in Fig. 3). Discontinuous high amplitude reflections make up the channel fill; the seismic facies of the levee consists of continuous and parallel

reflections but thin horizons of mass transport deposits are highlighted by transparent seismic packages. The surrounding slopes are affected by seafloor instability; in particular, a glide plane is evident in the Sardinian slope.

Fig. 5 Dip Sparker profile over the slope of the Olbia basin south of the Caprera Canyon (see fig. 3 for the location of the profile). In the upper slope, wedge-shaped seismic units with discontinuous reflections and sometimes v-shaped erosional surfaces can be interpreted as buried channelised depositional elements. The lower, steepest slope sector is, on the contrary characterized by erosional and by pass processes.

Fig. 6 Multibeam bathymetric map of the Mortorio and Tavolara turbidite systems (contour interval 20 m). The canyons feed isolated deep sea fans with a radial planform and a width between 5 and 7 km. The fans are characterized by very short sector with a single leveed chanel. Scallop-like slump scars are present in the Tavolara canyon walls.

Fig. 7 Multibeam bathymetric map of the Posada turbidite system in the Baronie basin (contour interval 20 m; location in Fig. 2a). A sharp, rectilinear slide scars in the southwestern portion of the fan, interrupts the Posada channel pathway. An around 15 km wide network of headwall scarps is present on the basin slope. The distal eastern portion of the Posada fan reaches the slope of the Baronie seamount, that concomitantly is affected by mass movement processes.

Fig. 8 Strike Sparker seismic profile of the Posada turbidite system (location in Fig. 2a). The steep continental slope is characterized by small offset extensional faults, and is affected by active slumping. A mass transport deposit (MTD) is buried below the actual Posada fan. The distributary channels of the Posada system are visible both at the seafloor and in the subsurface. Despite the thin sedimentary cover, sliding processes also affect the Baronie seamount slope.

Fig. 9 Multibeam bathymetric map of the proximal sector of the Gonone-Orosei canyon system (contour interval 20 m; location in Fig. 2b and 2b). The walls of the

canyons that make up the system are strongly affected by mass wasting processes; in addition slide scars are present in the surrounding slope sector.

Fig. 10. Bathymetric map from multibeam data of the Gioia and the Capo d'Orlando Basins in the northeastern Sicilian margin (contour interval 100 m; location in Fig. 1). The Capo d'Orlando is a completely silled basin bounded seaward by the volcanic slope of the Aeolian Islans arc. On the Contrary, the Stromboli slope valley connects the Gioia Basin to a deeper base level, ultimately feeding the Marsili deep sea fan (see Fig. 1). A channel levee system spans much of the Capo d'Orlando basin as evidenced by a positive bulge at the base of slope (see detailed bathymetric map of Fig. 15). A channel levee system is present also in the western part of the Gioia Basin. On the contrary, the Villafranca mass transport deposit corresponding with a re-entrant in the bathymetric contour characterizes the eastern part of the Gioia basin (see detailed bathymetric map of Fig. 11). On land, the metamorphic rocks of the Cabride units outcrop in the structural elevated areas. Tortonian to Quaternary clastic deposits are present in the uplifted the coastal basins of the Barcellona depression. Pleistocene deposits are also present in the Naso rige at an elevation of about 500 m. The boxes correspond with the detailed bathymetric maps of respectively the Gioia (Fig. 12) and the Cefaù Basin (Fig. 15).

Fig. 11. Bathymetric map of the Gioia Basin (contour interval 10 m). The Milazzo, Niceto and Mele channels originate a channel levee system that spans the western portion of the margin for a length of about 20 km. Note that at the mouth of the Mele channel an area with downslope convex contours is developed that can represents the site of deposition of unconfined flows at the exit of the channel. Sediment waves are develeopd on the right levee of the Niceto channel; they have a relief up to 50 m a wavelength of about. The eastern side of the basin is characterized by a reentrant bounded eastward by the Acquarone high. Here, the slope is steeper and is characterized by small gullies and by numerous scars. It corresponds with area of removal of sediments involved in the Villafranca mass transport deposits that has a width of about 10 km and span the whole margin down to the Stromboli axial Valley.

Fig. 12. Sparker Strike section over the Gioia Basin (location in Fig. 11) showing the channel levee system and the Villafranca mass transport deposit. The pattern of HARs of the Mele channel infill highlight that a migration toward the west has occurred through time. Beside the fill of the active channels, an abandoned channel fill is evident. The Villafranca mass transport deposits is characterized by a mainly chaotic seismic facies; however, some portions with coherent reflections point to the presence of undisrupted blocks embedded within the deformed body.

Fig. 13. Sparker dip section over the Gioia basin channel levee systems. In particular the line cuts the Mele channel showing a complex interfingering of the channel fill discontinuous reflections and the levee deposits. In the distal part of the line, reflections are more continuous and represent the interfingering of unconfined flow deposit at the mouth of the Mele channel and overbank flow deposits from the Stromboli slope valley.

Fig. 14. Dip section over the Gioia Basin illustrating the Villafranca mass transport deposits involving about 300 m of sediments. In the upper slope, the scar surfaces along with the evacuation of the sediments has occurred are evident. Note the apart from the proximal part where coherent reflections evidence undisrupted blocks, the Villafranca mass transport deposit has generally a chaotic seismic facies. It is generally characterized by a rough seafloor (see Fig. 11) and pressure ridges are developed where the deposits has moved past a basement high.

Fig. 15. Bathymetric map from multibeam bathymetric data of part of the CapoD'Orlando Basin (contour interval 10 m). Two distict bulges of channel levee deposits are evident at the base of slope. The western largest one is formed by the coalescing of the channel fill and levee deposits of multiple channels. The eastern one on the contary is formed by a single channel fill and related overbank levee deposits. Some of the channels are flanked downslope by lobes in the form of depositional bodies with mounded geometry. The salient feature of the Capo D'Orlando channel levee system is the high degree of degradation of the levees. Scars corresponding with the surfaces along which levee material has slid down the system are in fact ubiquitous. A structural control is evident with the western

channel that runs at the base of the slope and can develop a levee only in its right side.

Fig. 16 Dip Sparker seismic line over the western channel levee system of the Capo d'Orlando Basin (see location in Fig. 15). The flanks of the channels are affected by mass wasting processes as evidenced by evacuation surfaces (ES); areas of sediment removal (ES) are also observable in the distal part of the levee deposits. Mass transport deposits (MTD) with a chaotic to transparent seismic facies make up much of the channel infill, the recentmost coverage of the distal levee and the proximal part of the flat basin plain.

Fig. 17. Seismic sparker profile over the western channel levee system of the Capo d'Orlando (see location in Fig. 15). The lobe deposit at the mouth of the westernmost channel (see the bathymetric map of Fig. 15) mainly consists of a stack of seismic units with chaotic facies corresponding to mass transport deposits originated by the widespread processes of levee degradation. A more continuous pattern of seismic reflection, typical of sheet-like deposits characterizes the surrounding basin plain.

REFERENCES

ANTONIOLI, F., SILENZI, S., VITTORI, E., AND VILLANI, C., 1999, Sea level changes and tectonic mobility: precise measurements in three coastlines of Italy considered stable during last 125 Ky: Physic Chemistry of Earth (A), v. 24, p. 337-342.

BELLAGAMBA, M., NAPOLEONE, G., AND TRAMONTANA, M., 1979, Batimetria e morfologia delle aree settentrionale e centro-meridionale del bacino della Sardegna (Mar Tirreno): Atti del convegno scientifico nazionale, Progetto Finalizzato Oceanografia e Fondi marini, Roma, v. 2, p. 739- 751.

BORSETTI A. M., CURZI, P., DEL MONTE, M., FABBRI, A., NANNI, T., AND SAVELLI, C.., 1979 Ricerche geologiche nel bacino della Sardegna (Mar Tirreno): Atti del convegno scientifico nazionale, Progetto Finalizzato Oceanografia e Fondi marini, v. 2, p. 769-784.

CAROBENE, L., 1978, Valutazioni di movimenti recenti mediante ricerche morfologiche su falesie e grotte marine del Golfo di Orosei: Memorie della Società Geologica Italiana, v. 19, p. 641-649.

CIARANFI., N., GHISETTI, F., GUIDA, M., IACCARINO, G., LAMBIASE, S., PIERI, P., RAPISARDI, L., RICCHETTI, G., TORRE M., TORTORICI, L., AND VEZZANI, L., 1983: Carta neotettonica dell'Italia meridionale: Pubblicazione 515, Progetto Finalizzato Geodinamica, Bari.

FERRANTI, L., ANTONIOLI, F., MAUZ, B. AMOROSI, A., DAI PRA, G., MASTRONUZZI, G., MONACO, C., ORRU, P., PAPPALARDO, M., ULRICH, R., RENDA, P., ROMANO, P., SANSO, P., AND VERRUBBI, V., 2006 Markers of the last interglacial sea-level high stand along the coast of Italy: tectonics implication: Quaternary International, v. 145-146, p. 30-54.

GALLOWAY, W. E., 1998, Siliciclastic slope and base-of-slope depositional systems: component facies, stratigraphic architecture, and classification: Tulsa, American Association of Petroleum Geologists Bullettin, v. 82, no.4, p. 569-595.

KASTENS, K. AND MASCLE, J., 1990, The geological evolution of the Tyrrhenian Sea: an introduction to the scientific results of ODP Leg 107, *in* Kastens, K.A. and Mascle, J., et al., eds., Proceeding of ODP, Scientific. Results, v. 107, p. 3-26.

LUSTRINO, M., MELLUSO, L., AND MORRA,V., 2002 The transition from alkaline to tholeiitic magmas: a case study from the Orosei-Dorgali Pliocene volcanic district (NE Sardinia, Italy): Lithos, v. 63, p. 83-113.

MITCHUM, R.M., 1977, Seismic stratigraphy and global changes of sea level, Part 1: Glossary of terms used in seismic stratigraphy, *in* Payton, C.E., ed., Seismic Stratigraphy – Applications to Hydrocarbon Exploration: Tulsa, American Association of Petroleum Geologists Memoir 26, p.205-212.

MITCHUM, R. M. AND VAN WAGONER, J.C., 1991, High-frequency sequences and their stacking patterns: sequence stratigraphy evidence of high-frequency eustatic cycles: Sedimentary Geology, v. 70, p. 131-160.

MUTTI, E. AND JOHNS, D.R., 1978, The role of sedimentary bypassing in the genesis of fan fringe and basin plain turbidities in the Hecho Group system (south-central Pyrenees): Memorie della Societa Geologica Italiana, v. 18, p. 15-22.

NORMARK, W.R., 1974, Submarine canyons and fan valleys affecting growth patterns of deep sea fans, *in* Dott jr R.H., Shaver, R.H., eds., Modern and ancient geosynclinal sedimentation: Society of Economic Paleontologists and Mineralogists Special Publications, v.19, p. 55-68.

NORMARK, W.R., 1978, Fan valleys, channels and depositional lobes on modern submarine fans: characters for the recognition of sandy turbidite environments: Tulsa, American Association of . Petroleum Geologists, v. 62, p. 912-931.

POSAMENTIER, H. W., AND KOLLA, V., 2003, Seismic geomorphology and stratigraphy of depositional elements in deepwater settings: Journal of Sedimentary Research, v. 73, p. 367-388.

POSAMENITER, H. W., 2005, Application of 3D seismic visualization techniques for seismic stratigraphy, seismic geomorphology and depositional systems analysis: example from fluvial to deep-marine depositional environments, *in* Dorè, A.G. and Vining, B.A., eds., Petroleum geology: north-western Europe and global perspectives: Proceeding of the 6th petroleum geology conference, p. 1565-1576.

READING, H.G., 1991, The classification of deep-sea depositional system by sediment calibre and feeder system: Journal of Geological Society of London, v. 148, p. 427-430.

READING, H.G., AND RICHARDS, M.T., 1994, The classification of deep-water siliciclastic depositional systems by grain size and feeder systems: American Associations of Petroleum. Geologists, v. 78, p. 792-822.

RICHARDS, M., BOWMAN, M,. AND READING, H., 1998 Submarine-fan systems I: characterization and stratigraphic prediction: Marine and Petroleum Geology, v. 15, p. 689-717.

SARTORI, R., 1990, The main results of ODP Leg 107 in the frame of Neogene to Recent geology of Perityrrhenian areas, *in* Kastens, K.A., and Mascle, J., et al., Proceeding of ODP, Scientific. Results, v. 107, p. 715-729.

ULZEGA, A., 1987, Carta geomorfologica della Sardegna marina e continentale: Progetto finalizzato Oceanografia e Fondi marini.

VAIL, P.R., MITCHUM, R.M,, JR., TODD, R.G., WIDMIER, J.M., THOMSON, S., III, SANGREE, J.B., BUBB, J.B., AND HATLELID, W.G., 1977, Seismic stratigraphy and global changes of sea-level, *in* Payton, C.E., ed., Seismic

stratigraphy-applications to Hydrocarbon Exploration: Tulsa, American Association of Petroleum Geologists Memoir, v. 26, p. 49-212.

WALKER, R.G., 1978, Deep water sandstone facies and ancient submarine fans: models for exploration for stratigraphic traps: Tulsa, American Association of Petroleum Geologists, v. 62, p. 932-966.

WESTAWAY, R., 1993, Quaternary uplift of southern Italy: Journal of Geophysical Research, v. 98, p. 741-722.

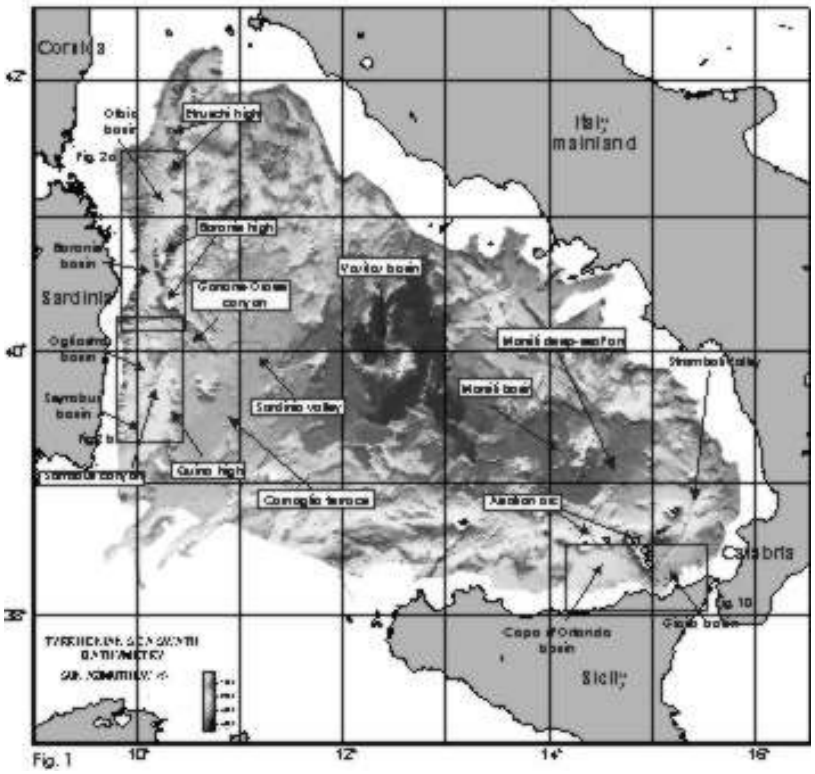
Corsica
Italy mainland
Sardinia
Sicily
Calabria
Vavilov basin
Marsili deep-sea fan
Marsili basin
Sardinia valley
Cornaglia terrace
Capo d'Orlando basin
10°
12°
14°
16°

Fig. 1

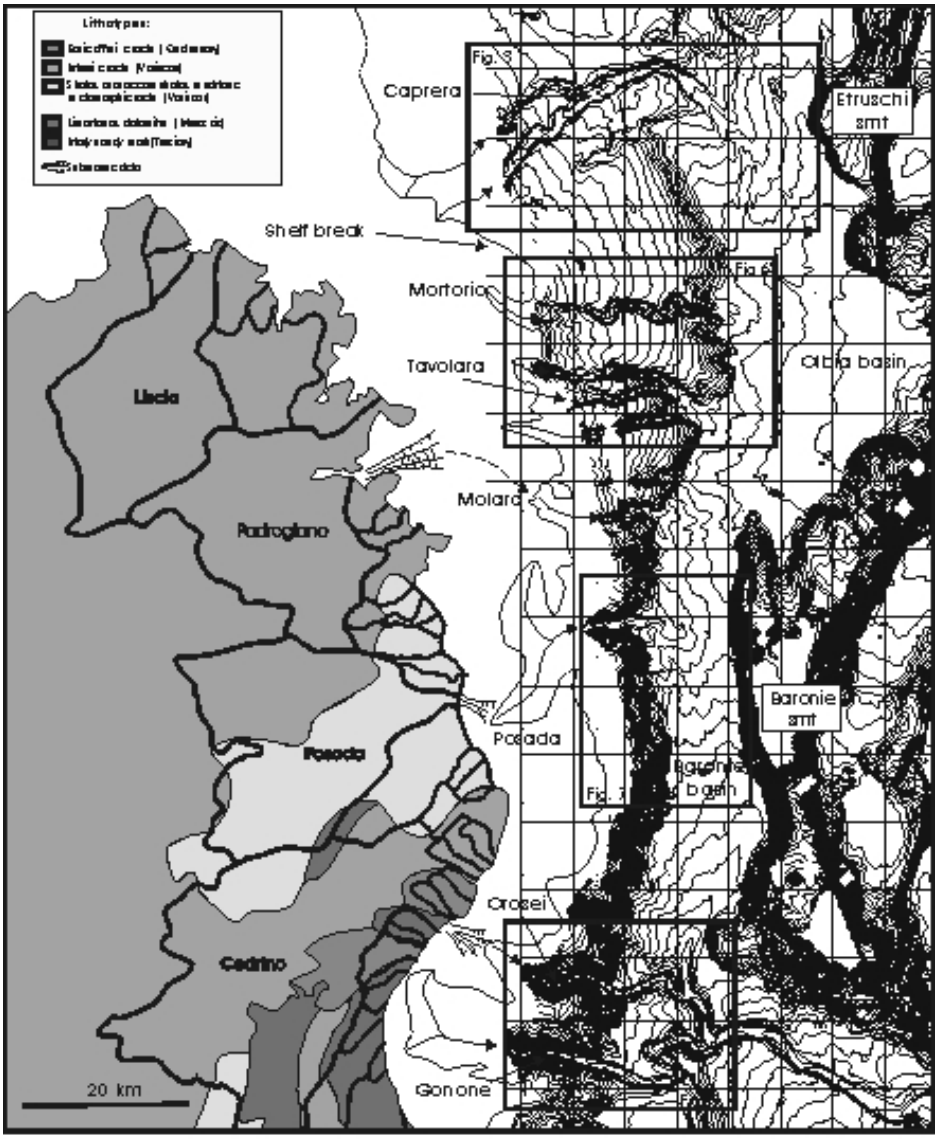
Caprera
Etruschi smt
Shelf break
Fig. 3
Fig. 4
Mortorio
Tavolara
Olbia basin
Uscio
Molara
Padrogiano
Posada
Baronie smt
Baronie basin
Fig. 5
Orosei
Cedrino
20 km
Gonone

Fig. 2 a

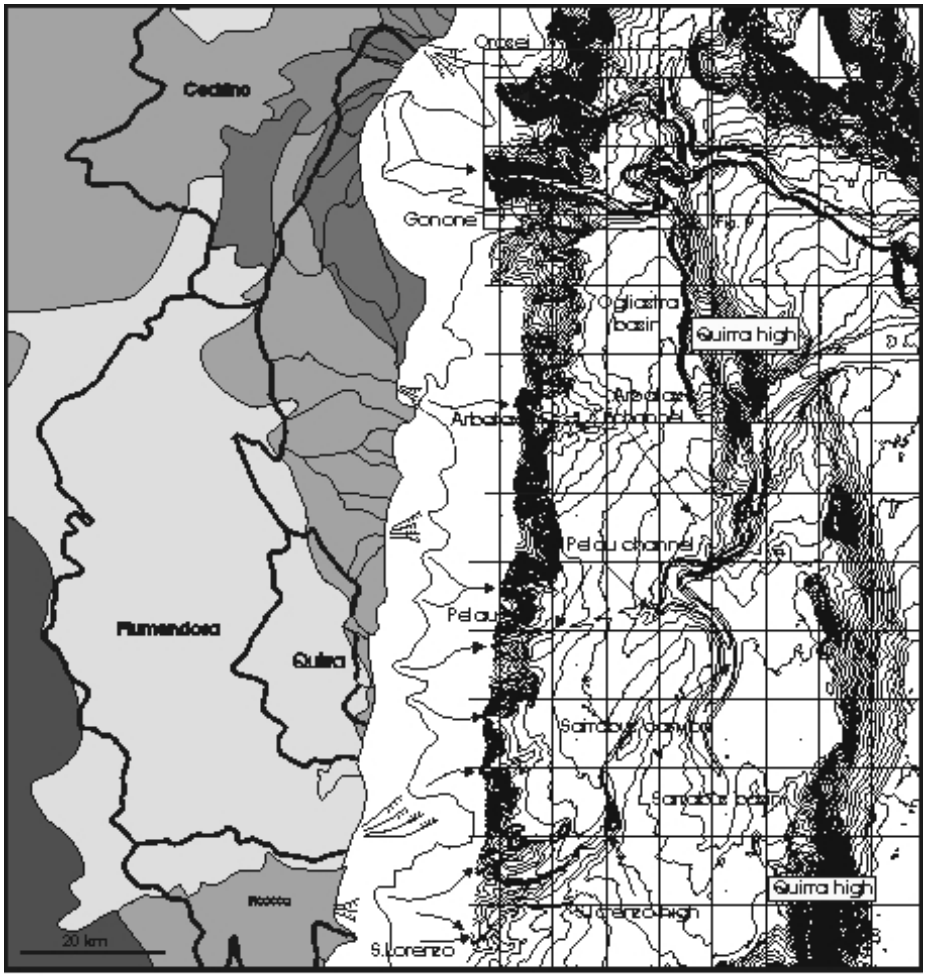
Cedrino
Flumendosa
Quirra
Rocce
20 km
Gonone
Arbatax
Pelau channel
Pelau
Quirra high
Quirra high
S.Lorenzo

Fig. 2 b

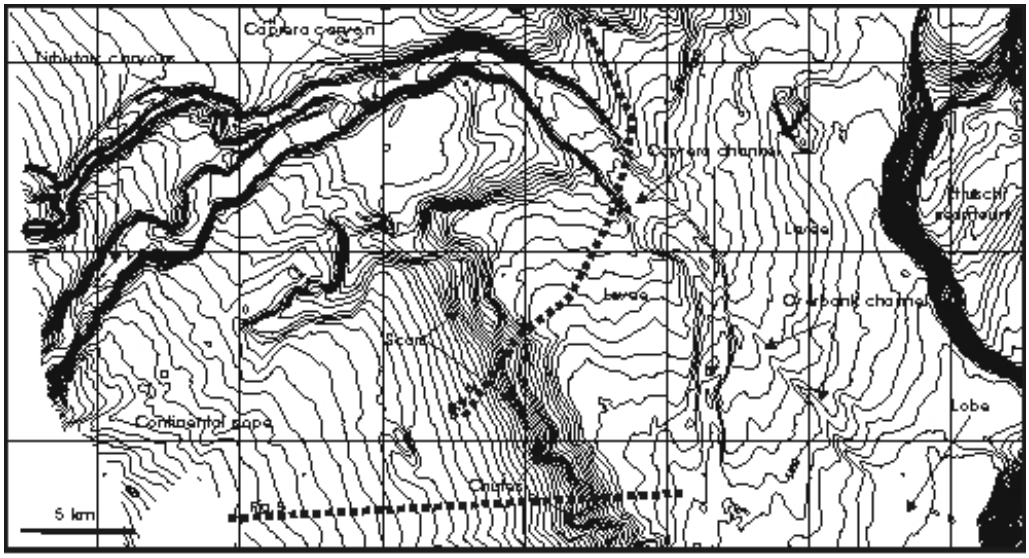
Capitara canyon
Tributary canyons
Capitara channel
Levee
Levee
Overbank channel
Scars
Continental slope
Channel
Lobe
5 km
Fig. 3

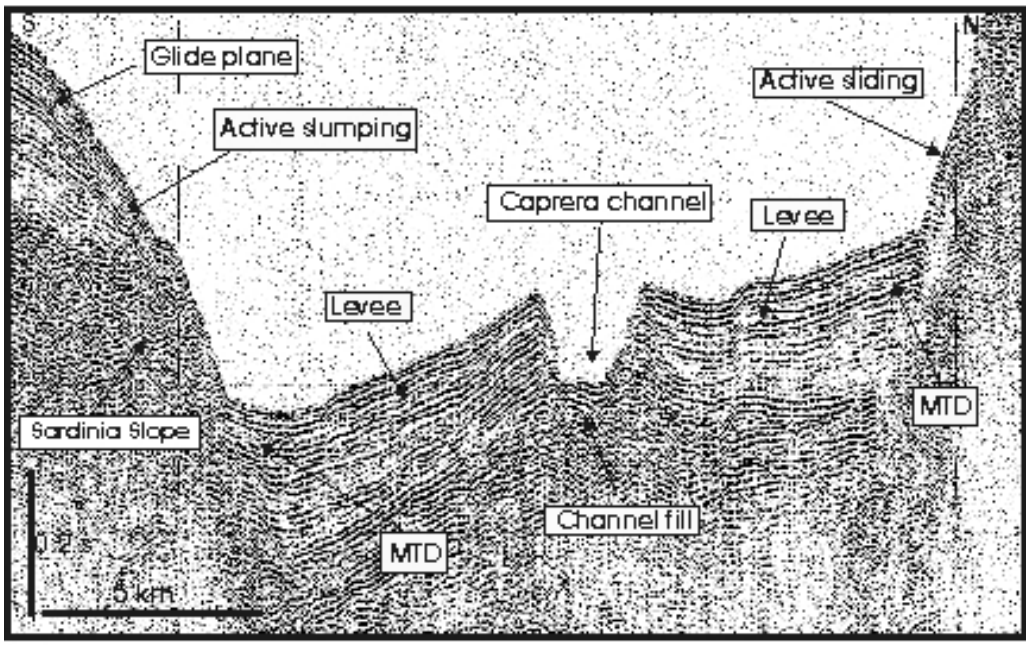
S
N
Glide plane
Active slumping
Active sliding
Caprera channel
Levee
Levee
Sardinia Slope
MTD
Channel fill
MTD
0.2 s
5 km
Fig. 4

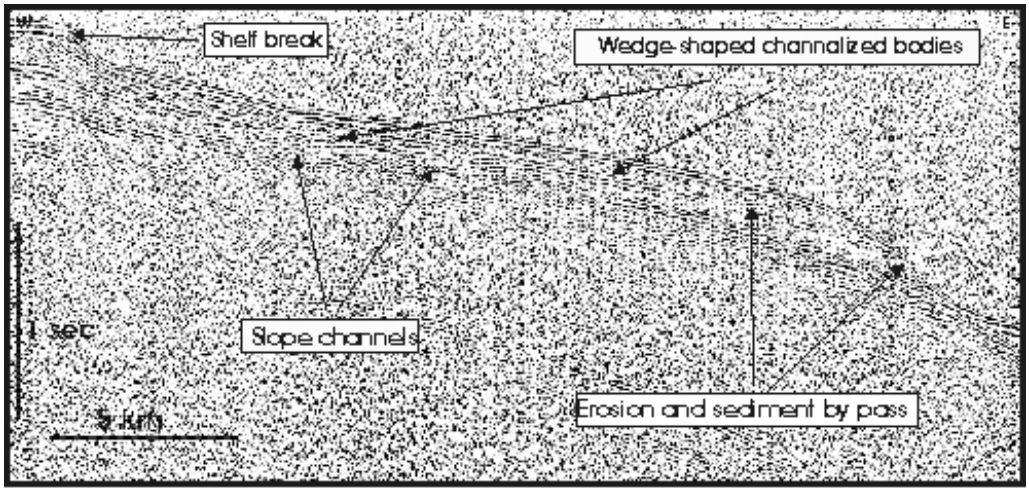
Shelf break
Wedge-shaped channalized bodies
1 sec
Slope channels
Erosion and sediment by pass

Fig. 5

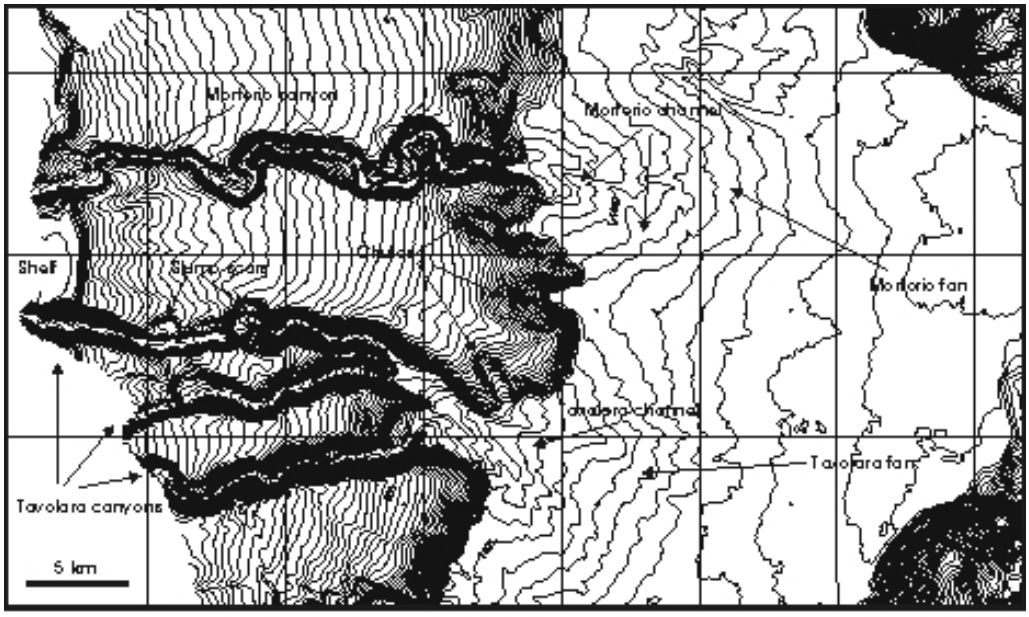

Fig. 6

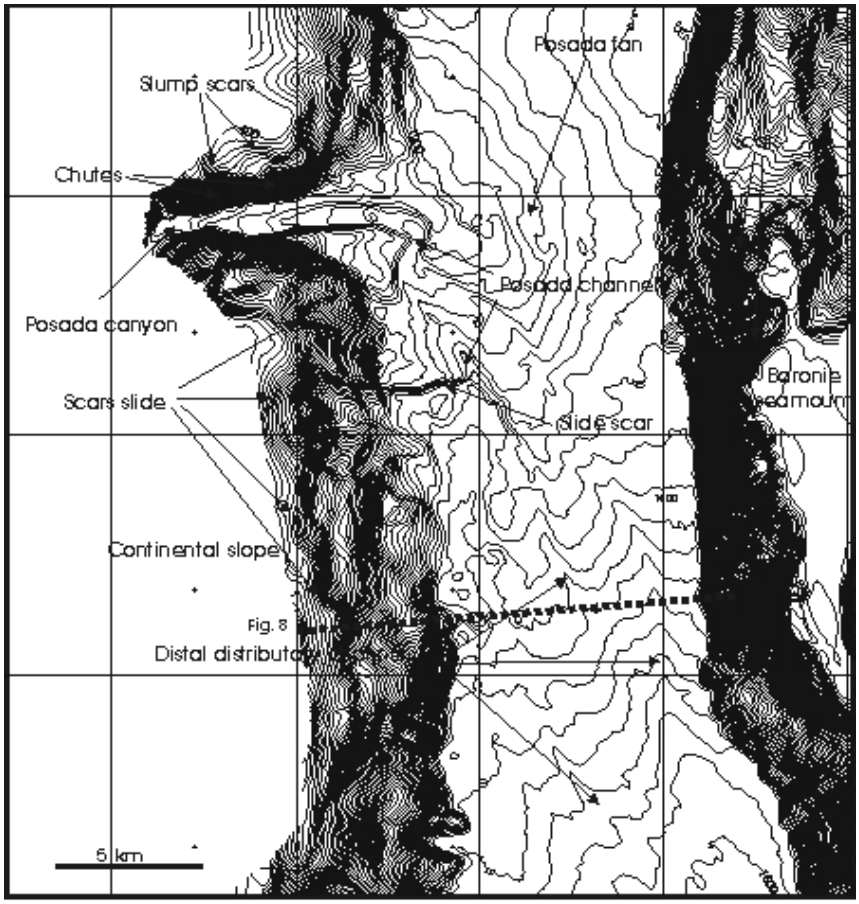
Posada fan
Slump scars
Chutes
Posada channel
Posada canyon
Baronia seamount
Scars slide
Slide scar
Continental slope
Fig. 8
Distal distributor
5 km
Fig. 7

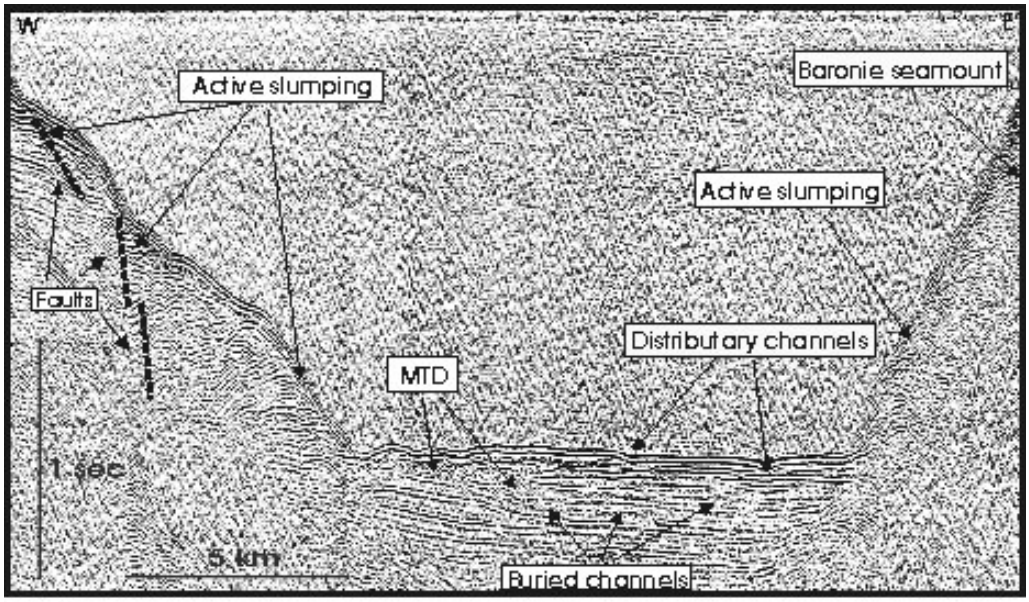
W
Active slumping
Baronie seamount
Active slumping
Faults
Distributary channels
MTD
1 sec
5 km
Buried channels

Fig. 8

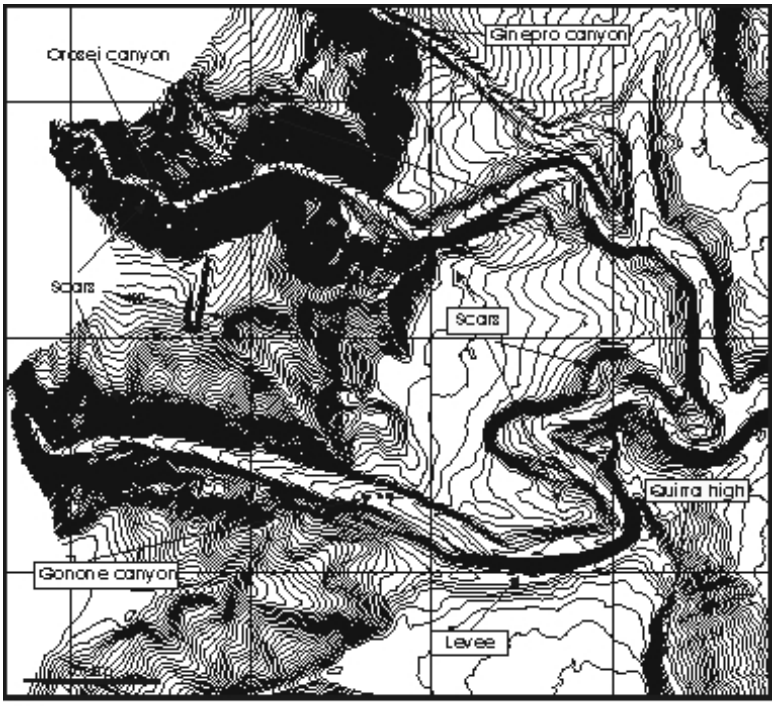
Orosei canyon
Ginepro canyon
Scars
Scars
Quirra high
Gonone canyon
Levee

Fig. 9

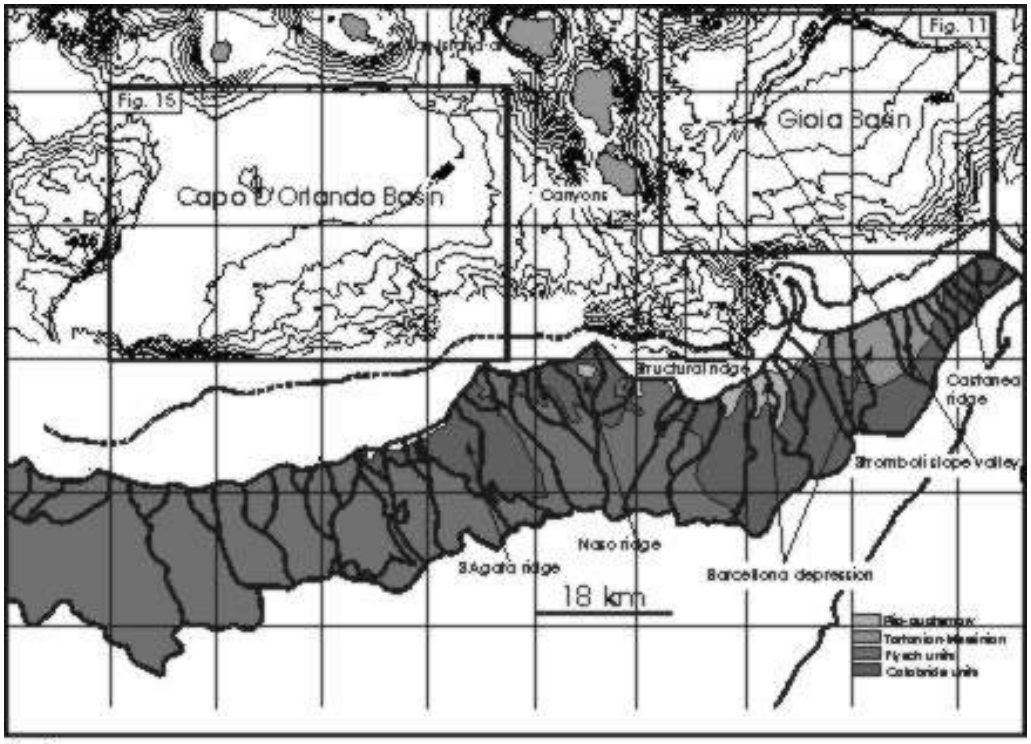
Fig. 11
Fig. 15
Gioia Basin
Capo D'Orlando Basin
Canyons
Structural ridge
Castanea ridge
Stromboli slope valley
Naso ridge
S.Agata ridge
Barcellona depression
18 km
Plio-quaternary
Tortonian-Messinian
Flysch units
Calabride units

Fig. 10

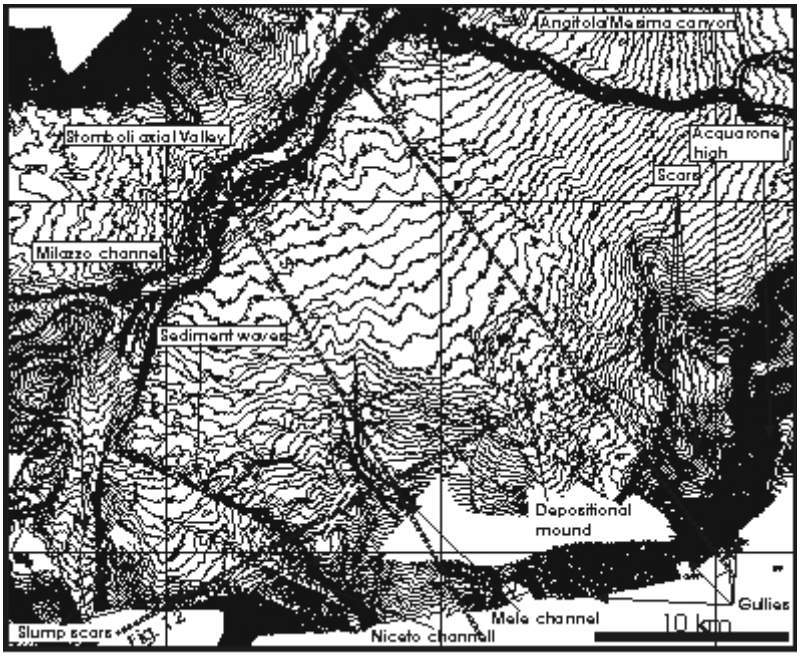
Angitola/Mesima canyon
Stromboli axial Valley
Acquarone high
Scars
Milazzo channel
Sediment waves
Depositional mound
Gullies
Mele channel
Slump scars
Nicoto channell
10 km
Fig. 11

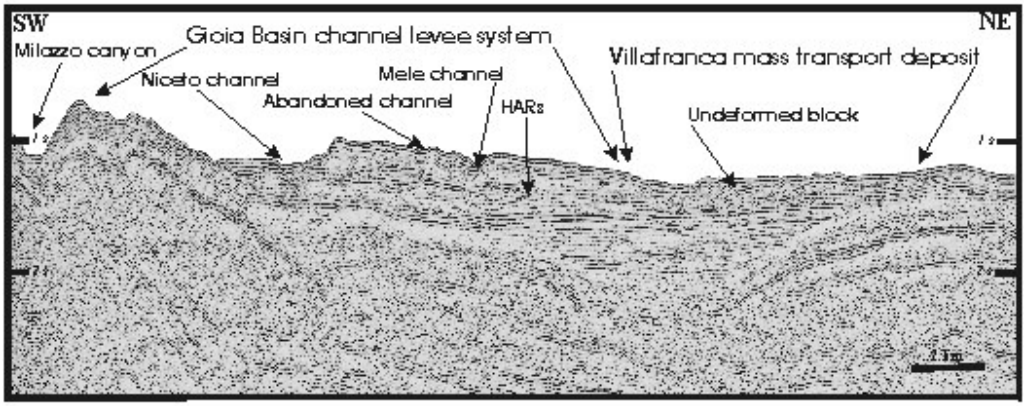
SW
NE
Milazzo canyon
Gioia Basin channel levee system
Villafranca mass transport deposit
Nicetto channel
Mele channel
Abandoned channel
HARs
Undeformed block

Fig. 12

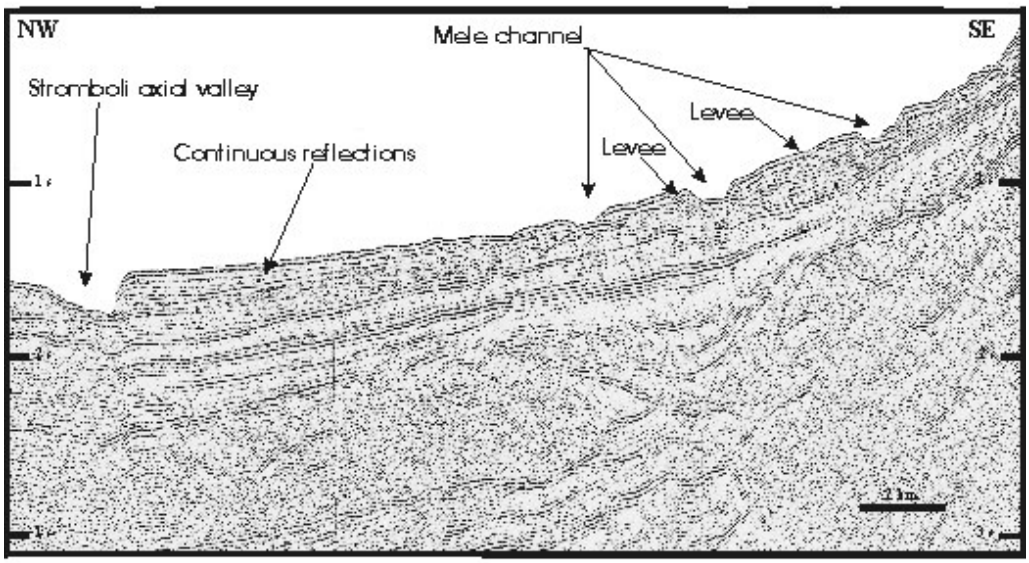
NW
Mele channel
SE
Stromboli axial valley
Continuous reflections
Levee
Levee
1 s
2 s
3 s
2 km

Fig. 13

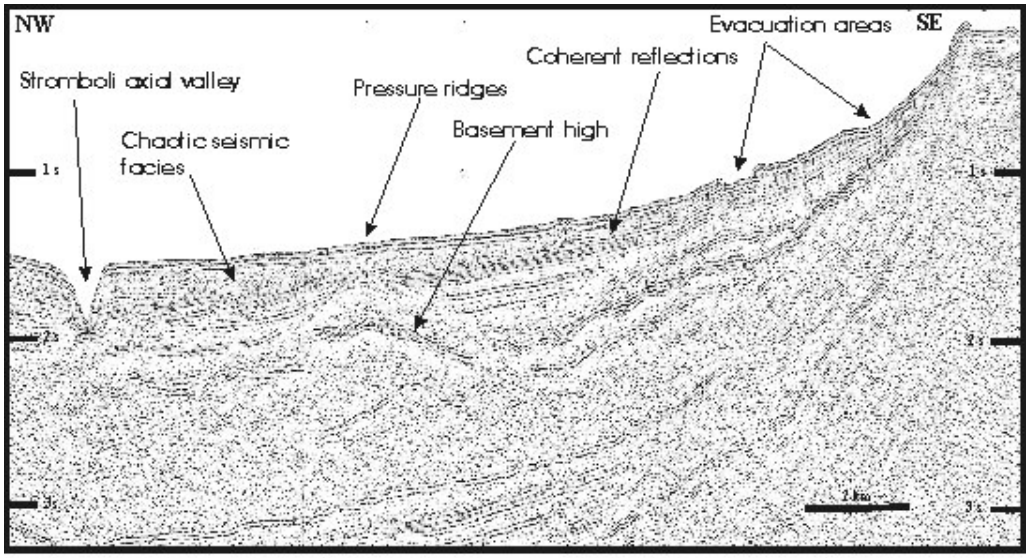
NW
SE
Evacuation areas
Coherent reflections
Stromboli axial valley
Pressure ridges
Basement high
Chaotic seismic facies
1 s
2 s
3 s
1 km
Fig. 14

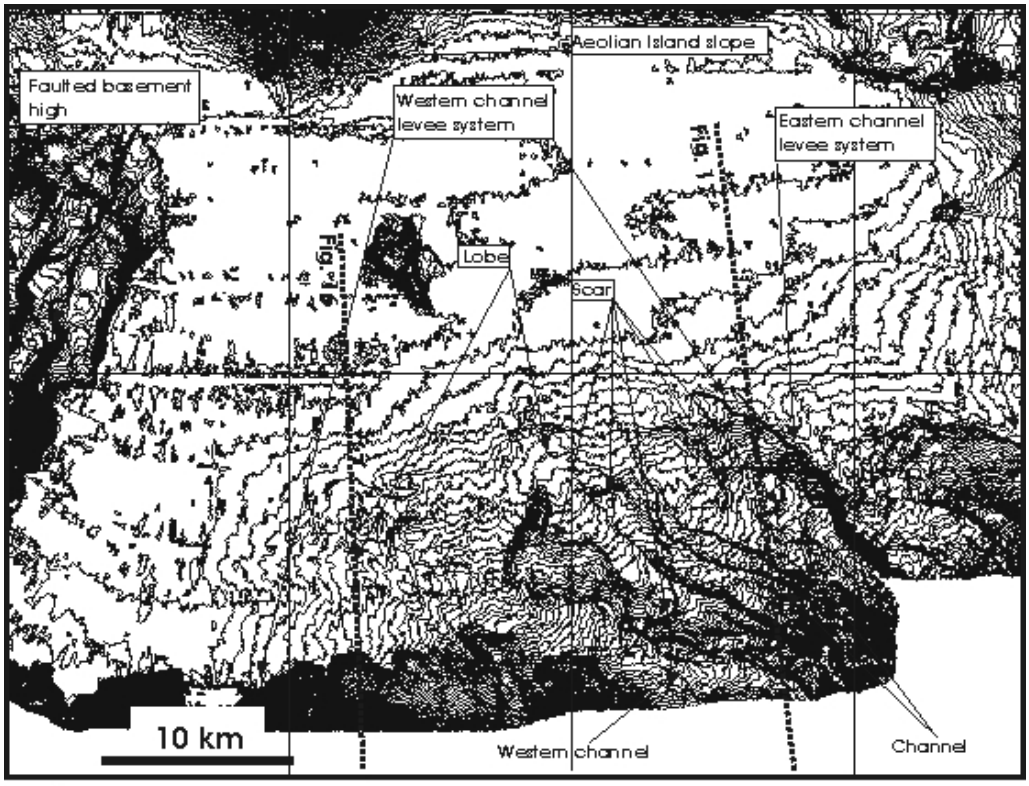
Faulted basement high
Western channel levee system
Aeolian Island slope
Eastern channel levee system
Fig. 16
Lobe
Scar
Fig. 1
10 km
Western channel
Channel

Fig. 15

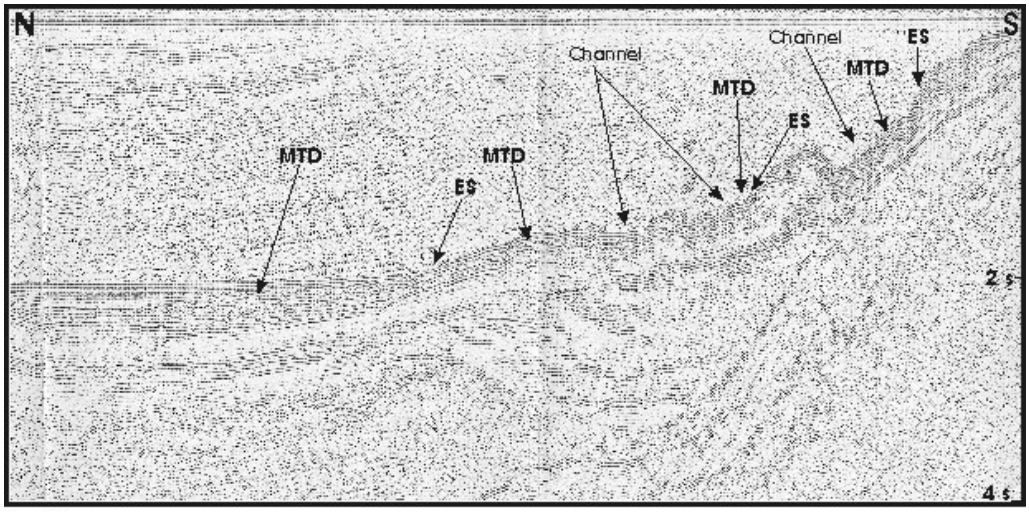

Fig. 16

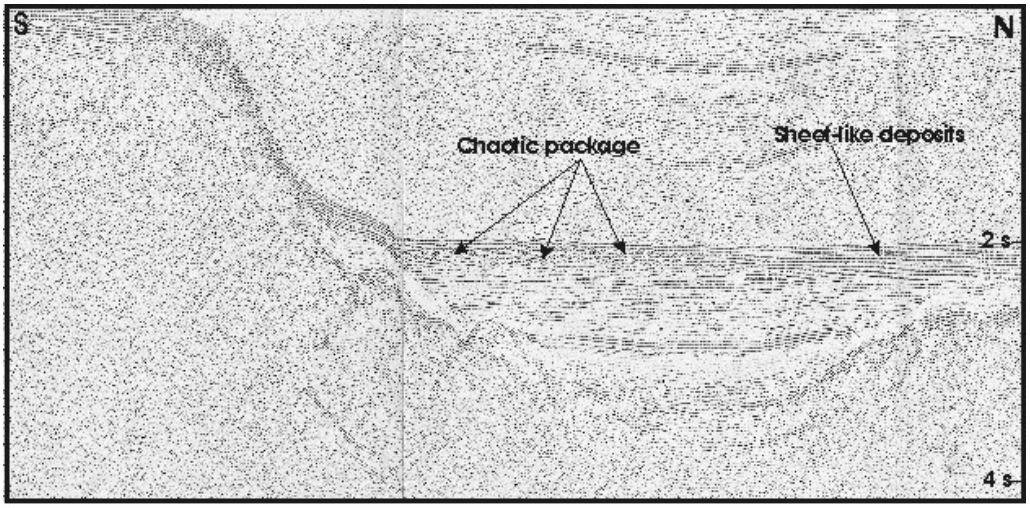

Fig. 17

Chapter 3

The Olbia basin

Introduction

The Olbia basin (OB) is the northernmost intraslope basin of the eastern Sardinian margin (Fig.1). In the northern sector it is flanked seaward by the Etruschi Seamount, whereas in the southern sector it is bounded seaward by the Baronie seamount (Figs. 1, 2, 3). The basin has a N-S length of around 65 km, with a maximum width in the centre of the basin of around 25 km; the basin plain lies between 1250 m and 1650 m of water depth (Figs. 2, 3). The OB represents a partially confined intraslope basin with a small bypass canyon incises in the eastern basin rim, where both the Etruschi and Baronie seamounts died out (Fig. 3). The canyon connects the OB to the lower Tavolara basin (TB), a small, circular depression lying at around 2000 m of water depth (Fig. 3). The OB is flanked landward by an around 20 km wide shelf, that narrows southward and by a 25 km wide, low angle continental slope (Figs. 2, 3). The continental slope is deeply incised by single canyon, and canyon systems, that at the base of slope develops small, radial deep sea fans: the Caprera, the Mortorio, the Tavolara and the Molara turbidite system (Figs. 2, 3).

The Caprera turbidite system (CTS), located in the northernmost sector of the basin, is the largest system of the OB and of the entire eastern Sardinian margin (Figs. 3, 4). In the continental slope, it consist of two tributary canyons that join in a single, 1 km wide canyon, at around 1000 m water depth (Fig. 4). At the base of slope, the canyon evolve in an around 20 km long leveed channel confined between the continental slope and the Etruschi seamount (Fig. 4).

3.1 The surrounding continental slope: morphology and seismic character

The morphology of the slope surrounding the CTS (Fig. 5) reflects the tectonic setting inherited from the rifting episode along the eastern Sardinian margin. The slope is articulated in an upper sector, from 300 to 500 m of water depth, averaging a dip of 2.4°, and a middle sector averaging a dip of 1.4° until 850 m of water depth

(Figs. 4, 5). Several circular depressions with diameter less than 1 km has been interpreted as isolated pockmarks (Fig. 4). The crossing Airgun seismic profiles shows hooked reflectors in correspondence of the pockmarks (Fig. 5a). In some cases the hooked feature cuts the entire sedimentary cover (~ 0.2 s) down to the acoustic basement whereas in another cases the hooks appear buried below weakly disturbed reflectors (Fig. 5a). Two distinct topographic highs (H1 and H2) stands out in the middle slope sector, between 650 and 750 m of water depth (Fig. 5).

The H1 is eliptical, around 2,5 km long, with a sublte relief of around 30 m (Fig. 5), flanked by a low relief, sinuous chute (Fig. 5). Internally it consist of strongly disturbed reflectors and the the acoustic basement below the structure is weakly reflecting (Fig. 5b). The slope reflectors plastered against the H1 high are faintly hooked (Fig. 5b). All of these feature lead to interpret this structure as a mud diapir due to the uprising of lower sediments.

The H2 is around 7 km long and 2 km wide stand around 30 m above the seafloor (Fig. 5c). Internally is made of irregular reflectors, overlayed by a thin sedimentary cover and with the slope reflectors onlapping on its left side (looking downslope) (Fig. 5c). A headless, wide chute flank the structure on the right side and is infilled by inclined, disturbed reflectors linked to slump and mass transport complex (Fig. 5c). With no evidence of fault associated with the high, and with the lack of blanketing in the basement below the structure, this feature could represent a buried carbonate mud mound.

The distal slope sector, between 800 and 1250 m of water depth, average a dip of 6°, due to its coincidence with the main extensional fault that bounds the OB (Figs. 4, 5). The distal sector is dissected besides by rectilinear headless chutes and by a network of wide, amphitheatre-like headwall scarps (Fig. 5). Slumping and mass movement processes are active, as truncated reflectors and marked glide planes reveals (Figs. 5a, 5b).

3.2 The Caprera turbidite system (CTS)

The CTS can be divided into five, large scale architectural elements, that proceeding downslope are:

(1) A proximal sector in the upper slope, where the system consists of two small tributary canyons (C1 & C2) with a SW-NE trend (Fig. 6)

(2) A middle sector characterized by a single canyon with an inital SW-NE trend and subsequently SE direction down to the distal slope sector (Fig. 7)

(3) A leveed channel, from the base of slope sector to around 1415 m of water depth (Fig. 8)

(4) A distal sector beyond the channel mouth, ending at around 1535 m of water depth (Fig. 9).

(5) A bypass sector, with an intraslope canyon, incised on the OB rim (Fig. 10).

3.2.1 The C1 and C2 tributary canyons

The C1 canyon has a lenght of around 17 km (measured along the canyon axis from the shallowest multibeam data) with rectilinear tracts alternated with a meandering sector (Fig. 6). In the proximal tract the canyon is around 500 m wide with a narrow V-shaped thalweg, that widens to 1.3 km downslope, averaging a dip of 2°. In the first turn of the meandering sector, in correspondence with a subtle entrenchment of the thalweg, an arcuate, 25 m of relief terrace is present (Fig. 6). In the final tract the canyon widens to around 1.2 km, showing a flat bottom floor scoured by two small relief thalweg with a very low dip (0.3°) (Fig. 6). The canyon walls has initial relief of around 160 m and 110 m, respectively for the right and the left wall, that loose relief downslope to 100 m and 50 m (Fig. 6). Both the canyon walls are affected by active slumping processes as the multiple scars reveal (Fig. 6). A slump deposit at the base of the right wall force the thalweg to change the pathway (Fig. 6). The C1 canyon appear partially filled by high amplitude reflectors (HARs) (Fig. 6a, 6b) capped by a thin package of chaotic reflectors interpreted as slump deposit, probably rafted down from the canyon walls (Fig. 6a). A marked incision of the V-shaped thalweg on the canyon infill suggests a rejuvenation of the erosional activity in this sector (Fig. 6a).

The C2 canyon has a lenght of around 16 km, deep incised on the slope with a negative relief of 180 m for both walls (Fig. 6). The initial sector is characterized by a narrow (100 m), V-shaped thalweg, flanked on the left side by a 4 km long terrace (Fig. 6). The terrace has a relief of around 80 m respect to the canyon floor with a gently erosional surface on its top (Fig. 6). Internally it consist of arcuate, parallel reflectors (Fig. 6b), and despite the unclear geometry of the contact between the terrace and the slope reflectors (Fig. 6b) this structure could be interpreted as a depositional internal levee.

In the bend sector the thalweg widens to around 500 m, with a dip of 0.3° (Fig. 6). In the right side of the bend sector, a series of perched, arcuate terraces, located at around 50 m up to the canyon floor are present (Fig. 6). A small relief lobe-shaped deposit, interpreted as point bar, is present at the base of the left canyon wall (Fig. 6).

3.2.2 The Caprera canyon

The Caprera canyon is around 9 km long with an around 70° bend that change the initial SW-NE pathway to the final NW-SE trend (Fig. 7). The canyon has a width between 1000 and 500 m, with a flat bottom floor scoured by a very low relief U-shaped thalweg (Fig. 7). The thalweg is flanked on the left side by a 4 km long, linear terrace with 35 m of relief and a maximum width of 250 m (Fig. 7).

The canyon walls have relief between 150 m and 130 m for the left and the right one respectively (Fig. 7), and are affected by mass wasting processes as suggested by the multiple wide, amphitheatre-like scars present on the uppermost sector (Fig. 7). As a confirm, marked glide planes are present on both the walls on the crossing seismic profile (Fig. 7a). Chaotic reflections make up the upper part of the canyon fill (Fig. 7a) suggesting that is composed primarily of slump deposits. In the bend sector, the left wall show evidence of retrogressive erosion on the surrounding slope (Fig. 7), whereas at the base of the right wall an inner -bend bar is present (Fig. 7). The bar elevates as much as 25 m above the canyon floor, is around 2 km long and has a maximum width of 500 m (Fig. 7). The chaotic style of the isobaths of the canyon floor beyond the bend sector, is probably related to slumps deposit, rafted down from the canyon wall and the surrounding slope (Fig. 7). At the canyon-

channel transition, the canyon show a flat bottom, scoured by a with very low degree (0.2°) U-shaped thalweg around 1 km wide (Figs. 7, 8).

3.2.3 The Caprera leveed channel

The Caprera leveed channel is around 18 km long, with a rectilinear 8 km long NW-SE tract, a bend sector and a subsequent 10 km long N-S tract (Fig. 8). The eastern levee extends for 10 km from the channel whereas the western levee is around 4.5 km of width (Fig. 8).

At the base of the slope the channel is around 1,3 km wide, with a flat bottom averaging a dip of 0.2° (Fig. 8). The crossing seismic profile show the leveed channel confined between the Etruschi seamount on the E and a basement high on the W (Fig. 8a): this setting has promote an asymmetry on the time-growing and the geometry between the levees of the Caprera channel (Fig. 8a). The channel fill is made up of predominantly chaotic reflectors, alternated with marked high amplitude reflectors (Fig. 8a): this setting could be related to phases of activity of the channel with deposition of coarse grained sediments alternated with stages of abandonment.

In the bend sector the channel thalweg show an abrupt entrenchment (Fig. 8) coupled with an erosion of the internal side of the western levee (Fig. 8). On the left side of the channel a probably abandoned thalweg is still visible and is separated by the active thalweg by an around 3 km long sedimentary ridge, interpreted as a left behind bar (Fig. 8). On the outside sector of the bend, in correspondence of a breach, a narrow, 10 km long V-shaped channel nucleates and incise the eastern levee surface with NW-SE direction (Fig. 8). At around 1500 m of water depth, the channel develops a small lobe around 5 km width, with a relief of less than 10 m (Fig. 8). On the surface of eastern levee small head-scarps with associated chutes are also present (Fig. 8), and in some case, the chutes develops small relief lobe-shaped deposit (Fig. 8). The western levee by contrary show an almost flat cross profile, with a dip of around 0.2°, with some few small chutes on the surface (Fig. 8). In the distal sector the Caprera channel has an almost flat bottom floor, with a slightly sinuous U-shaped thalweg (Fig. 8). A small arcuate terrace is developed in the right side of the channel with a relief of 35 mm respect to the floor, surrounded by a faintly scarps just 10 m high (Fig. 8).

3.2.4. The Caprera leveed channel: evolution inferred by seismic

A sparker seismic profile cross the eastern levee of the Caprera fan with a N-S trend (Figs. 8, 8b), provides additional information regarding the evolution of the Caprera leveed channel.

Two buried basement high partially confine the Caprera leveed channel (Fig. 8b): the nothern high has its top at around 0,25s below the seafloor, with onlapping high amplitude reflectors on its flank (Fig. 8b), wheras the southern high is deeper, buried below around 0.4 s of sediments (Fig. 8b).

A series of seismic units, enclosed between well marked high amplitude reflectors and interpreted as wide erosional surfaces, are identified confined between the basement highs (Fig. 8b). The lower seismic unit (LSU), marked at the base by a couple of rectilinear, high amplitude reflectors that mark the ignition of the turbidite system, is interpreted as the older stage of the Caprera channel (PaleoCaprera_1) (Fig. 8b)

A wide erosional channel-like feature with pronounced levee development represent the older NW-SE pathway of the Caprera channel (Fig. 8b). The levees have thickness between 0.05 s to 0.1 s (Fig. 8b); small channels and chutes scours the northern sector (Fig. 8b), whereas the southern sector is made of faintly disturbed parallel reflectors, onlapping against the basement high (Fig. 8b). A thin chaotic level (Fig. 8b), interpreted as small channel lobes deposit, or thin lenses of mass transport deposit, caps the levee in the nothern sector (Fig. 8b). The infill of the channel is made of chaotic reflectors (Fig. 8b): this is due to nature of the depositi (high-concentrated turbidity currents or debris flows) or due to migrations of the channel thalwegs.

The LSU is eroded by a wide V-shaped erosional channel-like surface (Fig. 8b), that mark the base of the upper seismic unit (USU). The channel-like feature (Paleo-Caprera_2) is about 6 km wide, with a marked flat bottom thalweg, without levees on both side of the channel (Fig. 8b). The channel appear filled by faintly layered reflectors, that probably consist of muddy sediments as consequence of the abrupt abandonment of the channel (mud plug) (Fig. 8b).

The younger, uppermost seismic unit (ASU) cap the USU and represents the eastern levee of the actual Caprera channel, that span with regular, parallel reflectors pinching out northward, interfingering with the Olbia basin plain reflectors. (Fig.

8b). Southward the levee is eroded by the the channels (DDC) of the Caprera distal distributary system (Fig. 8b).

3.2.5 The Distal distributary zone

The Caprera leveed channel ends at around 1415 m of water depth (Figs. 9). In front of its mouth, small relief erosive feature on the seafloor, interpreted as large scale scours are present (Fig. 9). This sector, characterized also by a very low dip (0.2°) is interpreted as a trumpet zone (*see* Mutti & Normark, 1987), a sector that mark the transition between the confined environment of the Caprera channel, to the unconfined basin plain environment. The wide, low relief scours are probably originated by the turbulence associated with the flow expansion processes at this crucial sector (*see* Pickering *et al.,* 1995). A crossing seismic profile (Fig. 9a) shows the low relief erosion of the trumpet zone on the seafloor (Fig. 9a). A thin lense of chaotic reflections are identified below the trumpet zone (Fig. 9a). The seismic profile show the LSU (Paleo-Caprera 1 channel) buried at around 0.2 s below the seafloor with the levees plastered against the basement high (Fig. 9a). As previously seen, also in this sector a marked erosional surface marks the base of the USU (Paleo-Caprera 2 channel) (Fig. 9a). The channel has a maximum thickness of 0.1 s, partially bounded by the top of the basement high (Fig. 9a). The channel fill is made of faintly layered reflectors (mud plug), with a predominance of chaotic reflectors in the sector that overlie the basement high (Fig. 9a).

At around 5 km downslope from the channel mouth, the formation of narrow distal distributary channels take place (Figs. 8, 9). In particular, the Dc1 channel (Fig. 9) nucleates as a single erosive feature at around 1500 m water depth, with a slightly curvilinear path of around 7 km, a width of 500 m and around 30 mof negate ve relief (Fig. 9). The Dc1 channel is confined on the right side by the Mortorio Fan, and the channel appear erosive on the distal portion of the fan (Fig. 9). The Dc2 channel consists of two small reaches that join into a single element (around 3,5 km long), with a very small negative relief, and flanked by small levees (Fig. 9). Beyond 1550 m of water depth no channel are traceable in the multibeam bathymetry (Fig. 9). However, the basin floor appear scoured by low relief, wide V-

shaped erosive features (VEF), that reach the distal sector of the Olbia basin plain (Figs. 9, 10), that represent the upslope portion of the bypass sector.

3.2.6 The bypass sector

The intraslope bypass sector nucleates in the eastern rim of the Olbia basin, at around 1650 m of water depth (Fig.10). It start with a narrow, steep (17°) incision W-E trending, around 600 m long (Fig. 10). It ends in a structural controlled terrace on the eastern flank of the Baronie smt at around 1900 m of water depth where it develops a small, circular plunge pool (Fig. 10). A lower bypass canyon starts at around 2000 m depth (Fig. 10), cutting the slope with a straight NW-SE trend. Also in this case, a circular plunge polls is develops (Fig. 10), and presumably originated by the sedimentary flows hydraulic jump due to the abrupt break-in-slope. The lower Tavolara basin appear completely flat and smoothed, without sedimentary features resolvable by the multibeam resolution (Fig. 10).

The Mortorio turbidite system

3.2.7 The Mortorio canyon

Besides the CTS, other slope canyons and system of canyons that, at the base of slope, develops small, unconfined deep sea fans, incise the slope of the OB: the Mortorio canyon and the Tavolara canyons system (Fig. 11). The sinuosity index of the canyons seems to decrease southward in response to the increased continental slope gradients.

The Mortorio canyon develops southward from the Caprera canyons, and start with a marked indentation on the shelf (Fig. 2). It has a W-E trend, with a length (measured along the longitudinal axis, from 400 m 1300 m of water depth) of around 35 km, to the base of slope, at around 1300 m of water depth (Figs. 11, 12).

The Mortorio canyon can be divided in two sectors: a proximal sector, between 400 m and 620 m of water depth, where the canyons is narrow (50-100 m of width), slightly incised on the slope, and a middle-distal sector, where the canyon is deep (up to 200 m) with a series of meandering sectors, and with a width of 300-500 m (Fig. 12). The two sectors are separated by a marked break in slope (60 m of relief, 20° of dip), similar to the subaerial "water falls and is interpreted as a purely erosional isolated step.

In the proximal sector the canyons wall show hybrid characters: the right canyon wall is steep and erosional, with truncated slope reflectors (Fig. 12a) whereas the left wall is less steep and show depositional characters, linked to a slope progradation (Fig. 12a). A MTD buried below the canyon floor confirm the high instability of the canyon environment (Fig. 12a).

In the first meander sector (S-meander) the thalweg narrows abruptly due to the presence of slump deposits, rafted down by the high degree (up to 20°) canyon walls (Fig. 12a). Mass wasting processes affect the walls also the subsequent rectilinear tract of the canyon (Fig. 12a).

The second sinuous tract is characterized by several 90° turns (Fig. 12). These meanders are interpreted as due to slumps processes linked to failure of the canyon walls. The inner bend terraces that are the result of a combination of mass-wasting processes associated probably with the flows undercutting action, and deposition by the turbidity currents, as seen for example in the Monterey canyon (Fig. 12). The

crossing seismic line seems to confirm this interpretation, showing a buried MTD overlayed by an inner bend bar (Fig. 12b). An embryonic, well defined second-generation slump, probably resulting from retrogressive failures at the apex of the meander is also visible (Fig. 12).
In the final, linear tract, canyon walls are up to 300 m of relief, while the canyon flat-bottom floor has a width of around 400 m (Fig. 12).

3.2.8 The Mortorio deep sea fan

At the base of slope, the Mortorio canyon develops an unconfined, around 12 km wide and 14 km long, submarine fan (Fig. 12). In the apical sector, the fan is scoured by a weakly sinuous, low relief, around 10 km long channel, that ends in the northern middle sector of the Mortorio fan, developing a small relief lobe (CML) in front of its mouth (Figs. 12, 12c). An headless, short (2.5 km) low relief channel is developed on the outside sector on the Mortorio channel (Fig. 12); it can be as an overbanking channel, due the flow-stripping from the Mortorio channel, althought it could also be ad old abandoned channel.
On the distal southern sector, the Mortorio fan is eroded by the Ds1 distal distributary channels of the Caprera fan, and generally the fan surface is scoured by very small relief chutes (Fig. 12). Crossing seismic profile show the thin sedimentary unit of the Mortorio fan, with a maximum thickness of around 0.15 s (Fig.12c). A marked, basin wide high amplitude reflector marks the base of the Mortorio fan (Fig. 12c). Infilled channels, buried below the Mortorio fan (Fig. 12c), representing older distributary channels of the deep sea fan.

The Tavolara turbidite system

3.2.9 The tavolara canyons system

The Tavolara canyons system consist of three W-E trending canyons (T1, T2, T3) developed on the continental slope of the OB, south to the Mortorio canyon (Fig. 11, 13). The three fairway join into a single, 2.5 km wide canyon in the distal slope sector (Fig. 13). At the base of slope, the Tavolara system develops an around 14 km wide and 11 km long unconfined deep sea fan (Fig. 13). The T1 and T2 canyons

(length of 23 and 14 km respectively) can be divided in two distinct sectors, separated by an abrupt step (Fig. 13); cyclic steps are found along the floor of both canyons, with, in one case, an associated plunge pool (Fig. 13). As the previous case of the Mortorio canyon, the proximal sector of the T1 has a rectilinear path with a lower negative relief that the distal sector (from 150 m to 300 m) (Fig. 13). Gullies and arcuate slide scars are identified along the canyon walls of the T1 canyon, with small slump deposit founded along the floor (Fig. 13). The crossing seismic profile (Fig. 13a), show a removal surface on the left wall of the T1 canyon, indicating a general instability of the canyon wall.

The T3 canyon has a length of 15 km, from 450 m to the junction with the T1-T2 canyon (Fig. 12). Otherwise from the T1 and T2 canyon , the T3 is narrow and deeply incised (up to 380 m) in the continental slope for its whole lenght and with a sharp, 90° turn in the final sector, prior to the junction with the others canyons (Fig. 13). The thalweg average a dip of 2°; subtle break-in-slope are founded along the thalweg of the canyon, but cannot be considered as pure erosive steps ; erosive terrace, small slump deposits and longitudinal bar are also founded along the canyon (Fig. 13).

3.2.10 The Tavolara deep sea fan

At the base of slope, the canyons system develop a radial, around 10 km of radius unconfined deep sea fan (Fig. 13). The upper Tavolara fan consist of a an erosional V-shaped valley bounded by low relief longitudinal ridge that gradually taper in width and relief to their downslope terminations (Fig. 13). The upper fan valley loose negative relief donwfan and progressively enlarge to 3.5 km of width, with a smooth U-shaped profile (Fig. 13).

No lobe-shaped deposit is found at the end of the main fan channel, that loose relief progressively and ends at around 1490 m of water depth (Fig. 13). The fan surface is highly channalized by both small erosive chutes and by low relief leveed channels (Fig. 13).

Discussion

1. The continental slope

The overall morphology of the continental slope of the OB, with an upslope low degree sector and an high degree distal sector, is the results of the presence of the main extensive fault of the basin. In the proximal sector, field of isolated and, in some cases, aligned pockmarks interrupt the otherwise flatness of the slope. The relation of the presence of pockmarks with buried gas hydrates has been reported in the literature (Schroot *et al.,* 2005; Judd, 1998) especially for the Norwegian margin (Berndt *et al.,* in press; Hovland *et al.,* 2005) and the Balearic promontory (Acosta *et al.,* 2002). However, a study focused on the Mediterranean regions, consider the oceanographic setting of the upper eastern Sardinian margin not favourable to allow the presence of gas hydrates (Klauda & Sandler, 2003). The lack of active volcanism in this sector of the Sardinian margin leads also to discharge a thermogenic genesis, as seen for example in the Balearic Promontory (Acosta *et al.,* 2002). Therefore the pockmarks could be related to gas escape as consequence of shallow-depth organic matter decay. This hypothesis could also be supported by the evidence that organic-rich sediments are abundant within the Pliocene-Pleistocene deposit of Mediterranean regions (cf. Ariztegui *et al.,* 2000, Kallel *et al.,* 2000).

Also the H1 mud diapir could be correlated to the rise of Plio-Quaternary material, as Acosta *et al.,* (2002) has suggested for the mud diapirs in the Balearic promontory. The H2 carbonate mud mound, probably hasn't reach a complete "booster stage" (*see* Henriet *et al.*, 2002); a probably change in the oceanographic conditions has stopped the growth of the mound (Henriet *et al.*, 2002).

The steep, distal sector of the slope is the loci of intense mass wasting and of sediments bypass. Headless chutes are develops only in the steeper sectors of the slope, however, the middle-slope chains of the pockmarks could promote the development of these erosive fairways, that, with a retrogressive failure mechanism, could evolve into a younger canyon-stage. The thin sedimentary cover of the slope, suggest a deposition through hemipelagic fall-out and, subsequently, where the canyon systems starts, by a combination of unconfined turbidites and overbanking form the slope fairways.

2. The Caprera Turbidite System

Canyons: morphologies and evolution

The tributary canyons of the CTS show marked differences in their overall morphology. Assuming that the two tributary canyon C1 and C2, situated on a very similar sector of the continental slope, are supplied by the same feeder system, characterized by the same type and frequency of sedimentary flows, it is difficult to explain their different setting. Here, two different explanation are proposed:

a) The internal levee hypothesis

If the terrace in proximal tract of the C2 canyon is interpreted as an internal levee, it is possible to assume that in a previous stage, this canyon was very similar in width to the C1. The subsequent growth of the internal levee has narrowed the width of the canyon. The growth of the levee could be related to a change in the type of sedimentary flows that fed the C2 canyon. Initial high energy, short duration flows act within the canyon promotes the excavation and the narrowing of the canyon floor. When the energy or the size of the flows decreases, the flow is not able to spill over the main canyon walls, and consequently deposit their finer parts inside the canyon walls, and progressively originate an internal, depositional terrace, in a similar way to the growth of the "classical" levee (*see* Gervais *et al.,* 2004).

b) Different ages

The wide, flat bottom thalweg of the C1 canyon could reflect a mature stage of canyon evolution, while the C2 canyon, with a narrow, V-shaped thalweg could reflect a younger stage of the fariway. The different ages of the tributaries could be due to a subtle shifting of the entry point, with the younger C2 canyon erosional processes are instead dominants. The perched, arcuated terraces identified in the outer sector of the meanders of C2 canyon, are presumably originated as consequence of the deepening of the canyon thalweg, confirming that the canyon is

in a relative young stage with the equilibrium profile reach not yet reached by the canyon.

The multiple slump scars, the buried removal surfaces and the glide planes identified along the Caprera Canyon, and in the proximal sector of the C1 and C2 tributary canyons, indicate that the widening of the canyon occurs mostly through failures of the walls. This process is active both during the youngs stages of the canyon evolution (C2 canyon) and in the "mature" stage, as network of multiple scars identified on the C1 canyon and the Caprera Canyon suggests.

The inner-bend bars, recognized on the internal side of the meander tracts of the tributary canyons and the Caprera canyon, can be the result of escavation/migration by the thalweg, coupled with the subsequent spilling of particle-laden flows (see Babboneau *et al.,* 2002). On the contrary, the steep external walls of the canyon bend sectors are the demonstration of the erosive behaviour of the sedimentary flows, that due to centrifugal force, increase their shear stress on the canyon walls (Babboneau *et al.,* 2002).

The Caprera leveed channel: effects of confinement on the levee morphology

The geometry and the evolution of the Caprera channel appear strongly controlled by both buried and superficial tectonic related topography. The relevant asymmetry in the morphology and the development of the two levee is explained infact both by the distance from the bounding slopes and by the presence of the buried basement high that prevent the growth of the western levee during the initial stages of the channel development.

In addition, these differences could also be explained as the result of a complex interplay between the Caprera channel plan-form and the effect of confinement by bounding topography. Mohrig *et al.,* (2006) has infact shown that variability in the levee form could be induced by irregularities in channel plan-form (such as sharp turns or meandering sectors) and are responsible of complex relationships between proprieties of depositing flows and the resulting levees form (Mohrig *et al.,* 2006).

The bounding topography of the Etruschi seamount slope force the Caprera channel to change its pathway thought avulsion and marked bend sectors. An improvement on the discharge rate in the eastern levee of the Caprera channel, due to the stripping of the finer particles from the flows approaching the bend of the Caprera channel

should be expected. The presence of the overbanking channel, with the small lobe developed beyond its mouth seems to corroborate this assumption.

Besides, it has been argued that, variability in levee form may be also influenced by the presence of a obstacle that confine the sedimentary flows. As show by Kneller and McCaffrey (1999), flows approaching a slope may be deflected parallel to the slope, while the less dense, upper parts ran up the slope, with a subsequently collapse backwards as "reflections" directed normal to strike of the slope (Kneller & McCaffrey, 1999). This scenario could be responsible for the low dip of the western Caprera levee: the reflections of the flows strip by the Caprera channel, could explain the flatten morphology of the western levee (Dykstra, *pers. comm.)*

The Caprera leveed channel: evolution

The subsurface analysis has reveal that the Caprera channel has experienced avulsion during its evolution, with a previous pure NW-SE trend of the channel (Paleo-Caprera1 and Paleo-Caprera2).

The passage from the paleo-Caprera1 leveed channel, to the paleo-Caprera2 that is deprive of levees, could be the result of a retrogradation of the turbidite system, from a proximal-middle leveed channel sector to a more distal trumpet-shaped zone.

The last avulsion of the system, from the previous pure NE-SW trend to the actual pathway has caused the rapid abandonment of the old Paleo-Caprera2 pathway, as inferred by the seismic facies interpretation.

A single active channel and avulsion processes have also been observed for very big scale deep sea fan, and has been especially well documented on the Amazon Fan (Damuth *et al.,* 1983; 1988, Pirmez & Flood, 1995), the Zaire Fan (Babboneau *et al.,* 2002; Droz *et al*., 2003), and at the small scale, on the Rhone Fan (Torres *et al.,* 1997). During the development of the new pathway, turbidity breach the levee and follow a path down the lee backside and along a topographic depression (Pirmez & Flood, 1995). A new channel segments develops downslope from the avulsion point (Flood *et al.,* 1991). The segment of the parent channel below the bifurcation point becomes abandoned and subsequently buried by the overbank deposit of the new channel system (Babboneau *et al.,* 2002).

The actual western levee mask entirely the pathway of paleo-Caprera 2, suggesting high discharge rate of sediments by flow stripping from the new Caprera channel.

The perched, abandoned thalweg on the bend sector of the Caprera channel, represent a relict of old pathway prior of the avulsion.

The active thalweg of the Caprera channel nucleate with an abrupt entrenchment sector after a very flat channel tract. This could mean that the break in slope due to the entrenchment, produce an acceleration of the sedimentary flows, that become erosive on the channel floor, with no remarkable deposition of the sedimentary load (see Pirmez *et al.,* 2000). The erosional processes in turn, bring new sediments into the turbidity current, that increase the flow thickness, being contrasted by the increase in the flow velocity ("*squizzing*" of the flow) (Kneller, 1995). Such complex interplay rules the behaviour of the flows, changing their "efficiency" and the ability of the flows to build levee facies (Pirmez *et al.,* 2000).

The distal distributary zone and the bypass sector

The large, low relief scours identified in front of the mouth of the Caprera channel (trumpet-shaped zone) may be attributed to the hydraulic jump and the associated turbulence accompanying the transition from a confined to unconfined environment and the subtle decrease of gradient (*see* Mutti & Normark, 1987; Morris *et al.,* 1998). These scours are generally associated with high energy turbulence flows, so this could indicate that moderate to high efficency flows may reach the distal part of the turbidite system (Morris *et al.,* 1998). Fields of large scours are mapped in the Bearing Sea (Kenyon & Millington, 1995) that are concentrated on the right-hand side of the channel, where it starts to expand into a trumpet-shaped mouth. There are also similar features on the Navy Fan (Normark *et al.,* 1979), and giant slates are founded also on the Rhone Fan (Kenyon *et al.,* 1995).

The distal distributary channels (DDC) and the bypass canyon could be interpreted as the 3rd stage of the fill and spill model of Sinclair and Tomasso (2002). In the studied case, the upper OB is almost entirely infilled, the bypass canyon is situated in the distal sector of the OB and the lower basin corresponds to the Tavolara basin.

As a consequence of the creation of new accommodation space and of a lower base level, the CTS responds with a series of adjustments

In the classical fan model (Normark, 1970; Walker, 1978), infact, in the sector beyond the channel mouth depositional processes prevailing (Pickering *et al.,* 1995 and references therein). Channel-mouth lobe (CML) are believed to have formed by

non-channalized turbidity currents spreading radially after exiting a confined channel and deposit their sedimentary load (Parson e*t al.,* 2002).

In the CTS case, the distal sector of the system is instead characterized by erosional processes as the DDC and the wide, low relief V-shaped valleys reveal. The creation of a new base level in the distal plain, cause a re-acceleration of the sedimentary flows, enhanced their erosive behavior, that, with a feedback relationship, contributes in turn to the development of the V-shaped valley and of the DDC. Increasing in velocity, mean the increment of the kinetic energy and turbulence of the flows that bring new sediment into the flows (Kneller & Branney, 1995). The sediment-laden flow may experience overbanking of the finer particles and this could explain the presence of the small levees of the DDC.

The V-shaped valleys represent the very distal prosecution of the distributary channels and are connected with the bypass canyon to the lower Tavolara basin. The progressive down-cutting of the inter-basinal canyon will define a base-level for the upper basin that is lower than the level to which the sediments accumulated during the fill of the upper basin. The result is progressive incision into the upper parts of the confined basin succession, through the V-shaped features.

3. The Mortorio and Tavolara slope canyons

Canyon and canyon systems are present in the low angle continental slope of Olbia basin. The canyons are incised on a relative thin sedimentary cover, and in some case they erode also the Messian acoustic basement. The enlargement of the canyon through mass failure of the wall seems to be the main factor that control the evolution of the canyons; however, the undercutting erosive action by gravity flows could promote the collapse of the walls. In addition it has been observed that in some cases, the meander formation is due to collapse of the canyon walls. The series of abrupt break break in slope along the canyons axis are very similar to the isolated and cyclic steps examined in details in consolidated fine-grained, subaerial channels and laboratory experiments by Parker & Izumi (2000). Using the Parker and Izumi model (2000), Parson *et al.,(* 2003), studying the Eel canyon has shown that near-critical turbidity currents are likely the cause of the formation of cyclic steps. Also the case of the Eel canyon, the steps within the canyons are not coincident with relevant tectonic structures, and the lithological heterogeneities has

been preferred to explain the presence of the cyclic steps (Parson *et al.,* 2003). Like plunge pools, cyclic and isolated steps are related to internal hydraulic jumps within the turbidity currents; at variant from the plunge pools, in the cyclic steps, the jump must be much smaller than the wavelength of the steps (Parson *et al.,* 2003). Episodic, short time-scale turbidity currents with near-critical Froude number dictate the morphologies of the cyclic steps (Parson *et al.,* 2003). Hyperpicnal activity can produce episodic turbidity currents, if the discharge of sediment is sufficiently short lived. The Mortorio and the Tavolara canyons are not directly fed by rivers, and are flanked by an around 20 km wide shelf, so it can be assumed that the hyperpicnal-type flows are very rare. Failure-induced turbidity currents, which are necessarily episodic, therefore represent a plausible mechanism consistent with the observed morphology and subsurface analysis of the Mortorio and Tavolara canyons. However, the efficient conversion of a failed mass into a turbidity currents is still a matter of debate (Marr *et al.,* 2001); a fully turbulent behaviour is infact extremely difficult to attain from a slope failure in any small–scale laboratory experiment (Parson & Garcia, 1998).

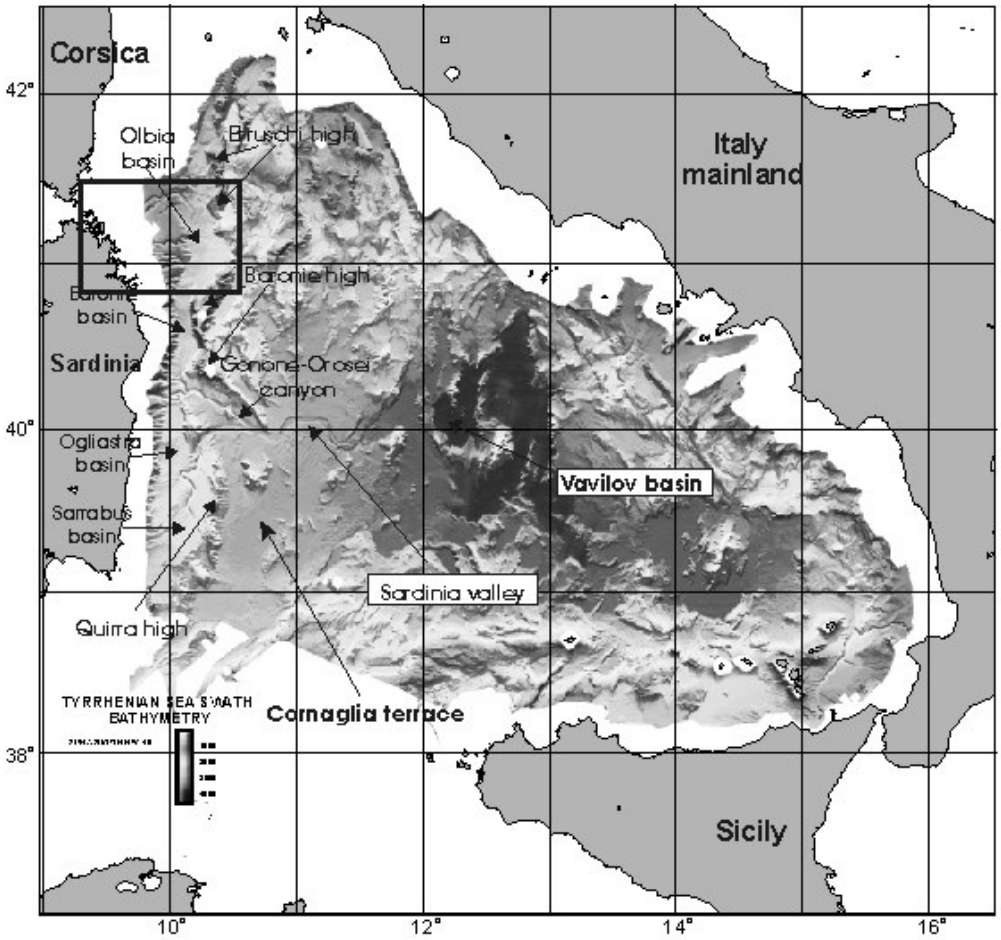

Fig. 1 Shaded relief image of the seafloor of the Tyrrehian sea. The upper intraslope basin and the bounding seamounts are indicated. The box corrispond to the bathymetic map in fig. 2

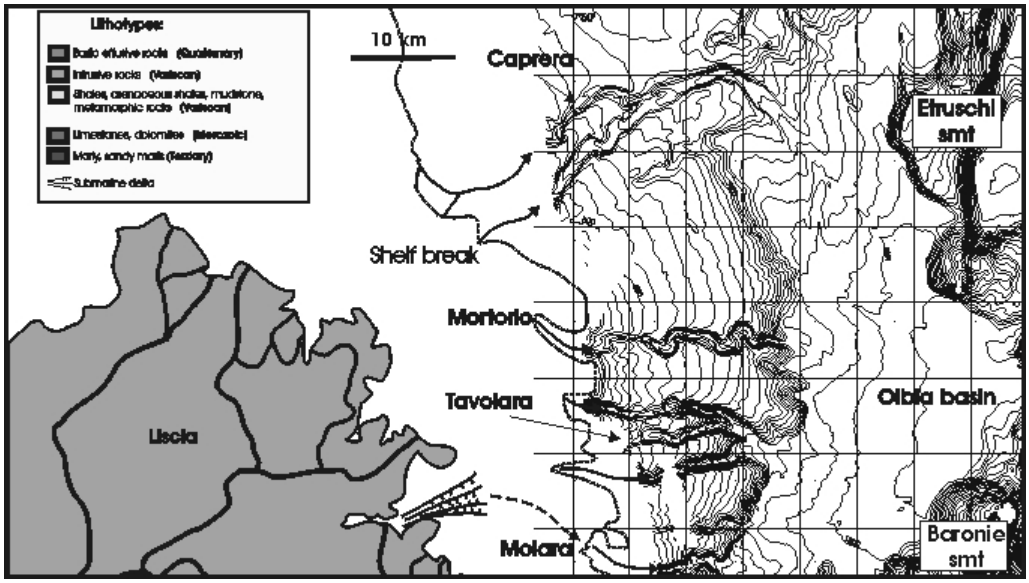

Fig. 2 Multibeam bathymetric map of the Olbia basin. The shelf break (dashed line) is taken from Bellagamba et al., (1979), whereas the location of the submarine deltas is from Ulzega et al., (1987). The map of the Sardinia Island with a schematic lithological subdivision has been simplified from Ulzega et al., (1987). The river drainage basins are also indicated with a solid black line. Contour interval 50m.

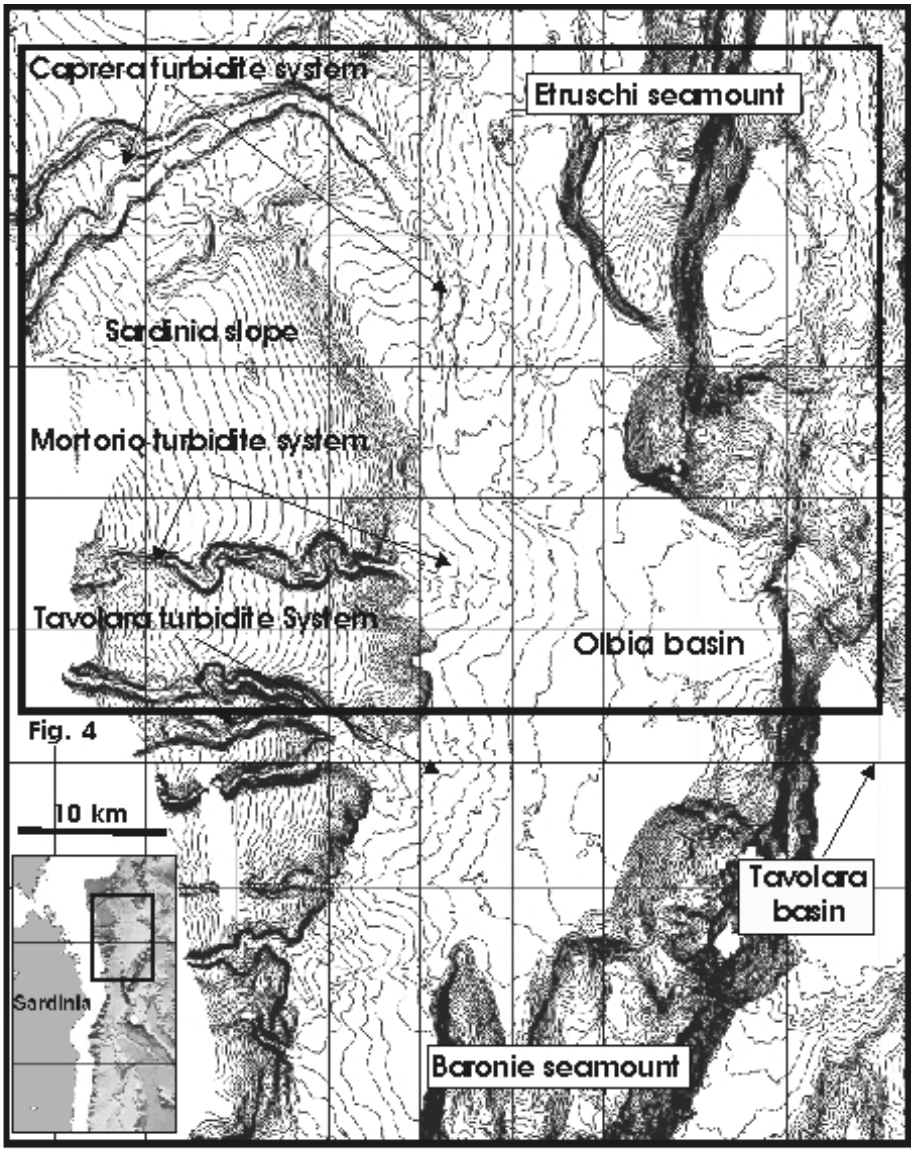

Fig. 3 Multibeam bathymetic map of the Olbia Basin and the lower Tavolara basin. The main turbidite system are indicated. Contour interval 20 m. The location of the Olbia basin is indicated on the map in the small box.

Fig. 4 Multibeam bathymetric map of the Capreta Turbidite System. The basic large scale elements of the turbidite system are indicated. C1 and C2: tributary canyons. DDC=Distal Distributary channels. VEF=V-shaped Erosive Features. BPC: Bypass Canyon. TB: Tavolara basin.Contour interval: 20m

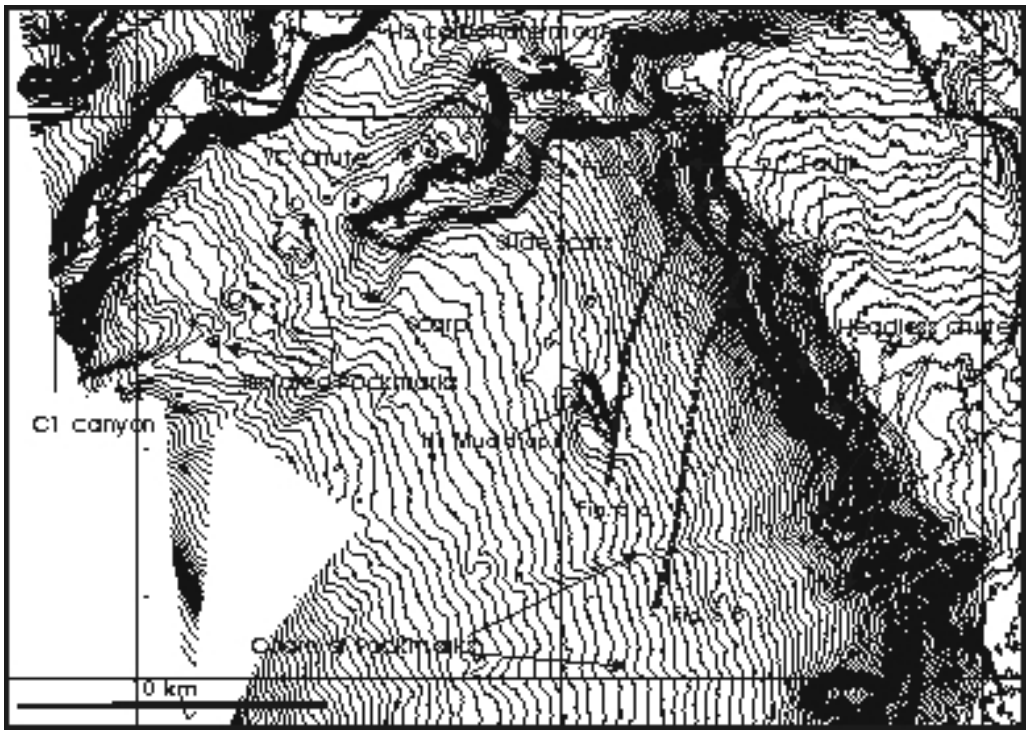

Fig. 5 Multibeam bathymetric map of the continenal slope surrounding the Caprera system. The main features descibred on the text are indicates. The dashed lines are the trace of the seismic profiles.Countour interval :10m

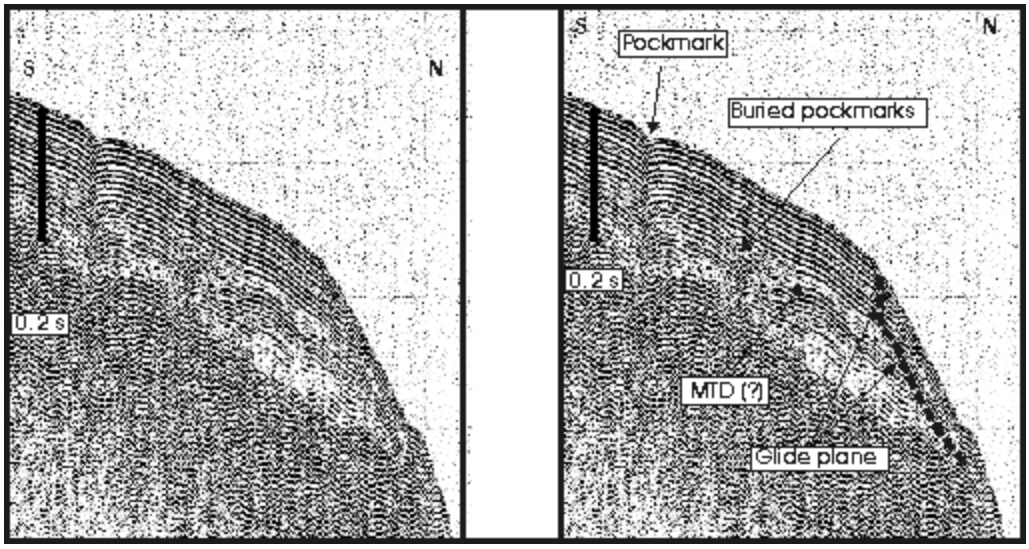

Fig. 5a. Air gun seismic profile of the middle-distal sector of the Olbia Basin.Tthe sedimentary succession above the acoustic basement, is around 0.2s of thickness made of continuous reflectors, in some cases interrupted by thin chaotic lenses of mass transport deposit (MTD). See Fig. 5 for the location of the profile.

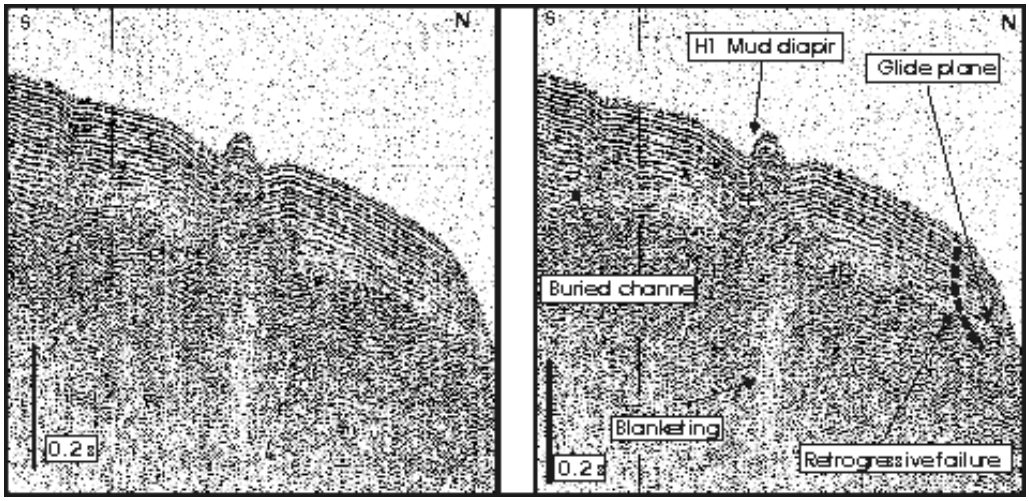

Fig. 5b. Airgun seismic profile of the middle and distal sector of the Olbia basin continental slope. See fig. 5 for the location of the profile.

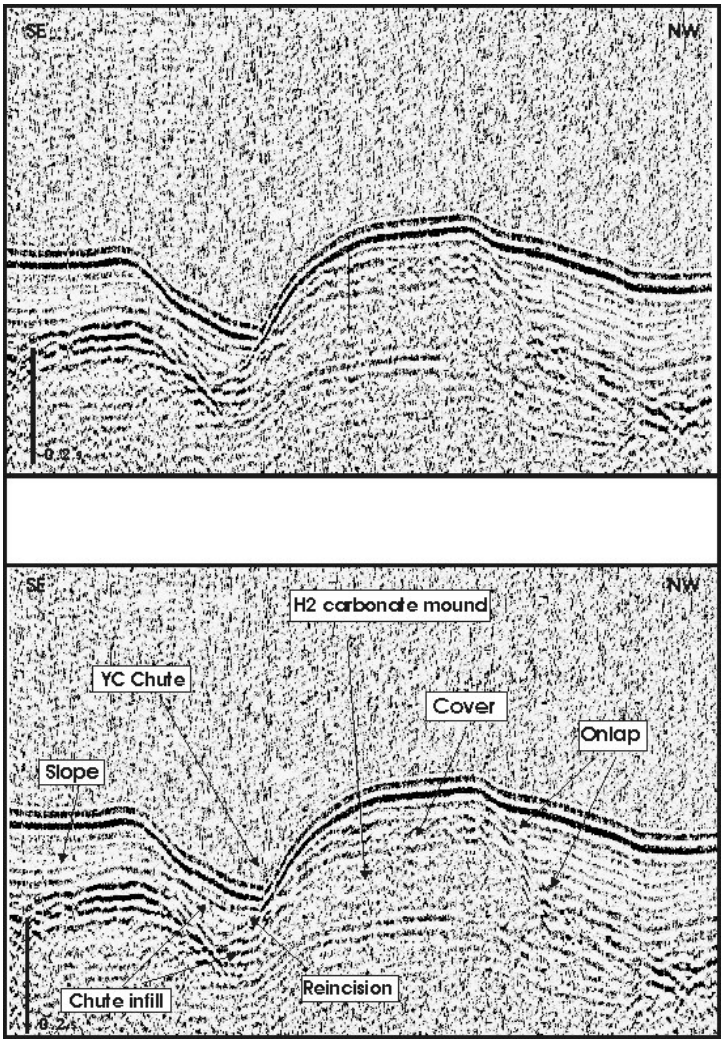

Fig. 5c Slope crossing Sparker seismic profile showing the Carbonate mud mound and the flanking YC chute. See Fig. 5 for the location of the profile.

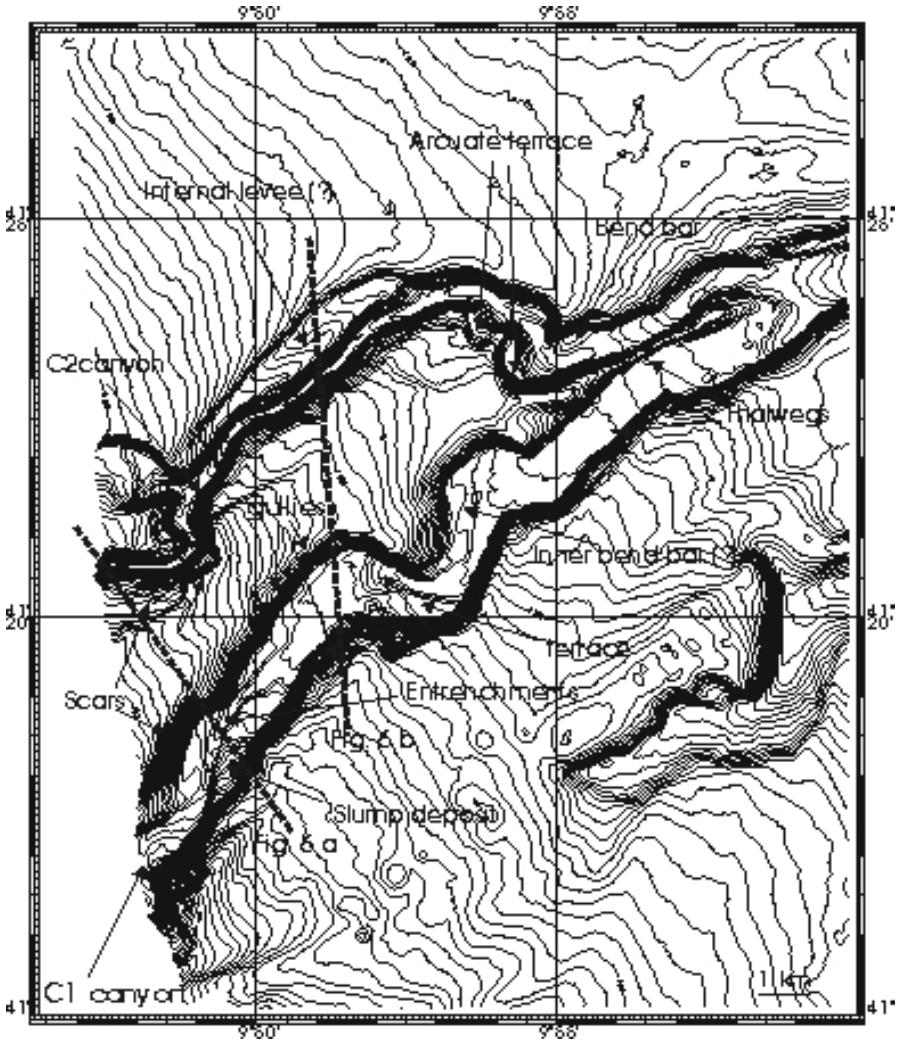

Fig. 6. Multibeam bathymetric map of the tributary canyons of the Caprera Turbidite system. The main morphological elements described in the text are indicated. The dahsed lines are the trace of the seismic profiles.Contour interval 10m.

Fig. 6a Sparker seismic profile of the tributary canyons C1 & C2. Truncated reflectors and removal surfaces, confirm that sliding processes are active along the canyon walls See fig. 6 for the location of the profile.

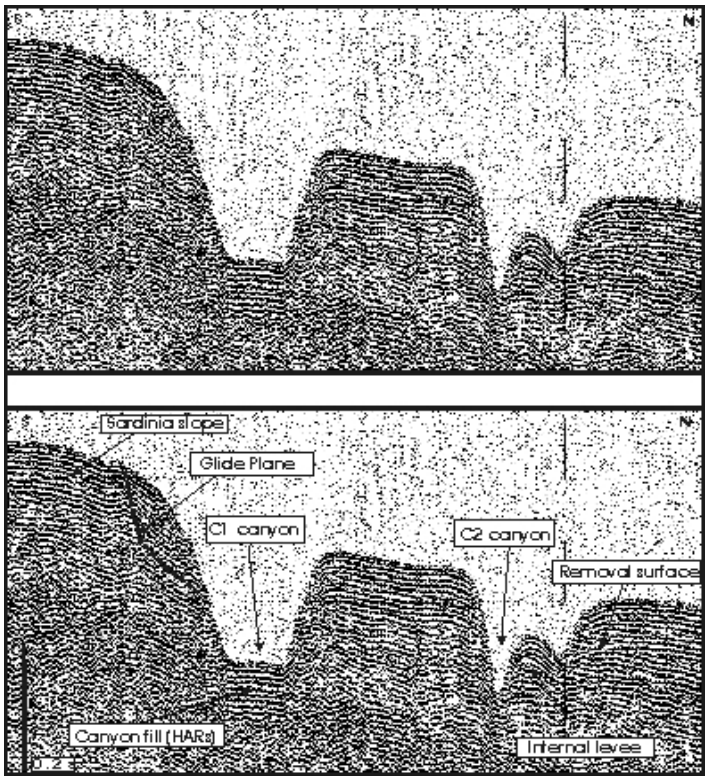

Fig. 6b Air gun seismic profile of the tributary canyons of the Caprera Turbidite System. Note the unclear geometry of the contact between the intpreted internal levee and the slope

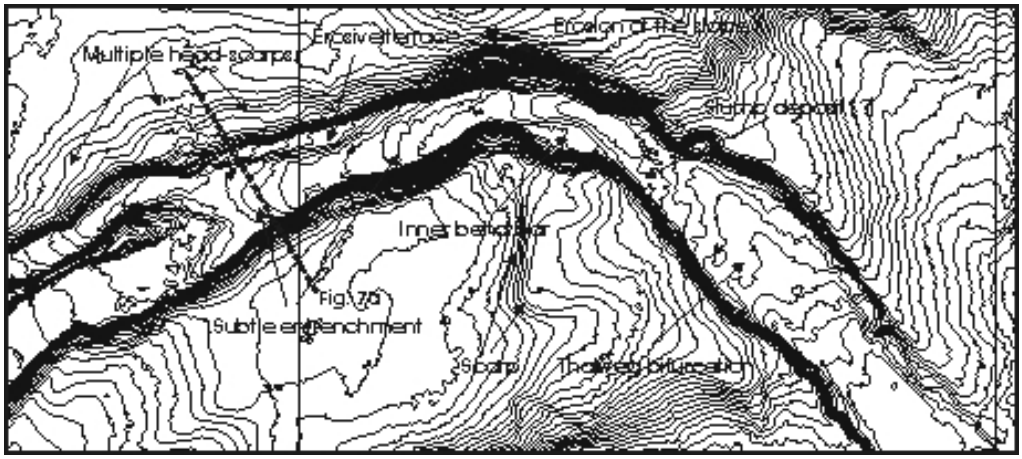

Fig. 7 Multibeam bathymetric map of the Caprera Canyon. Contour interval:10 m.

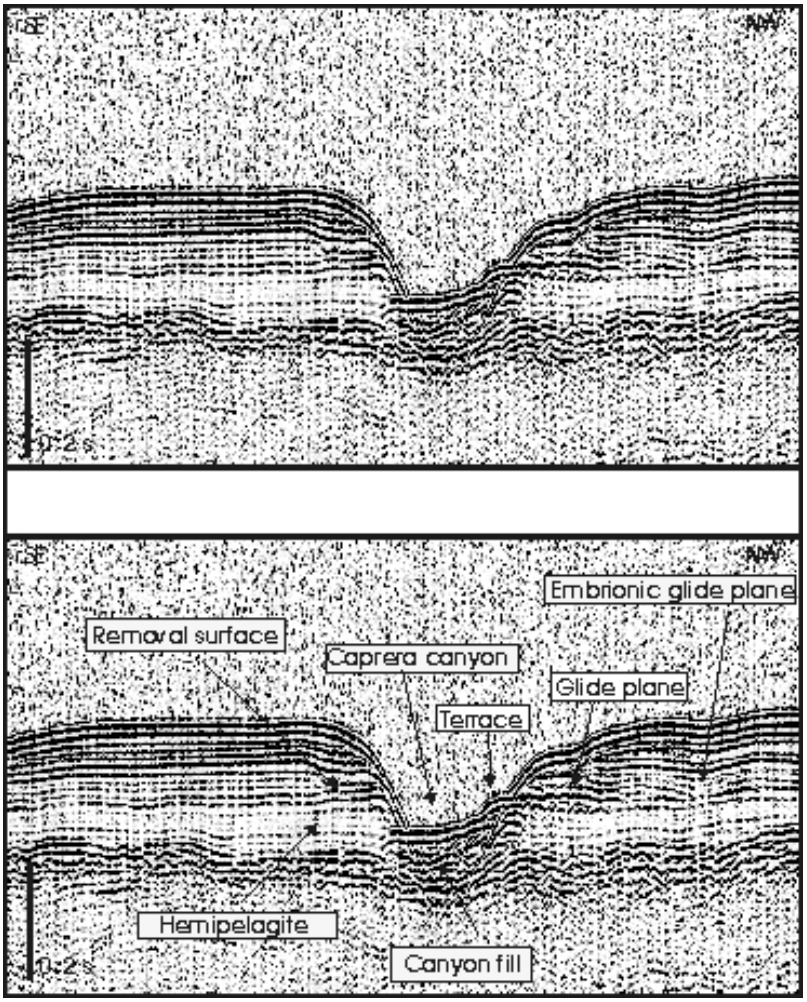

Fig. 7a Sparker seismic profile of the Caprera canyon. See fig. 7 or the location of the profile.

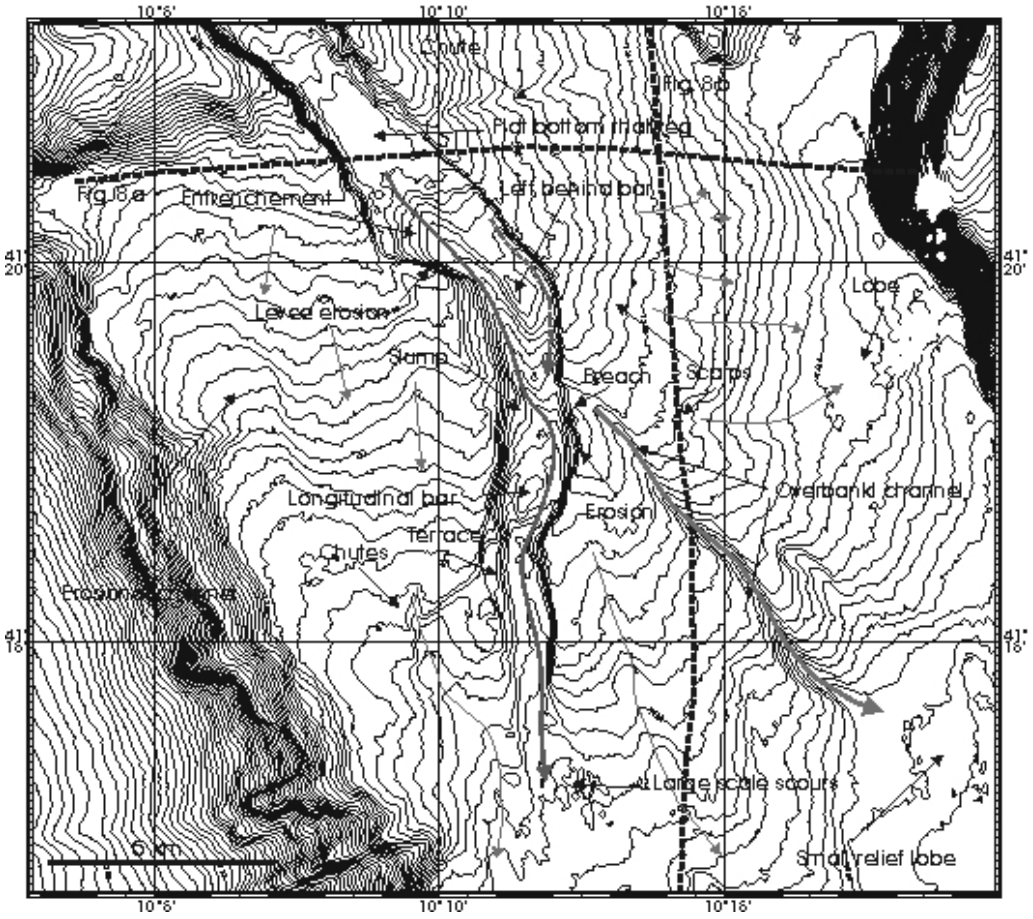

Fig. 8 Multibeam bathymetric map of the Caprera Channel. The main architectural elements described in the text are indicated. The blu lines are small chutes incised on the levees surface. The solid red line is the active thalweg of the channel; the dashed red line is the abandoned thalweg. Contour interval: 10m.

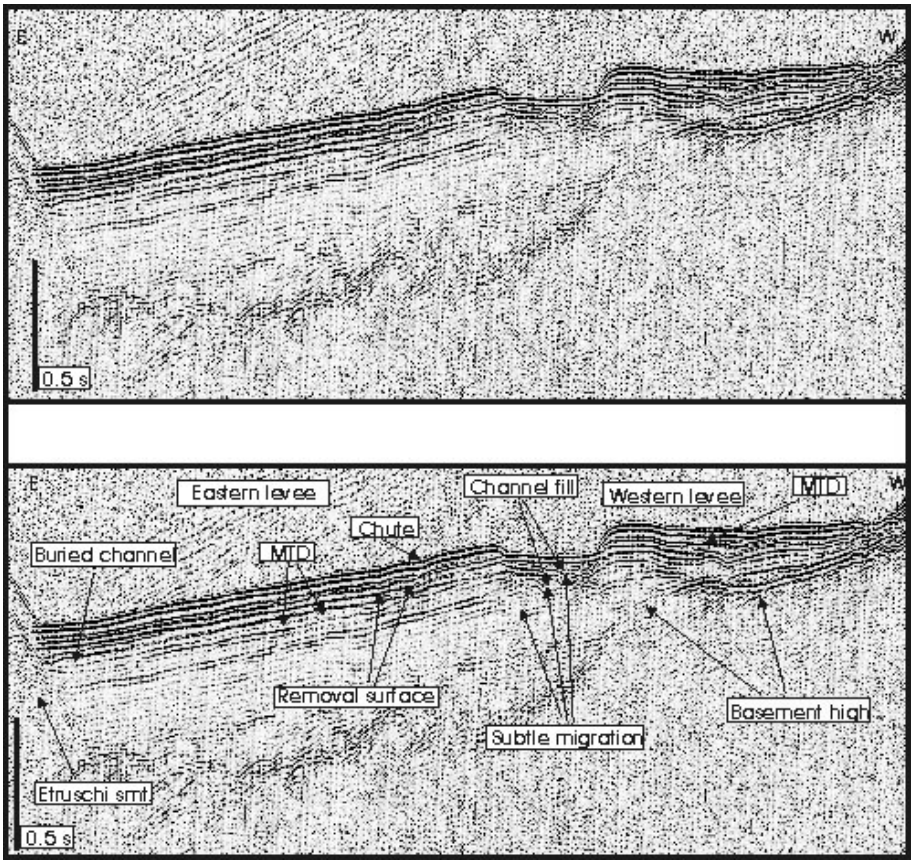

Fig. 8a Crossing sparker seismic profile of the Caprera Leveed channel. Buried removal surface, probably due to levee collapse, are identified on the eastern levee; thin lenses of mass transport deposit (MTD) are present on the subsurface of both levees. See Fig. 8 for the location of the profile.

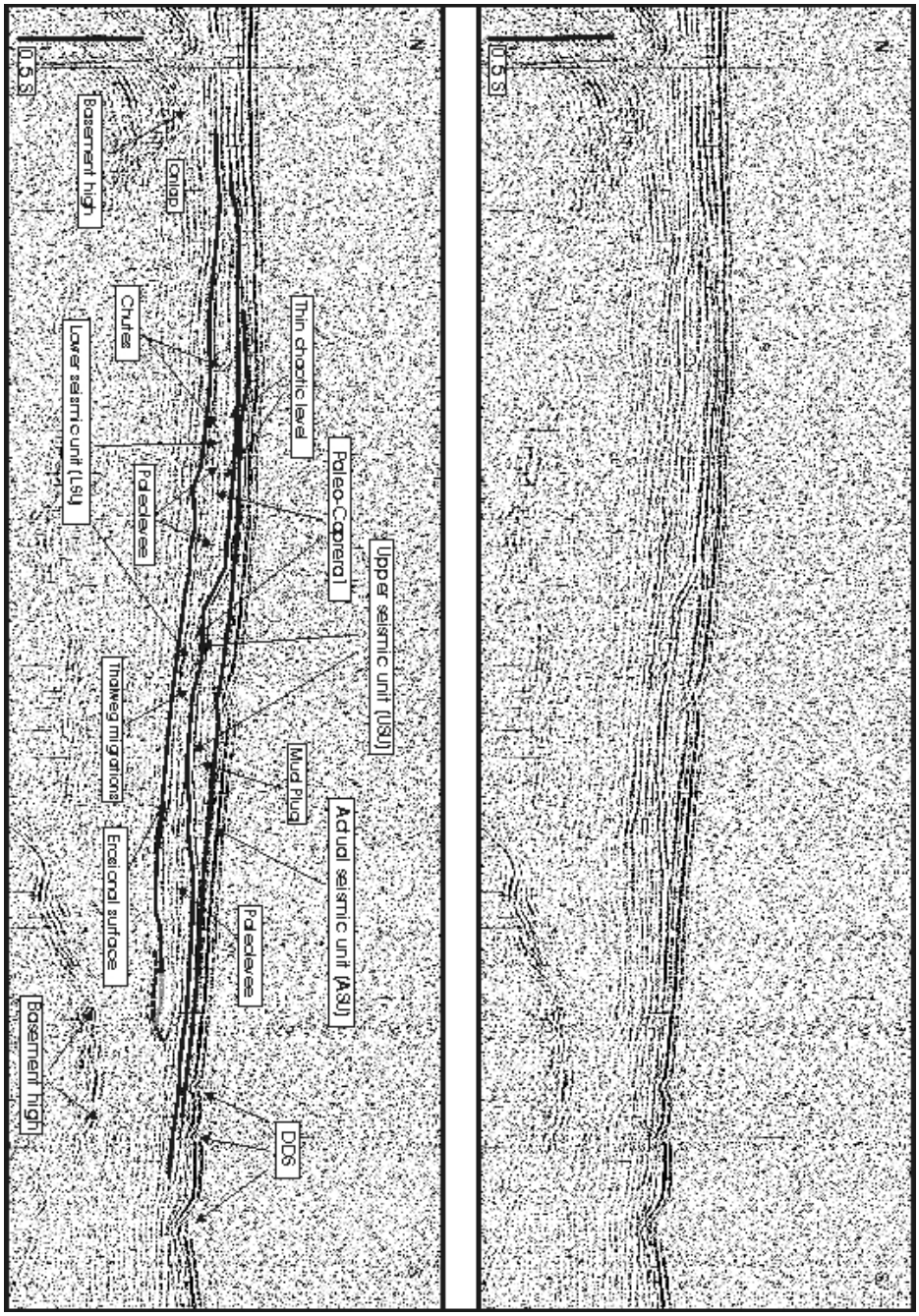

Fig. 8b Crossing Sparker seismic profile on the eastern levee of the Caprera leveed channel. See fig. 9 for the location of the profile.

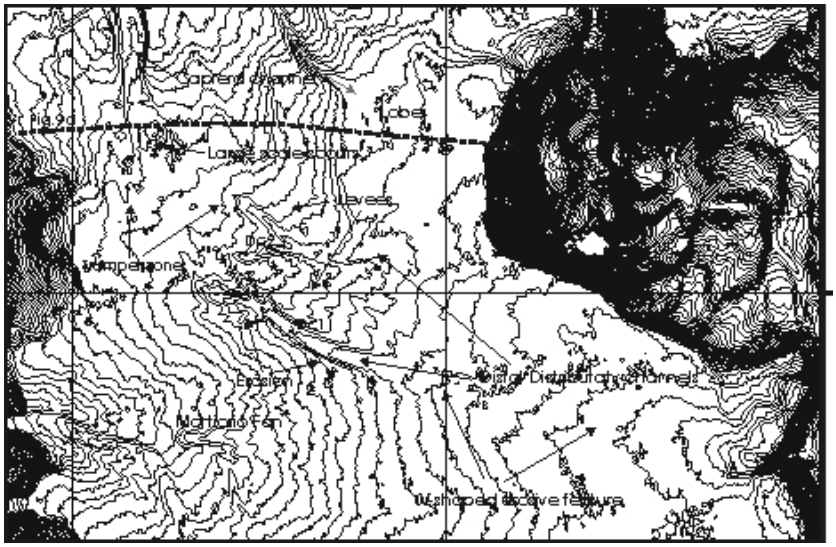

Fig. 9 Multibeam bathymetric map of the distributrary sector of the Caprera system. Contuour interval: 10m

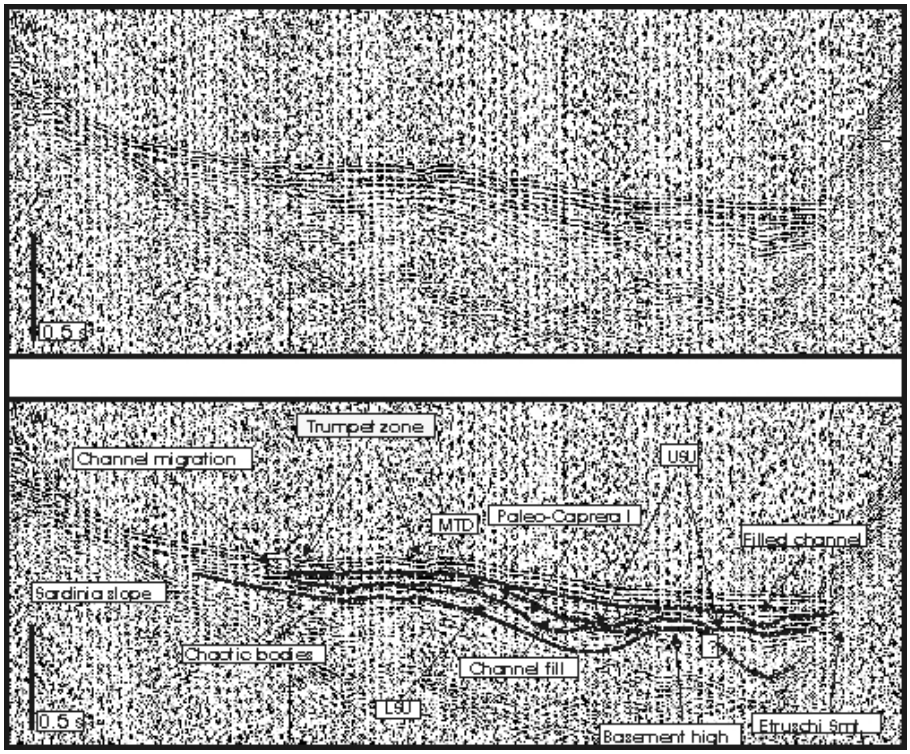

Fig. 9a Crossing sparker seismic profile of the distral distributary sector of the Caprera system. See fig. 9 for the location of the profile.

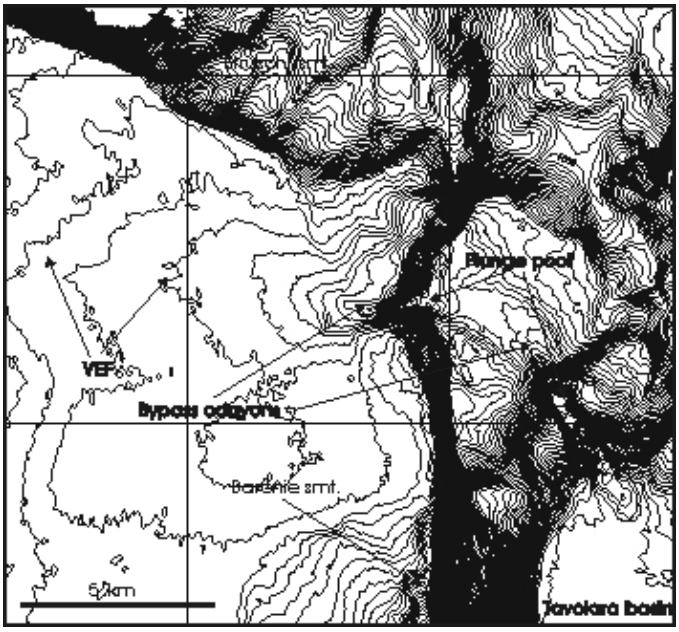

Fig. 10 Multibeam bathymetric map of the bypass sector of the Caprera turbidite system. Contour interval : 10 m

Chapter 4

The Baronie basin

Introduction

The Baronie intraslope basin (BB) trends N-S (Figs. 1, 2) is located southward form the Olbia intraslope basin and is delimited to the south by the Gonone-Orosei canyon system (Figs. 1, 2, 3). The basin is completely bounded seaward by the Baronie seamount (Figs. 1, 2, 3) a large basement horst originated during the rifting phase of the Sardinian margin. The BB is narrow, with an average width of around 11 km, and a maximum width of 14 km in the southern sector (Figs. 2, 3). The BB has a N-S length of around 53 km, flanks landward by a 15 km wide shelf that narrows to 10 km southward (Figs. 2, 3). The continental slope has a width of around 10 km, with a minimum of 6 km and has an average dip of 13°.
The basin plain has an average dip of 0.7° deepening southward from 1300 m to 1800 m water depth (Figs. 2, 3). To the south the BB plain merges with the northern reach of the Gonone-Orosei Canyon system (Figs. 1, 2, 3).

4.1. The Sardinian continental slope and the Baronie seamount slope

The continental slope flanking the BB is around 7 km wide, and is characterized by high slope angle (13°) due to its coincidence with the main extensional faults the basin (Figs. 2, 3) The slope sector between the Posada Canyon and the Gonone-Orosei canyon system is completely devoid of canyons, and with this respects it is a unique case in the entire Sardinian margin. However, in the southern sector of the basin, some small, headless canyon are present (Fig. 3).
South of the Posada canyon, for a sector around 14 km long, the slope of the BB is affected by a complex network of scars (Fig. 4). In the sector facing the Posada fan, the slide scars start at around 400 m of water depth, the slope average a dip of 10°, in the upper sectors with maximum values of 26° in the middle slope sector (Fig. 4). Small gullies and chutes are associated with the slide scars (Fig. 4). At the base of

slope sector, the jagged isobaths of the seafloor, and the low relief mounds (from 30 to 60 m of relief) are interpreted as slide deposits (Fig. 4). An around 1 km wide slide sheet is also recognized in the middle slope sector, rafted down from the steep (19°) upslope sector (Fig. 4).

In the southern sector of the basin, the continental slope is dissected by two headless canyons (Fig. 3, 10). The northernmost one has an around 2 km wide head composed by three narrow reaches starting from water depths of around 350 m (Figs. 3, 10). The other canyon nucleates at around 430 m of water depth, with a narrow amphitheatre-like head scar (Figs. 3, 10). At the base of slope both canyons develops tongue-shaped low relief lobe, around 7 km long aligned with a NW-SE trend (Fig. 10)

4.1.2 The Baronie seamount western flank

The Baronie seamount extends with meridian trend along the upper Sardinian margin for around 100 km, and can be divided in three distinctive sectors: a northern sector, with a subtriangular shape and a N27°E orientation, a central sector with a pure N-S trend, with and a southern sector, also it with a subtriangular shape with a N50° W trend. (Fig. 1). The Baronie seamount has two tops, lying at 162 m and 168 m water depth, characterized by a flat morphology and a thin sedimentary cover (Bellegamba *et al.,* 1979; Fabbri *et al.*, 1973). In the northern sector of the Baronie basin, the seamount has a relief of around 1200 m and around 950 m in the southern basin sector (Fig. 1).

The western flank of the Baronie seamount, that bound the BB is steep, averaging a dip of 27° in the northern sector, and 13° in the southern sector (Fig. 2).

The slope sector facing the Posada fan is characterized by a lower steepness respect to the surrounding slope, averaging a dip of 17°, whereas the surrounding sector average dip of around 30° (Fig. 5). A wide network of slide scarps are localized in the uppermost slope sector of the eamount facing the upper part of the Posada channel, with in some case, associated straight, narrow gullies that reach the base of the flank (Fig. 5). The jagged bathymetry of the portion of the Posada fan close to the Baronie flank could be due to the presence of mass and blocks fallen down from the seamount flank.

4.2 The Posada turbidite system (PTS)

The Posada system (PTS) represents the main turbidite system of the BB (Figs. 2, 3). It is fed by the Rio Posada, a torrential river with a small drainage-basin mainly within a metamorphic terrain (Fig. 2). Previous mapping work of the eastern Sardinia shelf area have show the existence of a submarine delta developed in the front of the Posada river (Ulzega *et al.,* 1987). In addition, in the shelf area, a northern tributary canyon of the Posada canyon was highlighted (Fig. 2). The Posada turbidite system could be divided in its large scale architectural elements (Fig. 3):

1. The Posada canyon in the shelf and slope sector.

2. The Posada fan and Posada fan channel in the base of slope and proximal basin sector.

3. The Distal distributary channel and the V-shaped valley in the distal basin plain sector.

4.2.1 The Posada Canyon

The Posada canyon nucleates in the continental shelf near the front of the submarine delta fed by the homonym river (Fig. 2). From around 1050 m of water depth (shallowest multibeam data available), the Posada canyon has a straight E-W direction that maintains until the base of slope at around 1220 m water depth (Figs. 3, 6). The slight offset of the base of slope entry point, suggests that is controlled by a W-E trending fault with those that mark the base of slope N-S trending faults (Fig. 6). The Posada canyon is deeply incised in the continental slope, with a negative relief of around 750 m (Fig. 6). The canyon thalweg is around 500 m wide, with a maximum width of 750 m at 1210 m of water depth (Fig. 6) and average a dip of 1.3°. A marked, ovoidal plunge pool is present along the canyon thalweg at around 1200 m of water depth (Fig. 6). It has a negative relief of around 30 m, with

a steep headwall toe and a width of around 400 m (Fig. 6). A 7 km long, erosive terrace with a relief of 40 m flanks the canyon thalweg on the left side (Fig. 6).
Both the canyon walls are steep (around 27°) and incised by some rectilinear chutes (Fig. 6). A wide amphitheatre-like scars occupies a large sector of the right wall with associated chutes that reach the canyon floor (Fig. 6). The crossing sparker seismic profile (Fig. 6a) confirms that the canyon walls are strongly affected by mass movement processes. A slide surface followed downslope by the related deposit is present in the left wall (Fig. 6a). The slide deposit has a relief of around 150 m, made up of chaotic reflectors (Fig. 6a). Irregulars reflections characterize the surrounding slope, suggesting that widespread mass wasting processes are promoting the canyon enlargement (Fig. 6a). Active slumping, is also shown by truncated reflectors in the right wall (Fig. 6a). The canyon thalweg is incised into chaotic bodies, interpreted as slump deposits that have reach the canyon floor (Fig. 6a).

4.2.2 The Posada fan

At the base of slope, the Posada canyon develops a small (9 km of radius) radial fan scoured by a fan channel (Posada channel) in the southern sector (Fig. 3).The fan spans the entire width of the basin, being confined eastward by the base of the Baronie seamount. (Fig. 2, 3). The Posada fan elevates of around 200 m with respect to the surrounding seafloor, with a steep apical sector (3°) and a more gentle distal sector, ending at around 1350 m of water depth (Fig. 7).

-Posada fan: nothern sector

In northern sector of the Posada fan, a series of amphitheatre-like scarps are present outside from the sharp turn of the Posada fan channel (Fig. 7). A headless channel, around 1.5 km wide develops downfan from the wider scars, and originates a small relief lobe in front of is mouth (Fig. 7). Large scour depressions are identified at the base of the largest scar, with diameter between 300 and 500 m and a negative relief of around 20-25 m (Fig. 7). The scour depressions has a crescentic apparence shape with a steeper headwall forming the concave side (Fig. 7). Low relief scars are also

identified shed in the middle and the distal parts of the fan, with in some case associated small plunge pools (Fig. 7).

-The southern fan sector: Posada fan channel

The southern sector of the Posada fan is scoured by the Posada fan channel (Fig. 8). At the base of slope, the fan channel maintain the W-E trend of the feeder canyon, but subsequently, in the apex of the Posada fan, it experience an abrupt 90° turn (Fig. 8). In the bend sector the channel shows a negative relief of around 70 m, with steep channel walls (Fig. 8). Downfan from the turn, the channel widens abruptly showing two distinct thalwegs (ThwA & ThwB) separated by a 3.5 km long sedimentary ridge (Fig. 8). The ThwA, situated around 30 m above the TwhB, is V-shaped, flanked leftward by a 20 m relief scarps that loose negative relief downfan, dying out at around 1320 m of water depth (Fig. 8).

The TwhB has an initial width of 250 m, that enlarge progressively downslope and is flanked by low degree, 30 m of relief scarp (Fig. 8). The ThwA probably represent the old Posada channel pathway (Posada1) that is actually abandoned, whereas the ThwB represent the active thalweg of the Posada channel (Posada2) (Fig. 8). Beyond 1300 m of water depth, the Posada2 channel develops an entrenchment sector and narrows to around 200 m of width, confined by steep lateral scarps with dip of 5° and relief of around 45 m (Fig. 8).

At around 1350 m of water depth, the Posada 2 channel is abruptly interrupted by a steep, rectilinear scarp (RS) (Fig. 8). The RS scarp roots at the base of the slope, is very steep (23°), around 3 km long, with a relief of 90 m (Fig. 8). This seafloor feature is interpreted as the headwall scarp of a large mass failure that has affected the southern portion of the Posada fan. The eastern sidewall of the slide scar coincides partially with the relict of the left wall of the Posada 2 channel (Fig. 8). Downfan from the RS scarp, the post-failure Posada channel pathway (Posada 3) flows into the new accommodation space created by the mass wasting processes as a subdue, wide U-shaped feature (Fig. 8). The Posada 3 channel is forced to flow around the slide-related topography, and the channel floor exhibits slightly jagged isobaths, due to the presence of large blocks that are still part of the MTD (Fig. 8). The low relief terrace on the left side of the channel, reveal the erosional character of the Posada 3 channel on the MTD (Fig. 8) The Posada 3 channel is imposed

above a thin lense of chaotic reflectors, interpreted as part of the MTD (Fig. 8a). Above the MTD, a thin blanketing, interpreted as a channel infill, reveals that the Posada 3 channel has also a subtle depositional character (Fig. 8a). The MTD that flank to the left the Posada3 channel consists of chaotic reflectors (Fig. 8a), whereas the infilling style of the basin plain consist of high amplitude, parallel reflectors scoured by very low relief channels (Fig. 8a). A series of buried, small channels are evident at varying depths below the seafloor (Fig. 8a). In some cases, the channels show thin depositional levees, with reflections dipping predominantly eastward (Fig. 8a) and appear predominantly filled with chaotic reflectors, indicating a coarse nature of the sediment infill (Fig. 8a).

To the east of the MTD, a narrow U-shaped thalweg, flanked by a 25 m of relief scarps is present, and is in line with the Posada2 channel upslope (Fig. 8). This thalweg is interpreted as a relict of the Posada 2 channel pathway antecedent to the mass failure of the Posada fan. The Posada 3 channel ends at around 1450 m of water depth, in correspondence of two small, elliptical mounds, that force the narrowing of the thalweg to just 400 m of width, concomitant with a marked V-shaped profile (Fig. 9). On the left side of the channel, an around 2 km wide lobe-shaped intrachannel sector is present, and is scoured by many small chutes that join donwfan into the V-shaped valley (Fig. 9). The crossing seismic profile of fig. 9a show the thick chaotic lens related to the MTD being eroded by the Posada 3 channel. The base of the MTD appears erosive on a lower seismic unit that is made of faintly laminated reflectors, likely consisting of fine grained sediments (Fig. 9a). The intrachannel lobe is emplaced over the MTD, and is interpreted as deposited by the Posada 3 channel following the mass wasting process (Fig. 9a). The eastern sector of the basin consists of high amplitude reflectors that are cut by a single erosional channel, representing the apical portion of the V-shaped valley (Figs. 9, 9a). A series of buried channels are present below the seafloor, shows predominantly erosive characters, with low relief profiles and filled by chaotic facies, although in some cases, thin levee units are present (Fig. 9a).

4.2.3 The Posada system: distal distributary sector

The distal distributary sector of the Posada turbidite system consists of a network of low relief channels, separated by lobe-shaped elevated areas (Fig. 9). The channels

show different characters, with both erosive and depositional features, and show a general NW-SE trend , joining downslope into the V-shaped valley (Fig. 9). Due to the large number of channels and their high variability, it has been very difficult to follow individual small channels and to determine their relationship.

The channels are not disposed in a braided pattern, but instead are straight, with length less that 5 km, generally 10-15 m in depth and around 100 from 300 m of width (Figs. 9, 10). Some channels appear to form a small bifurcating distributary system, whereas others appear as discontinuos segments not clearly related to any other channel features (Figs. 9, 10). Erosional channels, with both V-shaped and U-shaped thalwegs seems to be predominant, but some few channels are flanked by low relief levees (Figs. 9, 10).

Numerous, small, mainly erosive channels, filled with chaotic reflectors are identified starting from around 0.2 s below the seafloor (Fig. 9b). In some cases, especially in the eastern sector, the channels are characterized by wide, low relief erosional surfaces, in other cases the channels appears as discrete, narrow, V-shaped erosive features (Fig. 9b). The overlying most recent lobe-sector is build above a narrow buried channel, being laterally eroded by modern distributary channels (Fig. 9, 9b).

4.2.4 The V-shaped valley

The V-shaped valley is a 5 km wide trough that spans in the eastern part of the basin, flanked by the Baronie seamount slope. The submarine valley roots as a low relief erosive channels that join at around 1500 m of water depth (Fig. 9). The valley tends to deepens proceeding downslope, from around 100 m to 150 m at 1750 m of water depth (Fig. 10). It maintain a dip of around 0.5°, with an increment to 2° upslope from the junction with the Gonone-Orosei canyon system (Fig. 10). The valley is predominantly fed axially by the numerous distributary channels of the Posada system, and act as the lateral escape pathway to the deeper level of the Gonone-Orosei canyon system.

The erosional character of the actual submarine valley is suggested by the truncated high amplitude reflectors of the basin plain (Fig. 10a) and by the narrow erosive terrace that flank the trough to the left (Figs. 10, 10a). Wide, filled erosional surfaces, representing previous stages of the V-shaped valley are buried starting

from depth of around 0.15s below the seafloor (Fig. 10a). The paleo-valleys erode faintly layered parallel reflectors, interpreted as distal, basin plain sheet turbidites (Fig. 10a). The paleo-valleys are filled with intrachannel lobe deposits, that are in turn eroded by smaller scale erosive channels (Fig. 10a). An eastward migration and progressively narrowing of the erosional surfaces are observed (Fig. 10a).

Only in the very distal sector of the BB, the V-shaped valley receives sediment input from cross-basin, slope derived fairways (Fig. 10). Here, infact, a series of headless canyon incised on the Sardinian slope give rise at the base of slope to depositional lobes, scoured by intra-lobes channels that join V-shaped valley (Fig. 10). The jagged bathymetry of the lobes surface, and the planform tounge-shaped profile (Fig. 10), lead to interpreted these sedimentary bodies as formed mainly by debris flow deposits, or slump-derived high concentration sediment-gravity flows. Due to the very low relief of the lobe is, however, difficult to interpret the nature of the sediments that made up the lobes by the seismic analysis (Fig. 10a).

Discussion

The Posada Turbidite system

The PTS is developed in the Baronie intraslope basin, laterally bounded by the continental slope of Sardinia and by the Baronie seamount western flank. The BB can be considered as a partially silled basin with lateral escape path represented by the V-shaped valley that ends into the Gonone-Orosei canyon system (GO). The GO represent the fairways that allow the sediments discharged into the BB to reach the deeper sectors of the Sardinian margin.

- **Posada canyon**

The PTS is fed by the homonymous river, so it can be assumed that hyperpycnal, long-duration flows with linked sustained turbidity currents are the relevant type of gravity flows that fed the BB.

However, as the many slide scars and slump deposits identified along the Posada canyon and continental slope reveal, and despite the disagreement among the various authors, on the possibility of the flow transformation from a debrites to turbidity currents (Marr *et al.,* 1999), the importance of slump related surge-type turbidite currents cannot be ruled out. The Posada canyon could also be the situs of temporary storage for longshore derived sandy deposits, that being removed by floods, storm or by currents erosion.

The erosive terrace flanking the canyon floor may be the result of a rejuvenation of the erosion, as a consequence of the change in the base level due to subtle tectonic-activity or changes in discharge. Considerable discussions has arisen about the formation of plunge pools in submarine canyons (Garcia & Parker, 1989; Lee *et al.,* 2002). The origin of the plunge pool feature identified on the floor of the Posada canyon could be explained as the result of scouring during submarine debris flows. The channel damming by mass wasting of the canyon walls, periodic rockfalls of mass and big block can act as obstalcles for the flows, triggering the undercutting erosion of the following gravity flows around the obstacles.

- The Posada base of slope fan

The small width (less than 15 km) of the BB has a strong effect on the shape and the evolution of the Posada fan, preventing the development of a typical unconfined radial base of slope fan and forcing the entire turbidite system to develop its architectural elements parallel to the basin margins, and orthogonal to the direction of the feeding fairway.

The jagged bathymetry of the Posada fan sector closed to the Baronie seamount flank and the unusual low degree of the facing seamount slope, could represent the results of the interaction between the sedimentary flows with the opposing, bounding slope. Experimental work has shown that the body of the gravity flows are not able to surmount topography that is more than about 2.5 times the body thickness (Rottman, *et al.* 1985) or 1.5 times the head high (Muck & Underwood, 1990) and being effectively blocked. However, both theoretical and experimental work has shown that flows are capable to climb an opposing slope (Muck & Underwood, 1990). The flow stratification (FS) play a key role on the behaviour of the flow approaching a bounding slope, and if the FS is sufficient pronounced, the decouple of the flows along a dividing streamline can take place (Kneller & McCaffrey, 1999). The denser basal parts of the flows is deflected parallel to the slope, while the less dense upper parts run up the slope, and subsequently it collapse back down the slope (Kneller & McCaffrey, 1999). The flow that run up the slope can produce instability on slope sediments, with their subsequent remobilization as low-efficiency flows (i.e. grain flow or non-cohesive debris flow*)* that quickly comes to rest at the base of slope (McCaffrey & Kneller, 2004).

The Posada fan is made up of two distinct sectors: the nothern sector where dismantlement processes are dominant and the active upper fan located in the southern portion, dominated by a fan channel.

The dismantlement of the nothern sector could be the results of induce cyclic stress on the superficial sediments by the Posada channel overbanking flows. When a flow approaching an obstacles, or a sharp turn (as the case of the Posada fan channel), the height of flows become elevated because of the conversion of kinetic energy into potential energy (Parson *et al.,* 2003): this process is called superelevation (Hay, 1987; Peakall *et al.,* 2000). The result is that a turbidity currents can more easily abandon a confining channel, or flow over a steep obstruction (Kneller & Buckee,

2000). The high turbulence associated with spilled flows may trigger instability on the superficial sediments of the fan, leading the formation of wide scars and flute-like scours as documented both in modern small fan (Normark *et al.,* 1979) and outcrop examples (Lien *et al.,* 2003).

The Posada fan channels evolution

The morphology and the evolution of the Posada fan channel is controlled by the combination of the basin geometry and mass wasting processes. The sharp turn of the Posada fan channel in the upper sector of the submarine fan is reasonably the results of confinement by the lateral bounding slope of the Baronie seamount. The subtle westward migration of the Posada 1 channel to the active Posada 2 channel instead, can be presumably considered as the result of an internal process of the turbidite system.

By contrary, the passage from the Posada2 channel to the Posada 3 channel is clearly forced by the mass wasting episode that has affected the southern sector of the Posada fan. Additionally, the shape of the RS failure surface has been in turn controlled by the previous Posada 2 pathway, since its sidewall coincides, at least in part, with the weak preexisting surface of the Posada 2 left wall.

The channel entrenchment located just upslope form the toe of RS scars is the consequence of the lowering of the seafloor by the mass wasting. The lower base level promotes infact, an acceleration of the sedimentary flows, with velocities that exceeds the erosion threshold of the channel sediments. The slope adjustment is achieved primarily via entrenchment, resulting in a retrogressive erosion with a consequent upslope migration of the knickpoint (Pirmez & Beaubouef, 2000).

The mass wasting episode has also create a new accommodation space for the Posada channel: it is not bounded by lateral scarps, but rather the mass transport deposits (MTD) and the continental slope act as “containers” for the sedimentary flows. The mass wasting episode has forced the transition of the sedimentary flows from the confinement of the Posada 2 channel, to the less confined post-failure environment.

The MTD has also created seafloor topography, with several meter high mounds that deflect turbidity currents around the depositional mounds. This particular setting can represent the modern equivalent of the mass transport complexes

described by Pickering & Corregidor (2005) on the Miocene of the Pyrenees. The erosive character of MTD on the lower sedimentary units suggest a good mobility and fluidity of the mass sediment failure (e.g. Badalini *et al.,* 2000).

The large slide that has affected the Posada fan reveals the reorganization of a turbidite system through mass wasting processes could affect also deep sea fan in a passive margin as the case of the eastern Sardinian margin. A very steep continental slope, closely spaced from the submarine fan, despite the quiescent tectonic activity could promote instability and mass wasting in a similar way of the trust-related tectonic . Much of the literature regarding the MTD complex as a major component on the evolution and on the depositional style of deep-marine clastic system are infact focused on active basin, where tectonic processes provide a first-order driver on the fan growth (Pickering & Corregidor, 2005; Grecula *et al.,* 2003).

The distal distributary sector

At variance with the classical model of small sandy turbidite systems (Normark, 1978; Walker, 1978) where the distal sector of the fan is unchannalized and is the loci of prevalent depositional processes, the distal sector of the PTS remaining highly channalized far away from the mouth of the main fan channel and no channel-mouth lobe (CML) is recognized.

The distal regions of some submarine fans are often covered with intricate patterns of low relief, low sinuosity channels, as seen for example in the distal end of Gulf of Cadiz submarine fan (Akhmetzhanov *et al., in press*). However the process by which the turbidity currents are able to create a distributary network of channels remains only partially understood. The distributary channels of the PTS can be either depositional, predominantly erosional, or a combination of the two characters. Their dynamics are probably not the same of the major feeder, more stable channel and they are probably easily abandoned by shifting and reactivated. The channel brancing may results from variability in previous small scale topography, that can redirect the flow and promote lateral shift (as suggest for similar features by Gervais *et al.,*2006). In modern deep water environment, lobes are defined on the basis of morphology, generally lobate in plainview. They are interpreted as the result of flow freezing due to depletion at the termination of the channels (Normark, 1970; Mutti & Normark, 1991). In the PTS case lobe-shaped deposit are not founded in the front

of mouth of the channels, but are thought as correspondents to a series of discontinuous intrachannel lenses deposited on the lateral side of the distributary channels and being subsequently laterally eroded by the other channels or by smaller scale chutes.

The low relief morphology of the present day seafloor distributary channels , with represent their initial stage before they were eroded or filled. Once the flow is concentrated of the topographic low of the young-stage channel, the channel tends to narrows and deepens: the discrete V-shaped channels buried below the seafloor represent the "mature" stage of these elements.

Not all the channels are purely erosive, but in some cases show small irregular levees, indicating also a subtle depositional activity. As suggest by Piper *et al.,* 1999 for the lower part of the Huemene fan valley, these kind of small levees are probably built by deposition of the lateral, less erosive part of the flow, and not by a "pure" channel spilling. Experimental works lead by Marr *et al.,* (2001, 2005), has show the formation of several small, mildly sinuous leveed channels in a tank-scale mini fan. These channels display distal lobes, levee overflow splays and incipient avulsion (Marr *et al.,* 2005). The Posada turbidite system could provide a nature-scale modern analogue of small scale experiments, however, the evolution and overall morphologies of the distal channels elements, are in this case also strongly controlled by the basin confinement and by the presence of the escape fairway to a lower level.

The V-shaped valley

The lateral bounding slope of the Baronie seamount could play an important control on the behaviour of the sedimentary processes that act into the V-shaped valley. Field and experimental results have shown that a characteristic turbidite deposits pattern is produced by waning flows confined by a lateral slope (Amy *et al.,* 2004). Experiments has demonstrate dissimilar rates of flow expansion on the obstructed and unobstructed sides of the currents as the currents leaves the point source (Amy *et al.,* 2004). The bounding effect of the lateral slope allow the part of the flow close to the slope to preserve a higher concentration and higher SLFR (Suspension-Load Fallout Rate) compared with basinal locations (Amy *et al*., 2004). That means for a same flow concentration, the flows closer to the slope shown a weakly

depletive flow concentration due to the spreads out over a smaller area, whereas the flow portion away from the slope, due to the spreads out over a larger area, leading to highly depletive flow concentration, and deposit more sediments (Amy *et al.,* 2004). That could used to explain why the V-shaped valley, with its marked erosional character, is emplaced in the eastern sector of the BB, closely to the lateral bounding Baronie seamount flank.

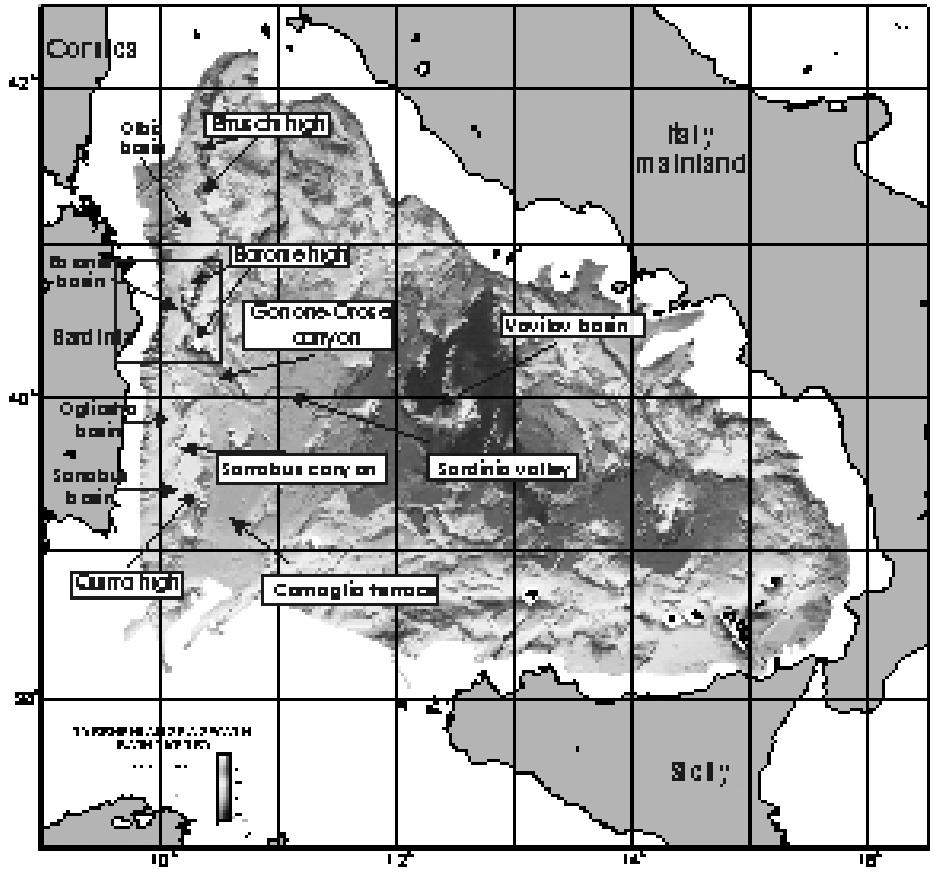

Fig. 1 Colour-shaded map of the Tyrrhenian sea from multibeam data. Depths are colour coded. The box correspond to the map of th Baronie basin (BB) in fig. 2

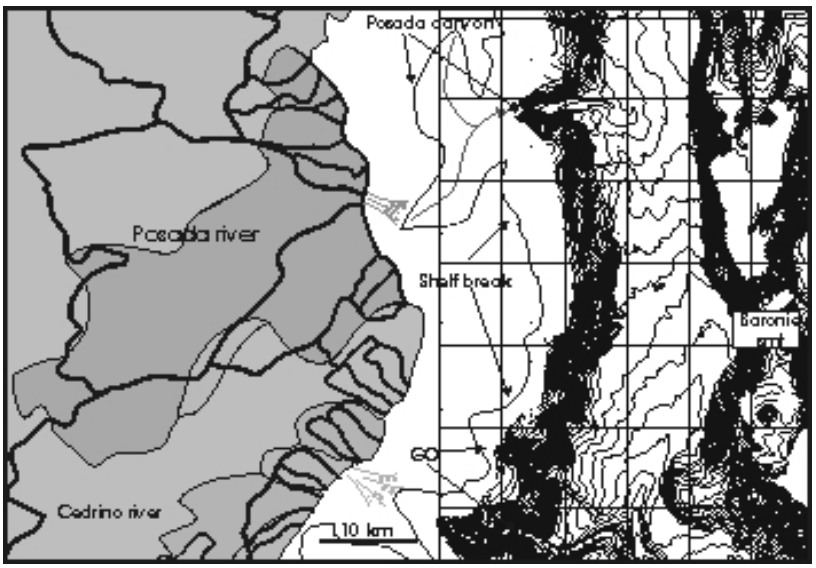

Fig. 2 Multibeam bathymetric data of the Baronie Basin. Contour interval: 50 m. GO: Gonone-Orosei canyon. The shelf break (dashed line) is taken from Bellagamba et al., (1979), whereas the location of the submarine deltas is from Ulzega et al., (1987). The map of the Sardinia Island with a schematic lithological subdivision has been simplified from Ulzega et al., (1987). The river drainage basins are also indicated with a solid black line.

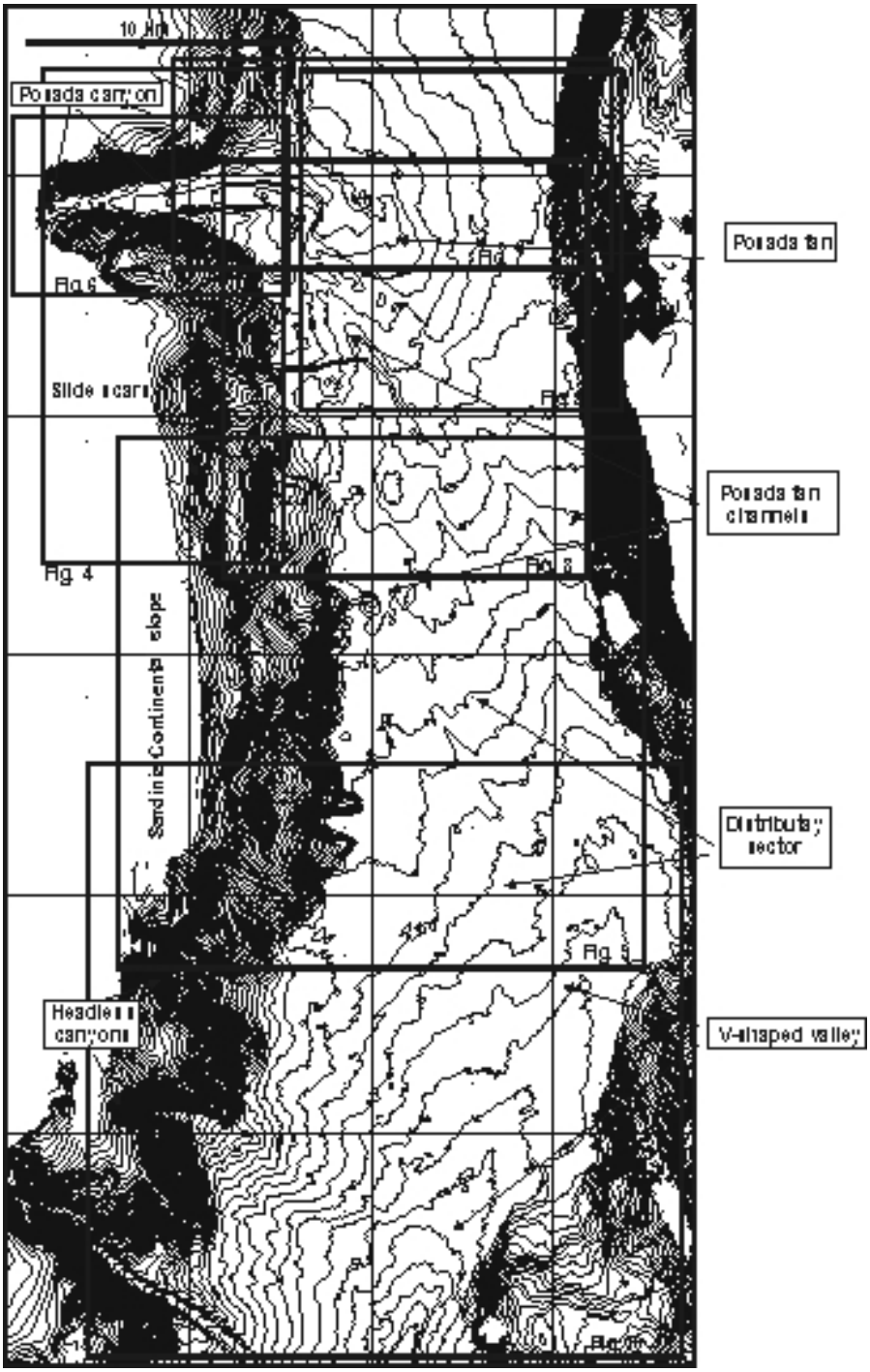

Fig. 3 Multibeam bathymetric map of the Baronie basn. The main large scale elements of the Posada turbidite system are also indicated. Contour interval: 25 m.

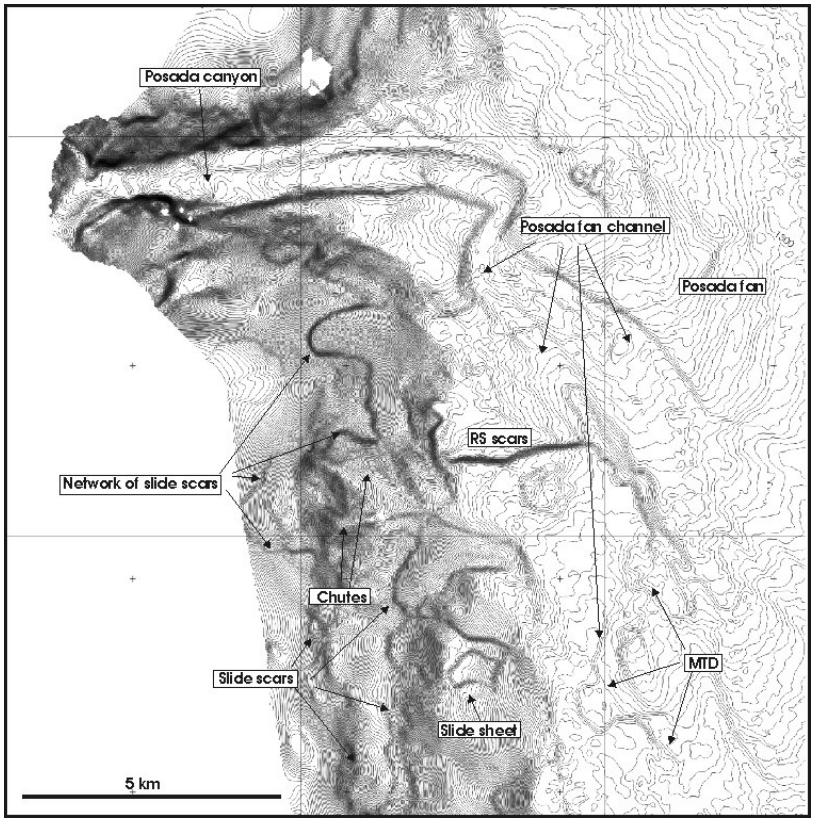

Fig. 4 Multibeam bathymetric map of the continental slope of the Baronie basin flanikng the Posada fan, the Posada fan channels. Contour interval: 5 m

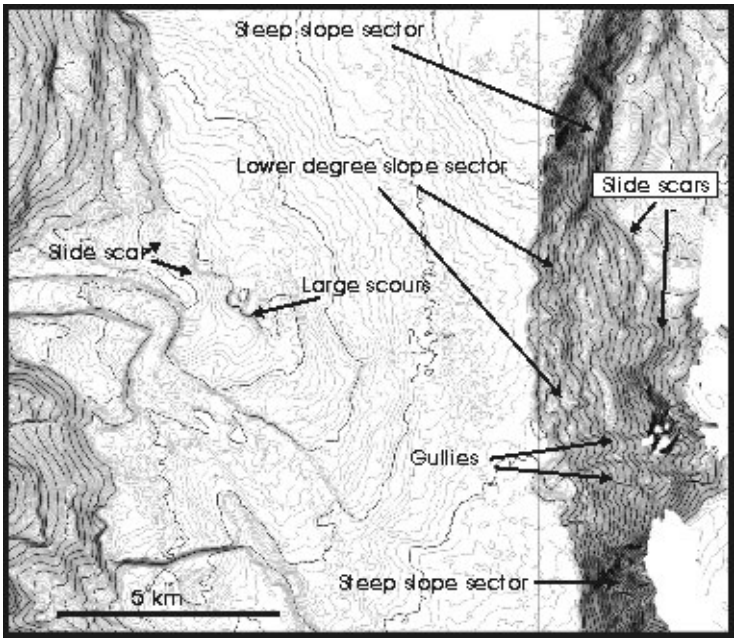

Fig. 5 Multibeam bathymetic map of the Posada fan and the bounding slope of the Baronie seamount. Contour interval: 5m

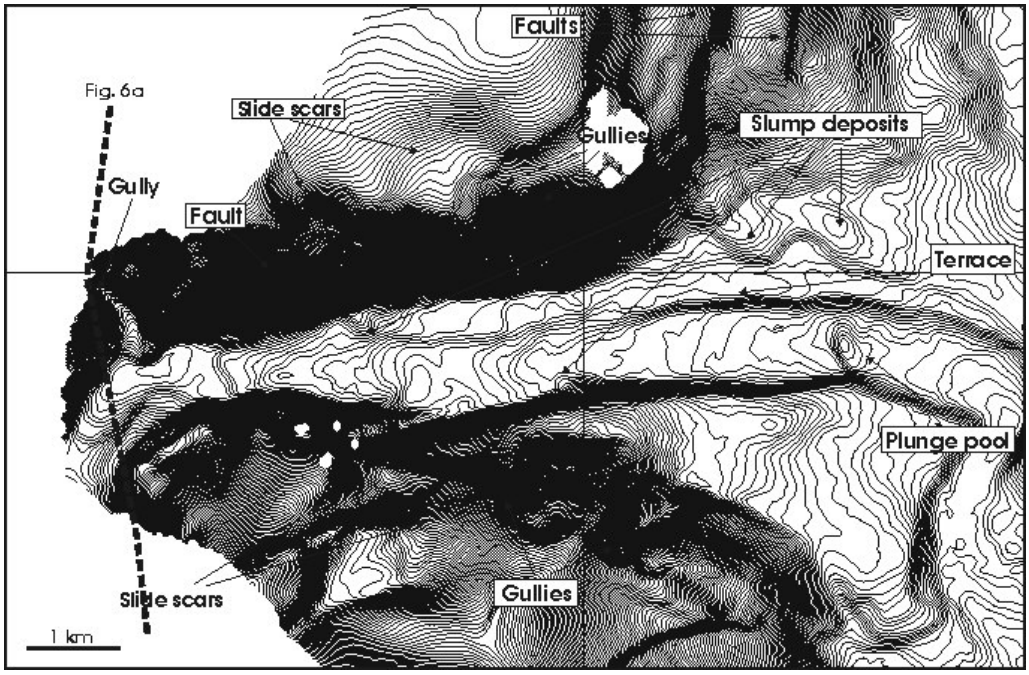

Fig. 6 Multibeam bathymetric map of the Posada Canyon. Contour interval: 5 m

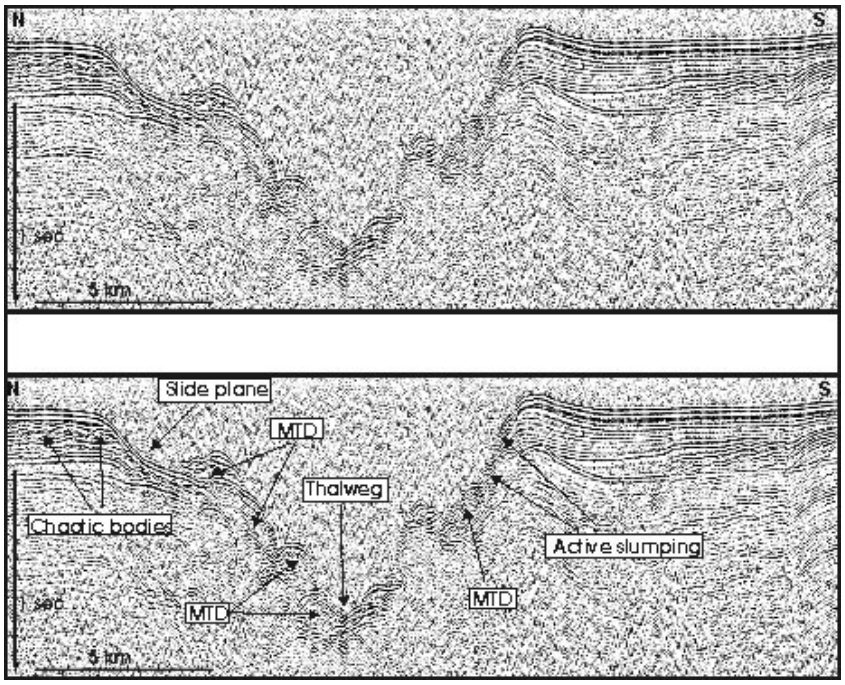

Fig. 6a Sparker seismic profile of the Posada canyon. See Fig. 6 for the location of the profile.

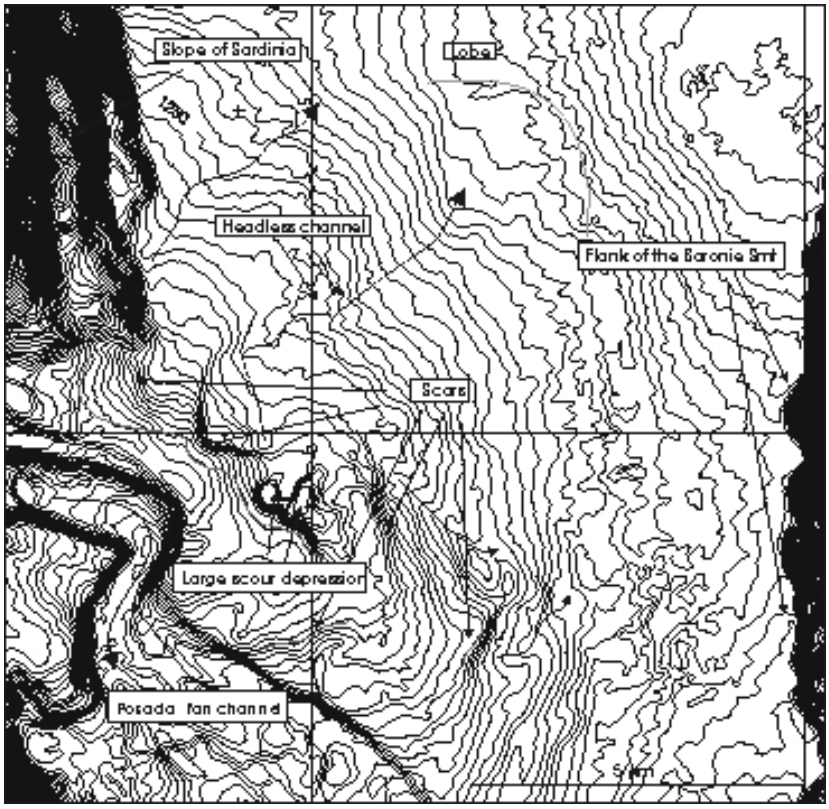

Fig. 7 Multibeam bathymetric map of the nothern sector of the Posada deep sea fan. Controur interval: 5 m

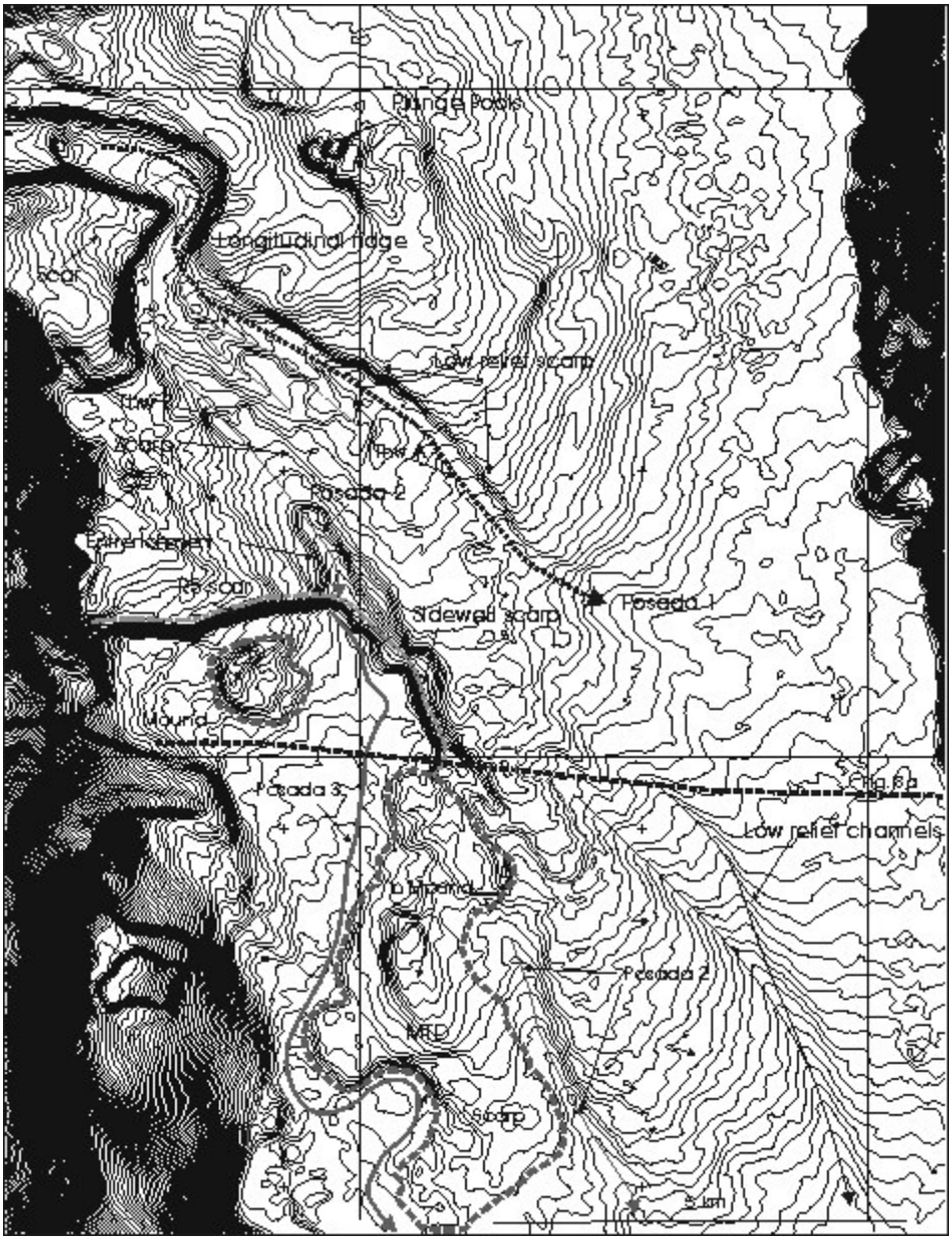

Fig. 8 Multibeam bathymetric map of the nothern sector of the Posada deep sea fan. Controur interval: 5 m

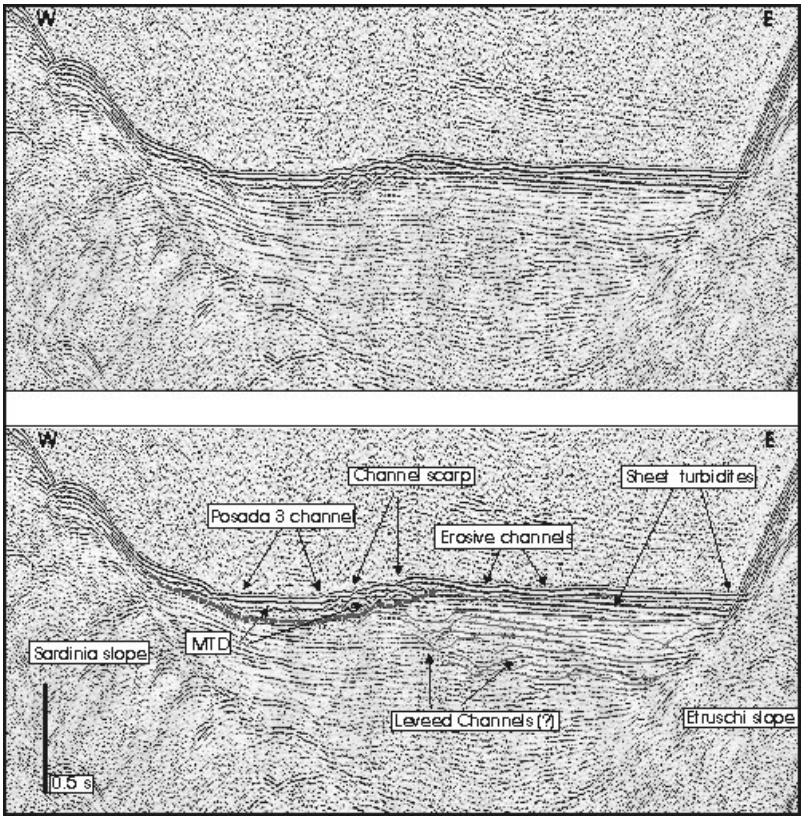

Fig. 8a Crossing sparker seismic profile of the middle sector of the Posada fan channel. See fig. 8 for the location of the profile.

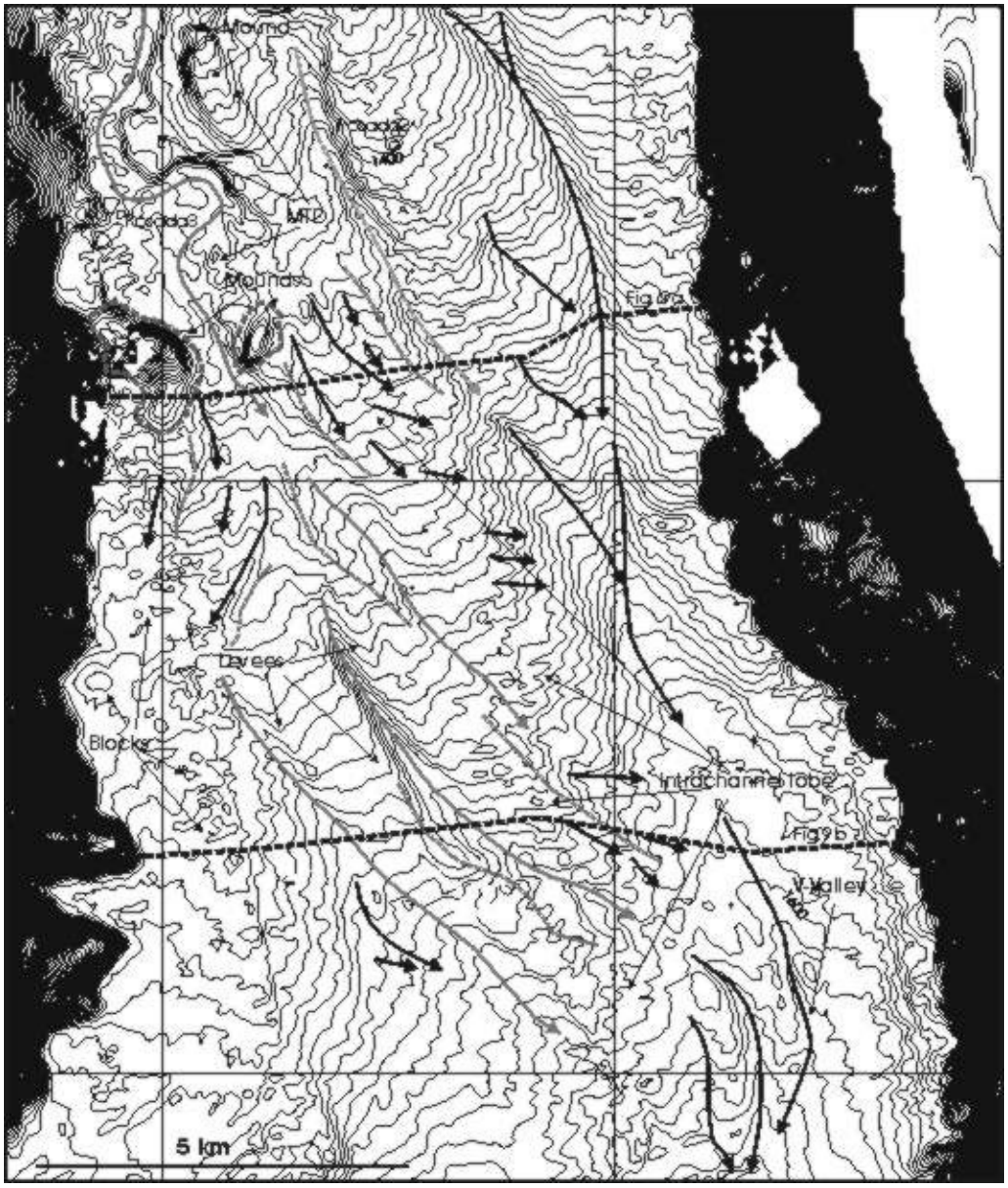

Fig.9 Multibeam bathymetric map of the distributary network of the Posada Turbidite system. Contour interval: 5m

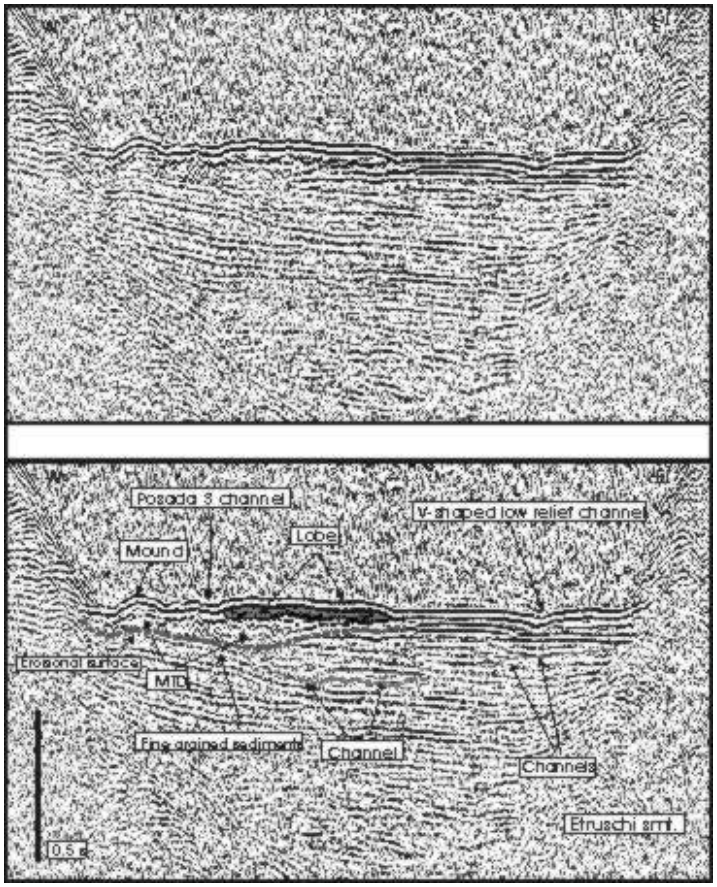

Fig. 9a Crossing seismic profile of the distal sector of the Posada fan channel. See Fig. 9 for the location of the profile.

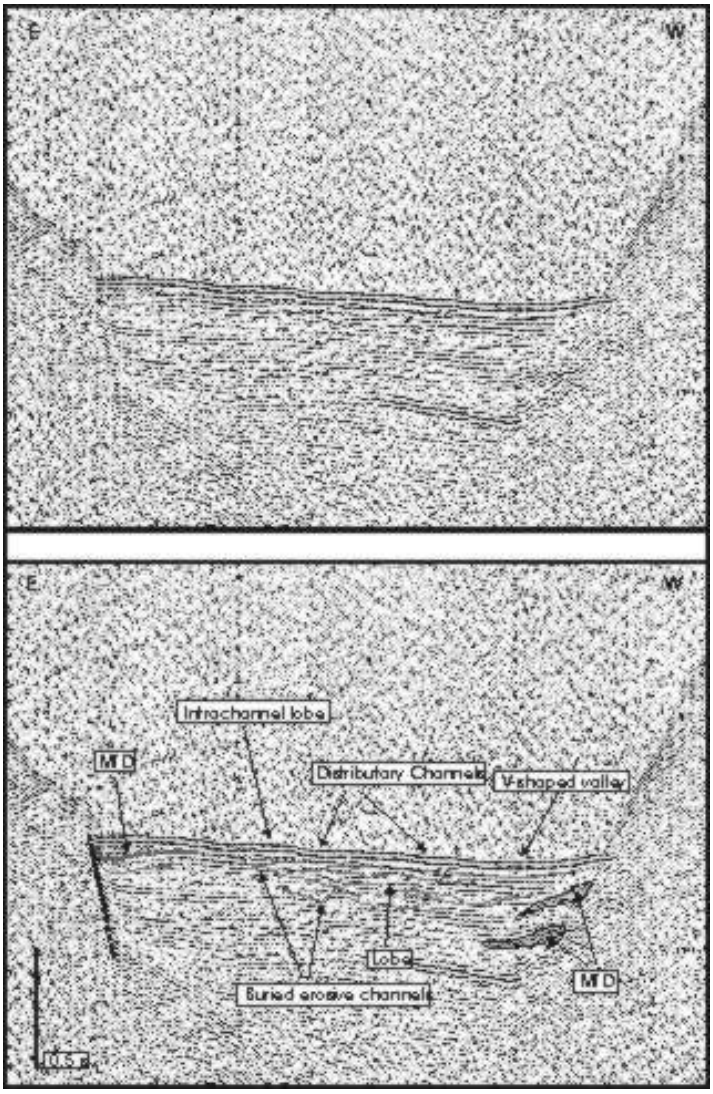

Fig. 9b Sparker seismic profile of the distributary sector of the Posada turbidite system. See fig. 9 for the location of the profile.

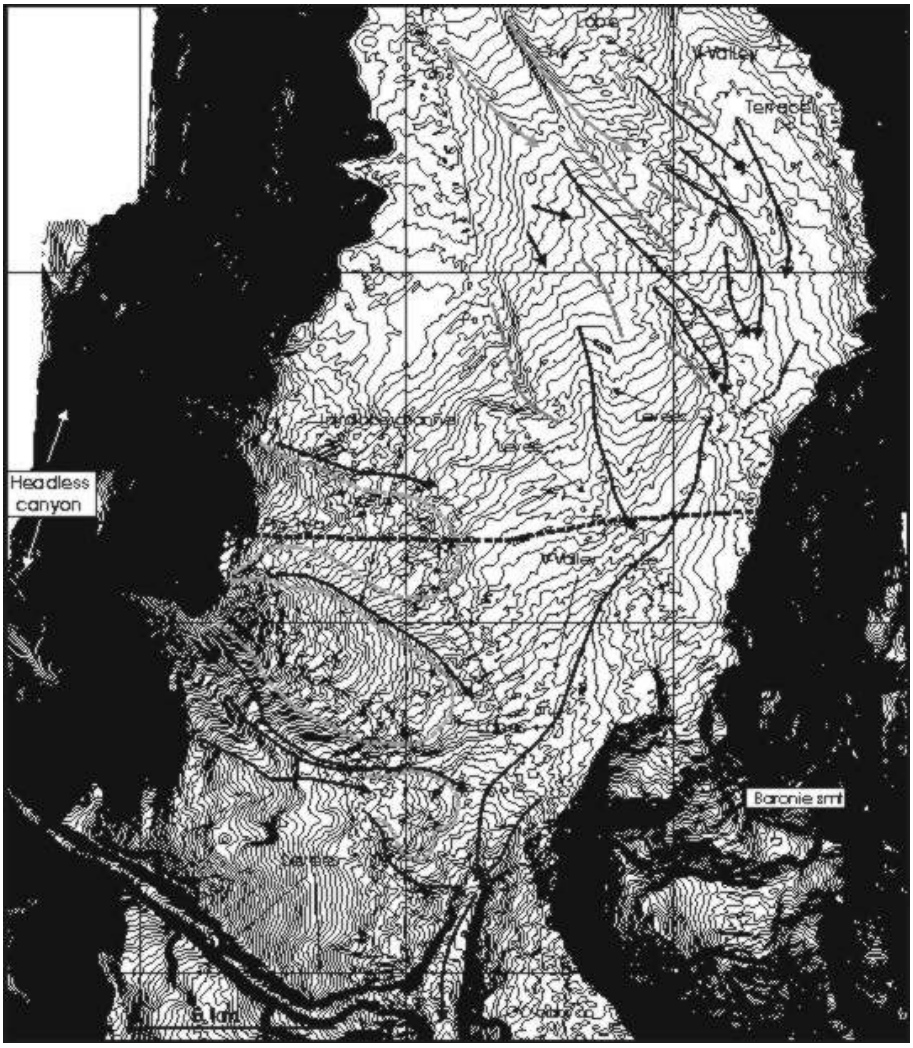

Fig. 10. Multibeam bathymetric map of the distal distributary sector of the Posada turbidite system and the V-Shaped valley.

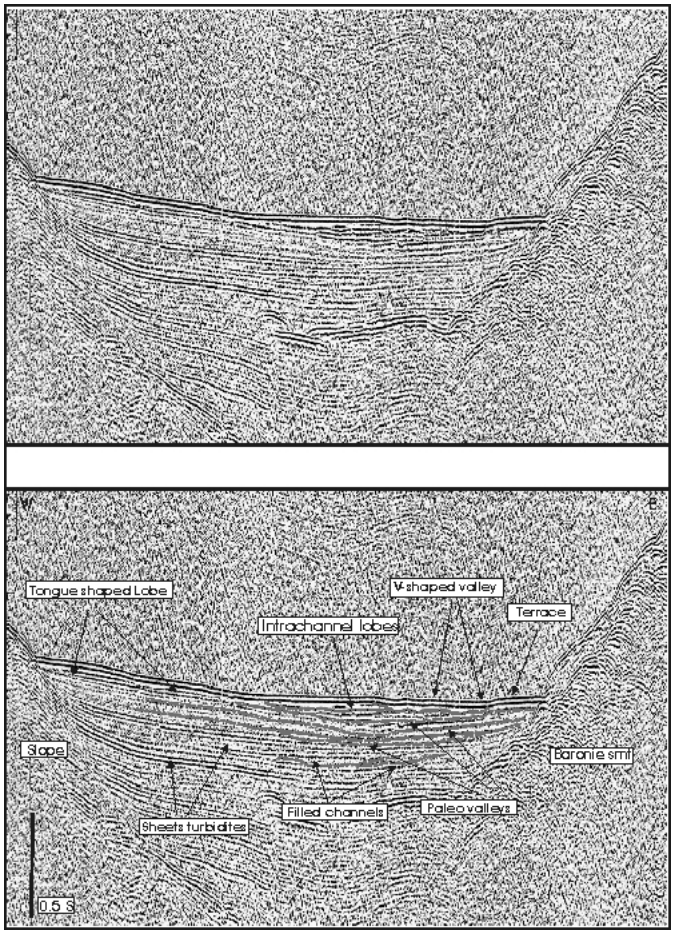

Fig. 10a. Sparker seismc profile of the distal distributary sector of the Posada Turbidite system and the V-shaped valley. See Fig. 10 for the location of the profile.

Chapter 5

The nothern Ogliastra basin and the Arbatax turbidite system

Introduction

The Ogliastra intraslope basin (OB) is situated in the southern sector of the eastern Sardinian margin, southward of the Gonone-Orosei canyon system (Fig. 1). The basin has a length of around 80 km, and a width ranging between 13 and 20 km (Figs. 1, 2). The basin is bounded northward by the 100 m high levee of the Gonone canyon, and southward by the San Lorenzo High (Fig. 2). The tectonic lineament of the Quirra High confines the OB to the east (Fig. 2). The Quirra high is a N-S trending tectonic horst inherited from the rifting phase, has a length of about 80 km with a relief respect to the OB plain of around 450 m, and is cut by the Sarrabus intraslope canyon (Figs. 1, 2, 3). The Sarrabus intraslope canyon, running along the axis of the OB represents the fairway to the deeper sectors of the margin (Figs.1, 2). The continental slope of the OB has a maximum width of around 18 km in the northern sector, and narrows southward to 7 km (Fig. 2). The OB continental slope average dip of 4/7° in the northern sectors, steepens progressively southward to 20°, reaching the maximum value of 33° in the lower sectors south to the Arbatax canyon (Figs. 2, 3).

5.1 The nothern sector of the Ogliastra basin:continental slope

Straight, headless canyons and chutes are the main morphological features of the nothern sector of the OB continental slope. (Figs. 2, 3, 4). (Fig. 4). The northern canyons are characterized by marked V-shaped profile, whereas the southern incision have a smoother profile, with U-shaped bottom and are closer spaced respect to the northern ones (Fig. 4). A progressive deepening of the headwall scarps moving southward is also observed (Fig. 4). Despite their erosional character, the seismic analysis show that, in some case, the canyons has hybrid characters. The seismic profile (Fig. 4a) show the slope reflectors truncated by

canyon walls, indicative of an erosional character whereas, in other case slope progradation within the canyon is observed (Fig. 4a) In other cases, incision are buried by passive backfilling and draped by a thin sedimentary cover above an U-shaped remnant topography (Figs. 4b, 4c). The drape consist of continuos parallel reflectors of moderate amplitude (Figs. 4b, 4c), interpreted as hemipelagic sediments deposited in a low-energy environments. The infilling of the canyons is often below the limits of seismic resolution and thus it is difficult to resolve the style of infilling. The slope incisions are characterized by repeated infill stages and subsequent re-incisions (Fig. 4a, 4b, 4c). The older incisions are generally wider with the respect to the younger ones, and are located in the same slope sectors, showing no appreciable migrational trends through time (Fig. 4a, 4b). Two distinct slope seismic unit are recognized: a lower unit, lying above the acoustic basement and made of discontinuous, high-amplitude reflectors, and an upper unit made of bedded, more continuous reflectors (Fig.4a, 4b, 4c). This setting could reflect a different progradational style of the slope, with changes in local conditions such as variations in sediment transport, in the rate of sediment supply and possible slope failure. The lower units seems to be related to a progradation cycle through unconfined deposition by debris flows, high concentration turbidites and mass wasting processes. The upper seismic unit suggest slope progradation through probably a combination of overbanking processes from the stripped currents flowing within the slope incisions, and by hemipelagic fall out.

At the base of slope the canyons develops very low relief (~5 m of deep) channel-like erosional features, separated by longitudinal and tongue-shaped sedimentary ridge that are near the lower limit of the multibeam resolution (Fig. 4). The multibeam reflectivity map of the base of slope sector show high backscatter lobate-shaped and tongue-shaped deposits that emanate from the base of slope and occupies the OB plain for a length of around 10 km (Fig. 5). A N-S Sparker seismic profile show the subsurface setting of the northern Ogliastra base of slope, from the levee of the Gonone canyon to the northern sector of the Arbatax deep sea fan (Fig. 6). The seafloor is flat with very subtle depressions associated to the low relief channels, separated by very gentle mounds, linked to the longitudinal ridges visible in the bathymetric map (Figs. 4, 6). The subsurface of the basin plain is dominated by the interfingering of small, thin lenses of chaotic reflectors, interpreted as small lobes, with high-amplitude, parallel reflectors interpreted as sheet, basin plain turbidites,

that appears in heteropic relationship with the lobes (Fig. 6). An around 0.2s thick lower seismic unit consisting predominantly of turbidite sheets is evident (Fig. 6). The sheet turbidites interfingers with several, very thin lense of chaotic reflections, probably related to small lobes deposited by debris flows (Fig. 6). A subtle southward migration trend of the lobe units is observed (Fig. 6). The overlying seismic unit is characterized by high amplitude reflectors basin plain turbidites, that also in this case interfingers with wider and, in some case thicker, lobate-shaped chaotic bodies (Fig. 6).

In the distal sector, the basin floor is scoured by a low relief V-shaped valley (less than 15 m of negative relief and dip of around 0.3°) that runs at the base the flank of the Quirra High with a N-S trend, and in the very distal sector joins into the Sarrabus canyon (Fig. 4).

5.2 The Arbatax turbidite system (ATS)

The Arbatax turbidite system (ATS) is the main turbidite system of the northern OB (Fig. 3, 7). In the shelf and continental slope the system is composed of a narrow canyon-slope channel system (Figs. 3, 7). The canyons indents the narrow shelf with the headwall developed in front of a small submarine delta (Fig. 2). At the base of slope it develops an around 18 km wide radial fan with up to 150 m of relief, that occupies much of the basin with its distal portions adjacent to the Quirra high (Fig. 7). Two narrow canyons, located around 8 km southward from the Arbatax canyon, develops a small fan that coalesce with the Arbatax fan (Fig. 7).

The upper sector of the Arbatax fan is scoured by a single, up to 50 m deep, sinuous channel that loses relief downslope after a series of sharp, 90° turns dying out in the middle fan sector where it develops a channel mouth lobe (CML) (Fig. 7). The distal portion of the Arbatax fan is channalized, with a series of straight channels, with both erosional and depositional characters that, in the very distal sector joins in the Sarrabus canyon (Fig. 7).

5.2.1 The Arbatax canyon-slope channel

The Arbatax canyon is incised the continental slope and is up to 450 m deep (at the shallowest water depth available from multibeam data); the canyon develops at the

junction of two faults with different trend: the main basin bounding fault, strikes N-S trend and a secondary SW-NE striking fault (Fig. 7). The walls of the canyon are articulated in a very steep basal sector (30°), and more gentle (10°) upper sector, with amphitheatre-shaped slide scars and associated gullies (Fig. 7). No slump deposits are recognized on the canyon floor (Fig. 7)

The seismic profile of fig. 7a, that cut the canyon about 5 km updip from the shallowest multibeam available data, shows that present day Arbatax canyon incised on a thin sedimentary sequence, that has fill a deeper, wider erosional surface (Fig. 7a). The canyon has experienced multiple cycles of erosion and susbquent filling stages, that progressively has narrowed the canyon (Fig. 7a). The right wall of the Arbatax canyon truncates the slope bedded reflectors, indicating erosional activity whereas the left wall has a predominantly depositional character, with a slope progradation unit (Fig. 7a). This unit covers a thick chaotic unit, interpreted as a mass transport deposit (MTD) probably rafted down from the canyon wall (Fig. 7a). The thalweg of the canyon is narrow, with a marked V-shaped profile, incised on part of the MTD (Fig. 7a).

In the multibeam bathymetry, starting from a water depth of 1150 m, the canyon thalweg is around 300 m wide, with a V-shaped profile, averaging a dip of 3° (Fig. 7). The canyon enlarge progressively downslope, loosing steepness and evolving into a U-shaped slope channel, with a steep right wall (up to 25°) and a more gentle, left wall (Fig. 7). The slope channel is confined within a small, tectonically-driven depression bordered to the left by a SW-NE striking fault (Fig. 7b). The right wall truncates parallel reflectors, indicating erosional character (Fig. 7b). The two slope seismic units previously described are still present, with the lower unit made up of discontinuous reflectors, and the upper unit made up of more regular, parallel reflectors (Fig. 7b). On the left wall, the Arbatax slope channel develops a low relief levee (Figs. 7, 7b), spans from 1200 m to around 1300 m of water depth (Figs. 7, 7b).

5.2.2 The Arbatax fan channel and the southern Arbatax fan sector

In the upper fan sector the Arbatax channel is deeply incised into the fan surface, with both sharp bends and straight segments (Fig. 7). The transition from the slope channel to a fan channel is marked by a change in the axial gradient, from 2.5° to

1.4°, with a minimum of 0.5° in correspondence of the first turn of the fan channel (Fig. 7). In the first straight path, the relief of the right wall diminish from 150 m to 20 m of relief , whereas the left wall, loose relief from 70 m to 60 m and increase the steepness from 8° to 14° approaching the turn of the channel (Fig. 7). In the first turn of the fan channel the outside wall top stand around 100 m above the channel floor, averaging a steepness of 15° (Fig. 7). The channel has a width of around 200 m, with a short entrenched sector with a dip of 3.5° followed by a gentle sector dipping at 0.7° (Fig. 7). The outside wall of the second turn has a relief of 50 m, with a steepness of 18° (Fig. 7), whereas in the internal sector an inner-bend bar, around 1 km wide, is present (Fig. 7). A small curvilinear, low relief channels is present on the outside sector of the turn (Fig. 7). This channel dies out at around 1560 m of water depth, just 1 km away from the Posada fan channel mouth, and has been interpreted as an old, actually abandoned pathway of the Arbatax fan channel.

A short sedimentary ridge around 30 m high, showing a smoothed surface, with regular isobaths, averaging a dip of around 2° (Fig. 7) separates the abandoned channel from the present day Arbatax fan channel. This intrachannel sector, is interpreted as an area of depositional activity by channel aggradation following the channel avulsion. The overbanking of the gravity currents flowing within the actual Arbatax fan channel, contributes to smooth the surface of the intrachannel area. The left wall of the Arbatax fan channel, by contrary, erode the Arbatax fan, with a step-like marked morphology (Fig. 7).

The mouth of the Arbatax channel is located in the middle fan sector, at around 1560 m of water depth (Fig. 7). In front of its mouth the channel develops an elongated channel-mouth lobe (CML) with a tongue plain-view shape, that extends for around 8 km beyond the channel mouth, and averaging a dip of 1° (Fig. 7). The lobe surface is poorly channalized, with some short straight chutes, that have dimensions close to the lower limits of the multibeam resolution (<5m). The multibeam reflectivity map (Fig. 7c) show a narrow, tongue-shaped, high backscatter body, starting from the Arbatax channel mouth, that is correlates with the CML (Fig. 7c)

Two marked, headless, low relief , straight channels are located on the right side of the CML between 1550 and 1650 m of water depth (Fig. 7). The channels shows different characters: the smaller one shows a marked v-shaped profile, indicating erosive character, whereas the larger one shows a U-shaped profile, and is flanked

by a very low relief levees (Fig. 7). Both channel loose relief proceeding downslope, and beyond 1650 m of water depth they are no more evident in the bathymetric map (Fig. 7). Although the data do not allow to make certain inferences on the nature of these channels probably they were connected with an old pathway of the Arbatax fan channel, currently disactivated. A concave-shaped slide scar flank the CML in the left side (Fig.7); the headwall of the scar has a width of 2 km, whereas two small relief erosive channel runs beside the smoothed side walls (Fig. 7). The two channels joins into one single elements, that ends at around 1660 m depth, developing a small relief lobe (Fig. 7).

A sparker W-E trending seismic profiles shows a mound, wedge-shaped body made of discontinuos, lenticular reflectors, with around 0.35 s of maximum thickness, buried at around 0.5s below the actual seafloor: is interpreted as the older stage of the deep sea fan (Paleo-Arbatax) deep sea fan (Fig. 7d). Onlapping high amplitude reflectors, that smooth progressively the mound topography of the deep sea fan, has been interpreted as the result of the abandonment stage of the Paleo-Arbatax fan (Fig. 7d). This lower fan unit is capped by a basin wide, high amplitude reflectors that marks the starts of the new stage of the deep sea fan (Arbatax1 fan) (Fig. 7d). The Arbatax1 fan consist of an around 15 km long wedge-shaped unit, made of curvilinear, discontinuous reflectors, with a maximum thickness of 0.15 s, loosing relief downfan (Fig.7d). In the upper sector, low amplitude reflectors could be related to a channel fill (Fig. 7d), whereas in the distal sector of the fan, a package of irregular reflectors could be related to a mass wasting processes (Fig. 7d). In the distal sector the Arbatax fan dies out abruptly against high amplitude reflectors interpreted as basin plain turbidites (Fig. 7d). Also in this case, the fan is capped by a couple of marked, high amplitude reflectors, traceable across almost the whole basin width (Fig. 7d).

The younger, present day Arbatax deep sea fan (Arbatax2) is a wedge-shaped unit, with a marked mound-shaped upper fan sector, with the relief that decreases downfan (Fig. 7d). An upper, low relief erosion on the uppermost sector of the fan is related to the abandoned Arbatax channel previously described in batymetry that show a subtle migration with a very thin filled sequence (Fig. 7d). The intrachannel sector, between the abandoned channel and the Arbatax fan channel consists of an erosional surface and an upper unit made of irregular reflectors interpreted as the result of the migration/avulsion of the upper fan channel with the

penecontemporaneus infilling of the intrachannel sector (Fig. 7d). The infilling unit consist of a lower package of irregular reflectors, capped by a thin package of faintly layered reflectors: this propably is due to a change in the sediments nature, from a coarse-grained particles size to fine grained sediments due to overspilling of the flows discharged by the Arbatax fan channel, also suggested by the bathymetric interpretation (Fig. 7, 7d). Downslope, the Arbatax2 fan is made up of moderate amplitude reflectors, interrupted in the middle fan sector by the slide surface that correspond to the previously described scars that flanks the CML to the left (Figs. 7, 7d). The slide surface is draped by a thin, blanked facies, indicative of very fine grained sediments (Fig. 7d). Very low relief, channel-like features scours the distal sector of the fan, that predominantly consist of high amplitude reflectors (Fig. 7d).
The distal sector of the fan, beyond 1700 m of water depth, is characterized by a around 12 wide belt of V-shaped erosive features (Fig. 7). The V-shaped erosive features narrows downslope, and join into a less than 1 km wide, low relief channels (15 m) channel (Fig. 7). The channel deepens further downslope, and at around 1880 m of water depth it evolve into a small bypass canyon, that joins into the Sarrabus intraslope canyon at around 2000 m of water depth. The by pass canyon is marked by an abrupt break in slope, from around 1.1° to 3° and by a deepens of the fairway to around 100 m of negative relief (Fig. 7).

5.2.3. The Arbatax fan: northern sector

The nothern sector of the Arbatax fan shows a different overall morphology with respect to the southtern fan sector (Fig. 7). This sector develops is devoid of upper fan channel and is rather mainly affected by mass failure and dismantlement processes (Fig. 7). In the apex sector of fan, outside from the 90° turn of the Arbatax fan channel many arcuate, crescent scars and small plunge pools are identified (Fig. 7). Proceeding downfan, a series of steep scars, alternated with small relief mounds, aligned with a SW-NE trend for a length of 5 km are present (Fig. 7). The steep scars (around 9° of maximum dip) have a wavelength of around 1 km and, together with the mounds, rapidly loose relief downfan (Fig. 7). In some cases, small, rectilinear gullies are present between the mounds and the steep sectors (Fig. 7). These features could be reasonable interpreted as the results of overbank processes from the gravity currents running within the Arbatax fan channel. A

similar morphological features are present on the Navy fan (Normark, 1971) and on the upper sector of the Monterey fan channel (McHugh & Ryan, 2000). The two authors has found overbank areas both along straight and curved segments of the channel path, that extend away from the levee crest (McHugh & Ryan, 2000). In particular, an overbanking area has been founded outside from the "Shepard Meander" of the Monterey channel, at water depth of 3450 m (the Arbatax channel depth is 1200 m); the bedforms are present on the backside of the outside levee crest, and interpreted by the authors as large sediment waves with crest that are sub parallel semi-circles extend away from the "Shepard meander" for around 15 km (McHugh & Ryan, 2000). By similarly, also this features, lying on the upper Arbatax fan, could be interpreted as formed by similar processes (Fig. 7e). However, a second interpretation is here proposed; these features in plainview are set in a well defined tongue-shaped body, around 3 km wide, and delimited by steep scars with a relief of around 15 m respect to the surrounding fan surface (Fig 7). This lead to also interpreted the whole body as a slide deposit (Sd1) of the upper fan sector (Fig. 7). As a confirmation for this hypothesis, the tongue-shaped deposit lies above a wider (5,5 km), lobate-shaped body, around 6 km long and traceable down to around 1650 m of water depth (Fig. 7). At its end, the body is marked by a steep scar (3°), whereas its surface is channalized, especially in the distal sector (Fig.7). This feature is interpreted as a slide deposit (Sd2) of the upper-middle sector of the Arbatax fan; an upslope concave-shaped scars, located at water depth of around 1500 m in the middle fan sector (Fig.7) is interpreted as the headwall scars of the Sd2 slide. The crossing seismic profile (Fig. 7f) supports the interpretation of this feature as a displaced mass, evidencing the concave upward (scoop-shaped) failure plane that truncates the middle amplitude reflectors of the Arbatax fan (Fig. 7f). The Sd2 unit is made up of irregular reflectors, but in the inner, deeper part of the slide body a regular seismic subunit of plane bedded reflectors is also present (Fig. 7f). The upslope headwall scar of the Sd2 trunk the fan reflectors, and is capped by an thin, irregular seismic unit that could be related to a mass transport deposit, or debris flow deposit (Fig. 7f) A thick, wedge-shaped seismic unit made of chaotic reflector is buried below the Arbatax fan at around 0.15s below the seafloor, is interpreted as a big mass transport deposit (MTD) that being in turn eroded by the slide plane of the Sd2 slide. Southward, the MTD loose relief and progressively interfingers with the high amplitude reflectors of the distal fan and of the basin plain (Fig. 7f).

A lower, wedge-shaped seismic unit, buried at around 0.35s, made of discontinuous, curvilinear reflectors could be related to the Arbatax1 fan (Fig. 7f). It has a thickness of 0.15 s, thinning downfan, interfingering with high amplitude reflectors of the distal basin plain of the Ogliastra basin (Fig. 7f).

Discussion

The continental slope of the Nothern Ogliastra basin

The evolution of the continental slope of the nothern Ogliastra basin occurs through the alternation of constructional stages (slope progradation), and destructive stages (multiple slope incisions). As inferred by the seismic analysis, the constructional stages have happens through different phases: an early stage characterized by deposition by unconfined, high density turbidity currents or debris flows, and a successive phase of deposition by less concentrated turbidity currents or trough hemipelagic fall out.

During the incision phase, the slope deposition is disactivated and destructive, erosional processes take place mainly in canyons. Apparently the slope incisions develops independently of the fluvial inputs, due to the very few, ephemeral, small drainage basin rivers on this sector of Sardinia island (Fig. 2). Longshore currents probably fed the continental slope, with temporary sediment storage on the narrow shelf (Fig. 2). However, it seems reasonable that much of the sediments is caught by the Arbatax canyon, that is the main slope incision of the nothern Ogliastra basin, and is the only incision that develops at the base of slope a remarkable deep sea fan. The slope canyons shows different morphological and subsurface characters: in bathymetry they show both U and V-shaped profiles, straight, closely spaced and localized along strike. The subsurface analysis has show that not all the slope incision are actually active, and along their paths the canyons alternate erosive tract with depositional tracts. Studies on the origin of submarine canyons, and more generally slope incision, have proposed different explanation and different evolutive models. Twichell & Roberts (1982) and Farre *et al.,* (1983) used modern U.S. eastern margin slope morphologies to suggest that these canyons were initiated by failures at the base of slope, followed by erosion that progressively migrates upslope. However, Pratson *et al.,* (1994) working on the New Jersey slope have shown that the buried canyons (mostly Pleistocene) are initiated by sediment-flow erosion on the upper continental slope, that then extend downslope by successive erosive events. On the middle to lower slope sectors, flows captured within remnant topographic lows of underlying buried canyons, periodically re-excavate them (Pratson *et al.,* 1994). The eventual focus of sediment drainage into a single slope

conduit may lead to the formation of the submarine canyon (Pratson *et al.,* 1994). The buried incisions of the nothern Ogliastra slope and their inherited topography can continue to influence where the incision initiation occurs, anchoring its formation at specific sites along the slope. After the filling of the older incisions infact, if the tapering by the draping sediments cover has failed to smooth-over the depression, a series of sea floor troughs remain (see Pratson *et. al.,* 1994). These remaining depressions catch the sediment flows coming from the shelf break and upper slope sectors, and confined them to follow the former paths to the base of slope sectors, and they eventually excavate and deepens the former routes.

The incision that existing today on the slope surface, are generally more narrow with respect to the older, buried incisions. This suggests that the erosion processes that produced the relief of the modern incision are linked to an early phase of (canyon) formation or due to less intense erosional activity of the sedimentary flows.

Finally, the fact that not all of the incisions are active at the present day, seems lead to discard a main sea level fluctuations control on these systems. Fulthorpe *et al.,* (2000) working on Miocene slope incision off New Jersey has show infact that the presence or absence of incision along the margin must be dictated not only by fluctuations in the sea level, but by a subtle changes in local conditions or regime variables. These includes the efficiency of downslope sediment transport, rate of sediment supply, grain size, and possible slope collapse (Fulthorpe *et al.,* 2000). The buried, closely spaced, thin lobes founded at the base of slope, interfingering with the basin plain turbidites of the Ogliastra basin are linked to the old slope incision, deposited during slope erosional stages. Acutally, the very low relief lobate-shaped deposit at the base of slope, supporting the hypothesis of a young-stage of the present day slope incisions of the Ogliastra slope.

The Arbatax turbidite system

The Arbatax turbidite system consist of a slope canyon-channel and a base of slope deep sea, small radial fan that spans almost the entire width of the nothern Ogliastra basin (Fig.7). The canyon do not face wide onland drainage river system, however it roots in front of a small submarine delta (Fig. 2). Small, sand-rich submarine fan receive their sediment from close and small source areas (Bouma, 2000a, b). It is well established that sand from littoral drift is intercepted in the heads of submarine

canyons and funnelled downslope from the shelves to sand-rich fans (Howell & Normark, 1982; Nelson, 1983; Reading & Richards, 1994). Examples of sand-rich fans which are fed by canyon heads extending relatively close to the beaches on a narrow shelf are the Redondo and the Dume fans off California (Haner, 1971; Piper *et al.,* 1999), and western Mexico (Underwood & Karig, 1980) where the coastal system receives sediment from a number of local or regional rivers. Sand-rich fans in general may also be fed directly by a local river (Nelson, 1983; Nelson *et al.,* 1999). The limited size of the rivers system coupled with the proximity of the source area, as the case of the Arbatax turbidite system, is commonly reflected in the compositional immaturity of the sand-rich submarine fans (Link *et al.,* 1984), in contrast with the sediments character of the large passive margin fans (Shanmungam & Moiola, 1988). The fact that the Arbatax canyon develops in front of submarine delta lead to the hypothesis that seasonally-flood hyperpicnal flows may contribute to feed the system with long duration, sustained turbidity currents. In addition, the evidence of mass failure founded along the canyon pathway, support that also surge type, slump derived debris flows or turbidity currents are common feeder agent as the case of the Posada.

The several stage of erosional and filling phase experienced by the Arbatax canyon are probably related to the controlling factors such as the rate of sediment supply, the type and the behaviour of sedimentary flows, with only a subtle control by external factors such as sea level fluctuations. Schwalbach *et al.,* (1996) concluded that canyon and fan activity in the small modern fans off California continued during a phase of rising sea level. There, canyon headward erosion rates have been equal to or greater than the transgression rate, and the canyon-fan system have remained linked with their sediment sources (Schwalbach *et al.,* 1996).

The Arbatax deep sea fan cycles (Arbatax1 & Arbatax2) are divided by a marked, basin wide draping surface, that mark the disactivation of the older system (Arbatax1), and the start of the younger stage (Arbatax 2).

Bouma's (2000a) review indicates that sand-rich canyon-fed fans often continue to build even during high stands, although normally at a lower pace. Construction of the fans increases when more sediment is available, during wet centuries and when the shelf becomes narrowest (relative sea level lowering) (Bouma, 2000a). However, much of the literature on sand-rich fans, is focused on system located in narrow, tectonically active margin (Schwalbach *et al.,* 1996, Normark *et al.,* 1998) that

probably allows the system to remain active during sea level rise. By contrary the Arbatax is located in a relative young, narrow passive margin, so caution is need in considering how this system, during its evolution, has enjoined a degree of "eustaic immunity".

The present day Arbatax fan is partially confined by the flank of the Quirra high, with the southern fan sector that faces the bypass zone of the Ogliastra basin to the deeper intraslope canyon of the Sarrabus Canyon. The asymmetry in the plainview shape of the deep sea fan, with a wider southern sector could be the result of the coupling of the regional dip of the basin, and the effect of the confinement effect on by the nothern Quirra seamount topography.

The morphological and subsurface analysis has revealed that the nothern sector of the fan is probably completely abandoned, and affected by dismantling processes through large mass failure. According to the plainview morphology of the slided mass, and the geometry of the failure surfaces, the motion of the displaced mass is rotational (*see* Hampton *et al.,* 1996), with a very short runout. However, the interpretation of the overbank area on the outside sector of the Arbatax channel turn, testifies that also a sediment supply is furnished to this sector of the fan, mainly through the spillover of the upper, less denser part of the sedimentary flows confined within the fan channel.

The overall morphology of the southern sector of the Arbatax fan is in good agreement with the conceptual models developed for the small, coarse grained submarine fans off the west coast of the North America by Normark (1970). The upper fan infact, is characterized by a slope channel with a very subtle levee that represent the continutation of the submarine canyon, and by a main upper fan channel. The Arbatax fan channel has experiences avulsional process, and display a series of both active and inactive distributary channels in the middle fan sector. The sedimentary flows move downslope from the submarine canyon via the fan channel, that it is sites of depositional processes (aggradation, overbanking area, small relief levee), and it also site of erosional processes (steep erosive walls, entrenchment sector and erosional surfaces).

Once the flows have reaches the Arbatax middle fan sector, flows become unchannlized, and the fan channels ends; from there, the flows can spread laterally to form the CML. This case appear very similar to what have described Normark *et al.,* (1979) for the Navy submarine fan.

In general, the channel lobe transition zone separates well defined channels or channel fill deposit from well defined lobe or lobe facies (Wynn *et al.,* 2002). Channel lobe transition zone are commonly associated with a break in slope (Wynn *et al.,* 2002), and this is visible in the Arbatax system, with a passage from 2.3° to 1° of degree. The sediments of the transition zone reflects the effects of flows undergoing a hydraulic jump, which occurs when flows pass from a relatively high-gradient and channalized condition to flatter and smoother unchannalized regions.

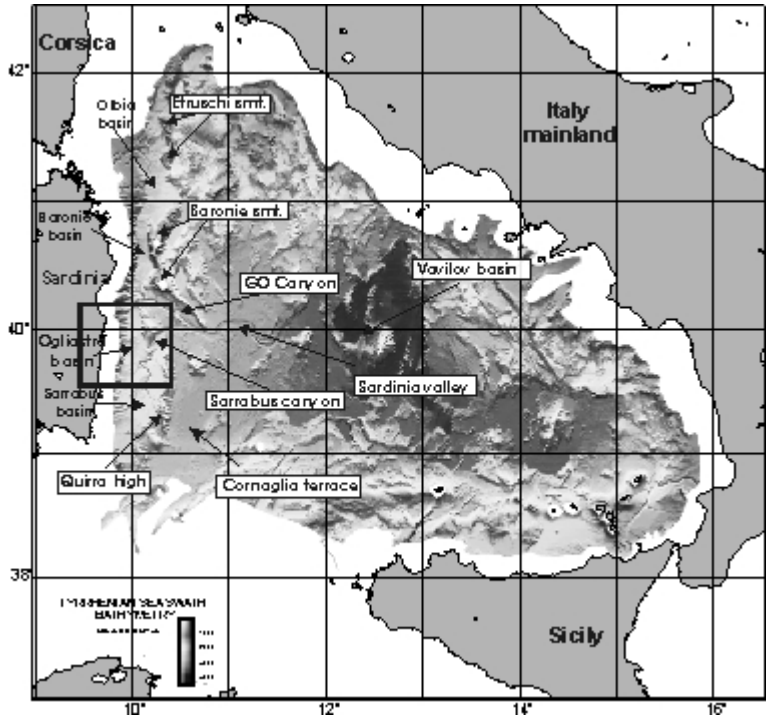

Fig. 1 Shaded relief bathymetric map of the Tyrrhenian sea. Depths are colour-coded, illumination from the NW. GO Canyon: Gonone-Orosei canyon system. The box corresponds to the bathymetric map of Ogliastra Basin in Fig. 2.

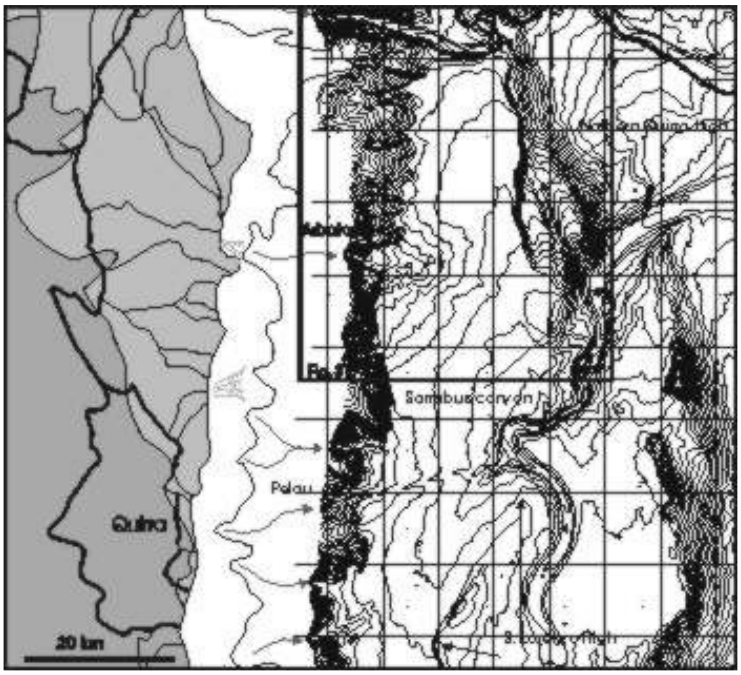

Fig. 2 Multibeam bathymetric map of the Ogliastra basin. Boxes correspond to the distinct sectors discussed in the text. The shelf break (dashed line) is taken from Bellagamba et al., (1979), whereas the locationof the submarine deltas is from Ulzega et al., (1987). The map of the Sardinia Island with a schematic lithological subdivision has been simplified from Ulzega et al., (1987). The river drainage basins are also indicated with a solid black line.The box represent the nothern sector of the basindescribed in the text. Contour intreval: 50 m.

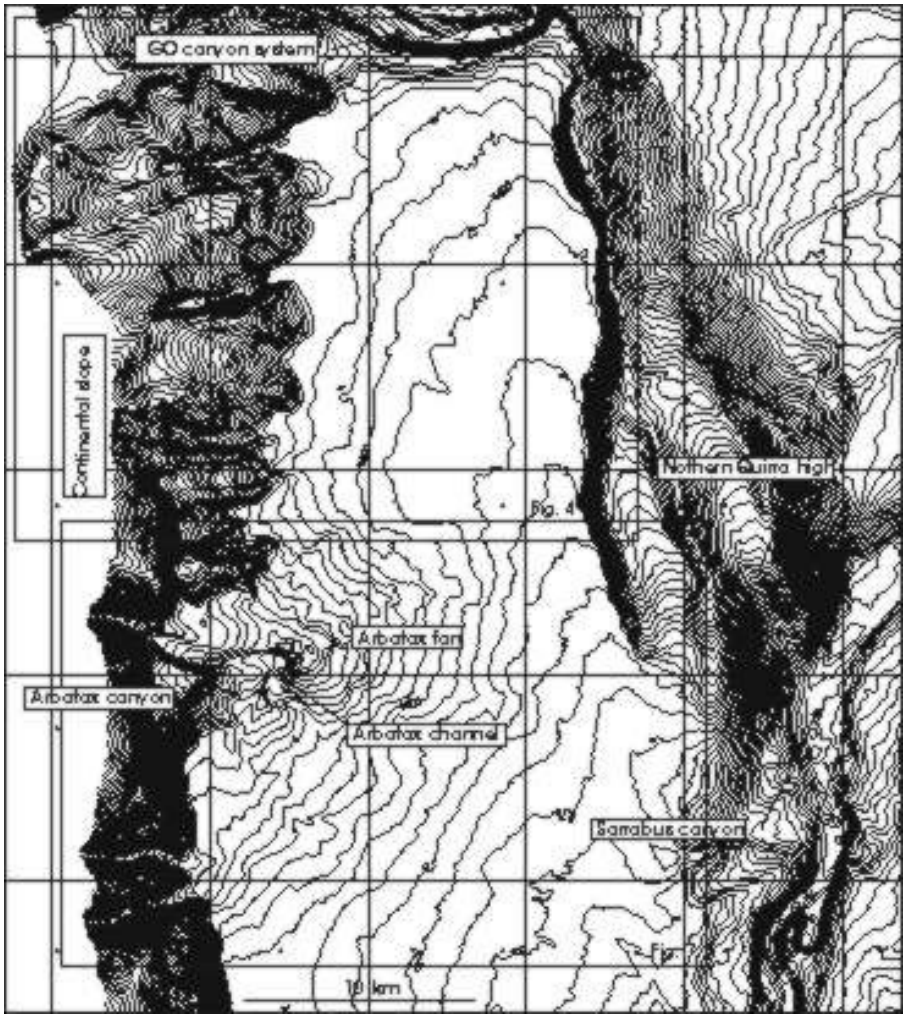

Fig. 3 Multibeam bathymetric map of the nothern sector of the Ogliastra basin. The manin large scale archectural elemets of the basin described in the text are incidcated. Contour interval: 20m

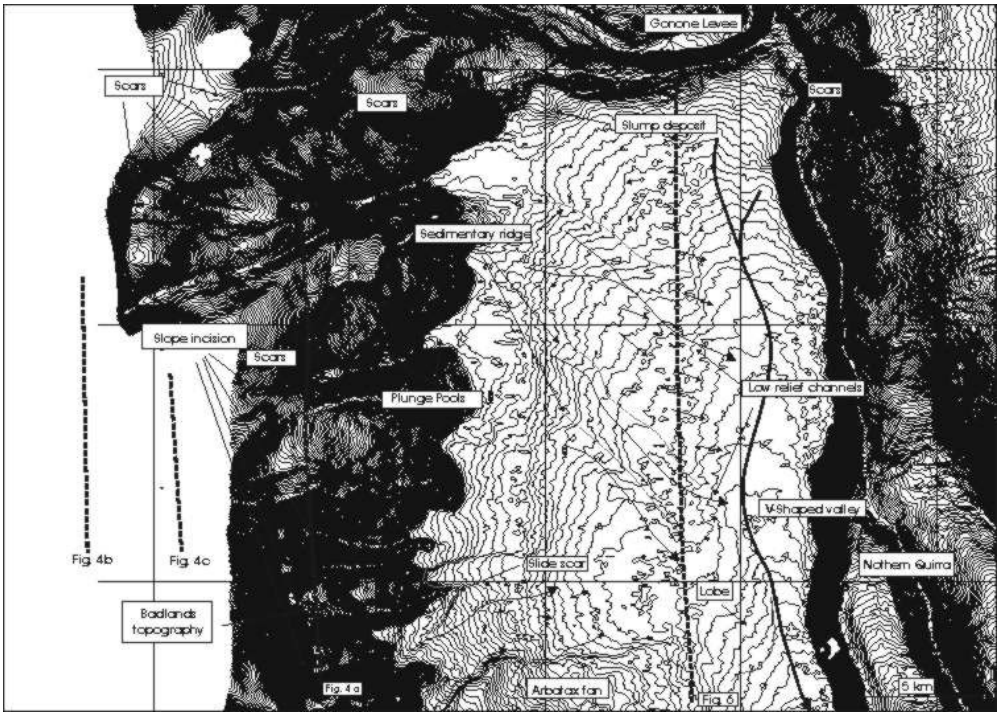

Fig. 4 Multibeam bathymetric map of the slope and base of slope sector of the nothern Ogliastra basin. Contour interval: 5m.

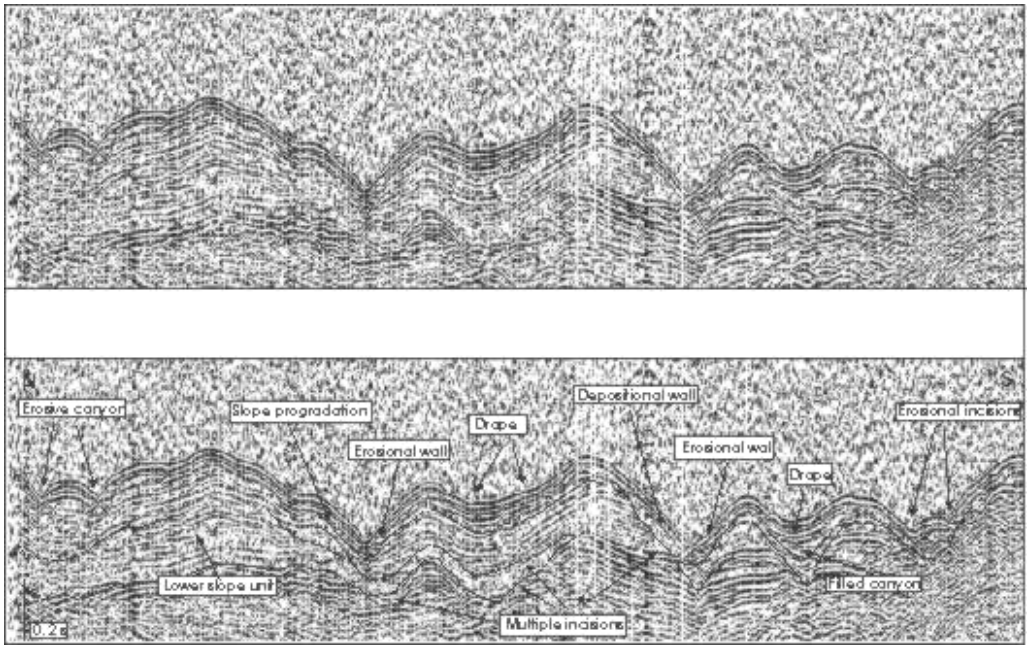

Fig. 4a Sparker seismic profile of the slope sector of the nothern Ogliastra basin

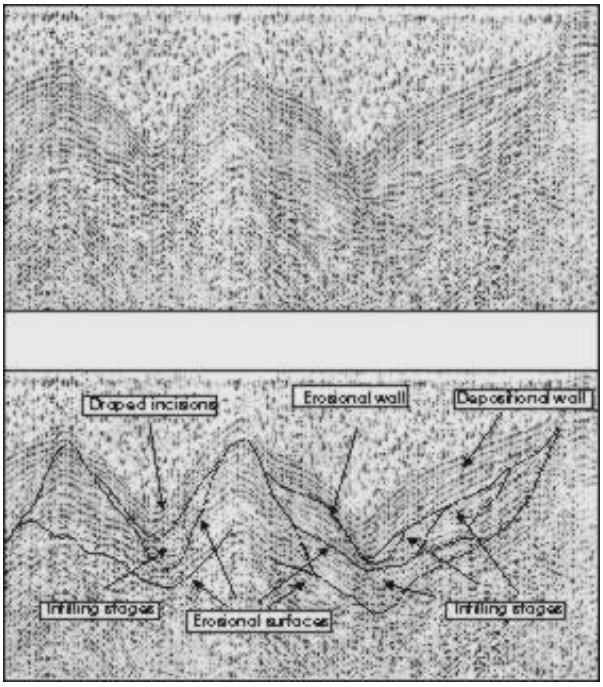

Fig. 4b Sparker seismic profile of the slope incisions of the nothern Ogliastra basin.

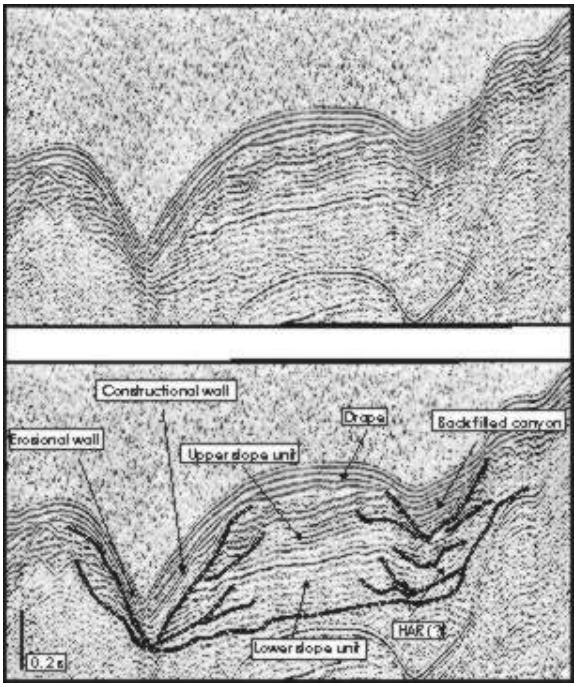

Fig. 4c Sparker seismic profile of the continental slope incision. See fig. 4 for the location of the profile.

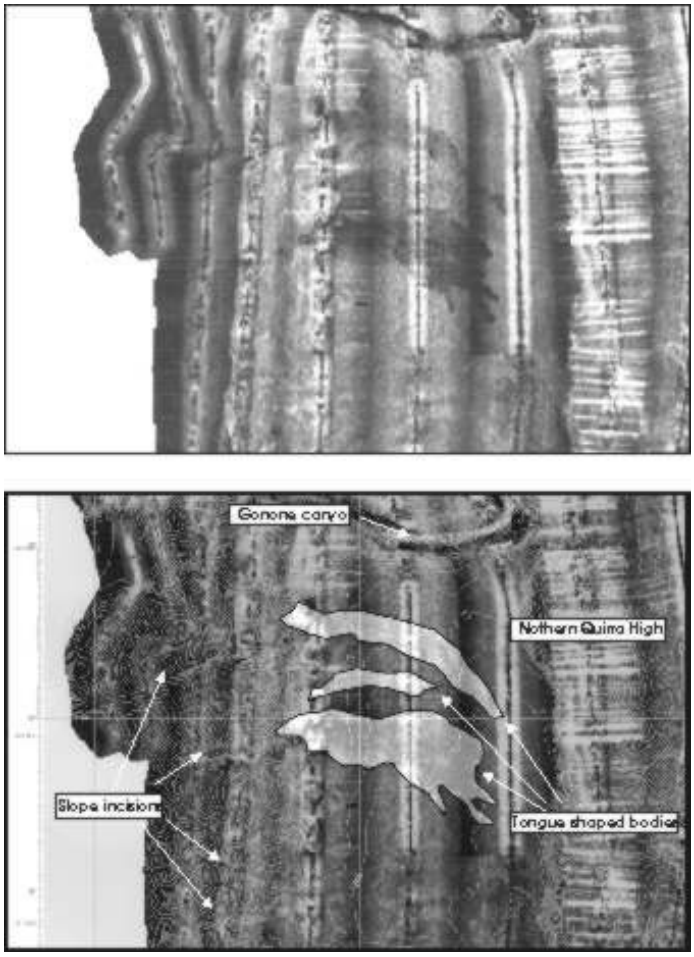

Fig. 5 Multibeam reflectivity map with the mutilbeam bathymetric map of the nothern slope sector of the Ogliastra basin. Contour interval: 25m..

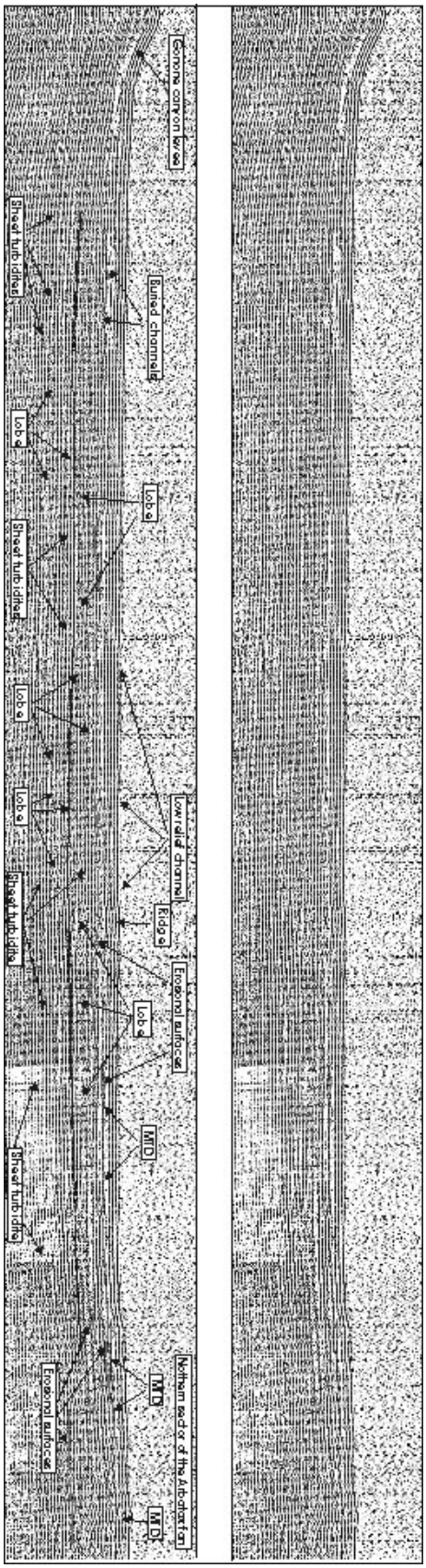

Fig. 6 Sparker seismic profile of the base of slope sector of the nothern Ogliastra basin. See Fig. 4 for the location of the profile.

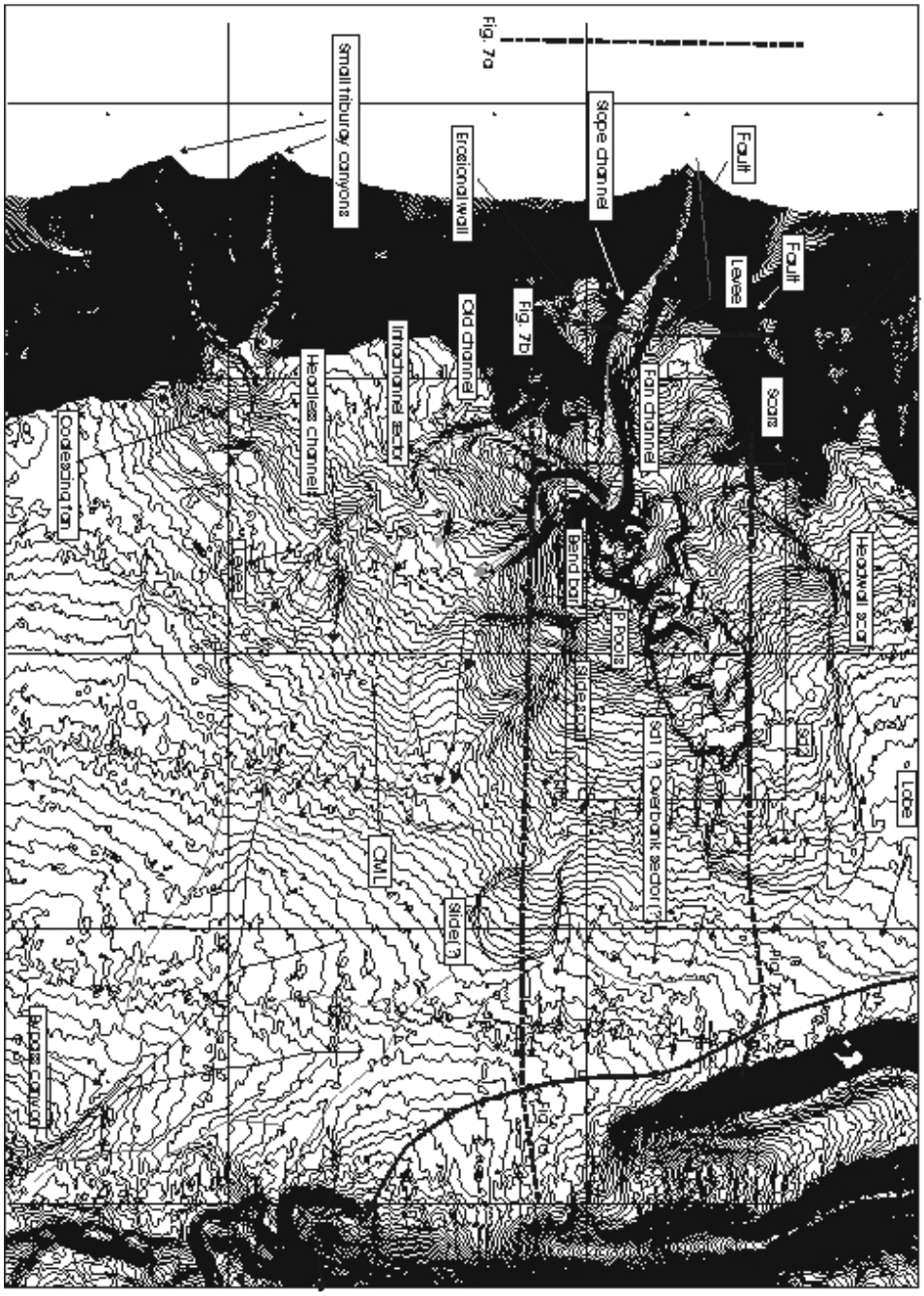

Fig. 7 Multibeam bathymetric map of the Arbatax turbidite system. Contour interval: 5m.

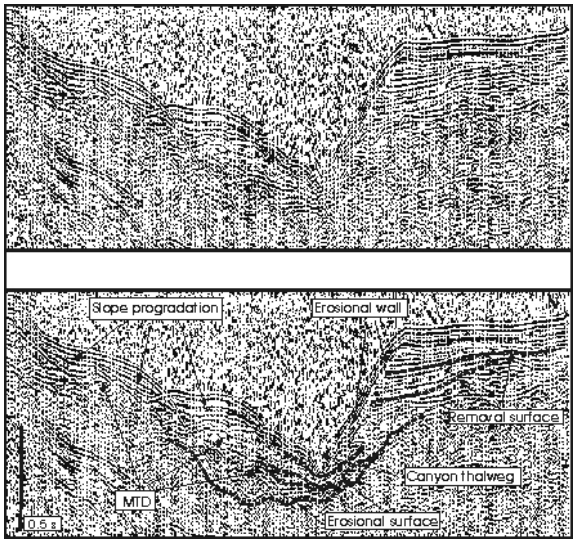

Fig. 7a Crossing sparker seismic profile of the upper sector of the Arbatax canyon. See Fig.7 for the location of the profile.

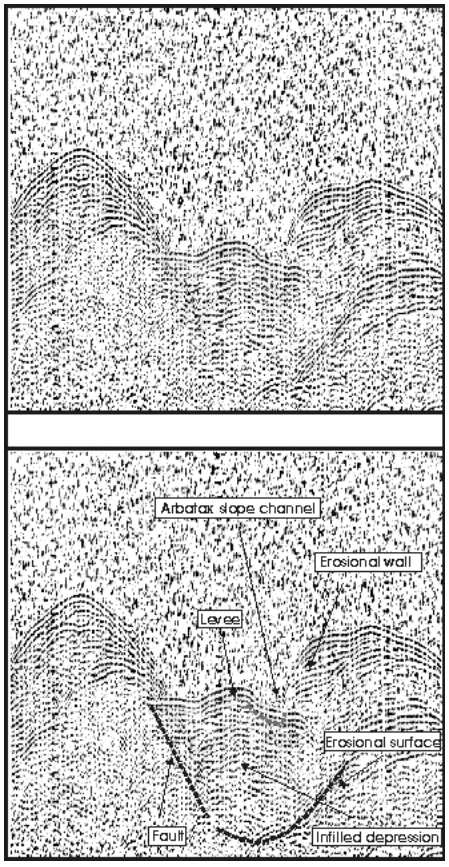

Fig. 7b Crossing seismic profile of the Arbatax canyon-slope channel. See fig. 7 for the location of the profile.

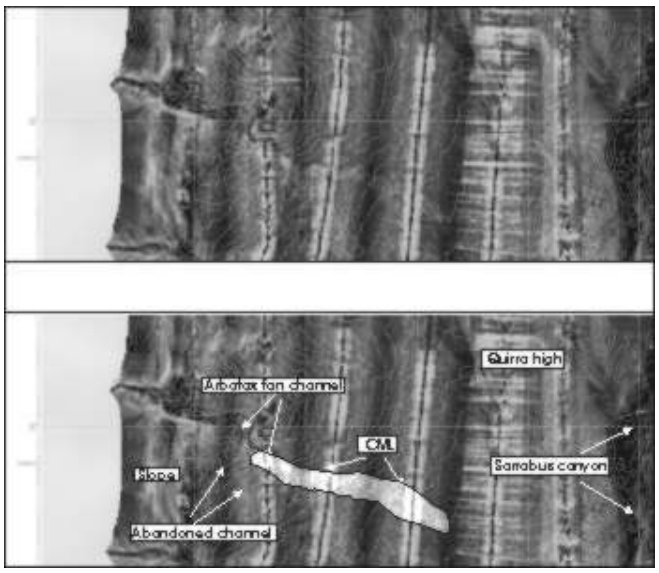

Fig. 7c Multibeam reflectivity map of the Arbatax fan, showing the interpreted extension of the Arbatax channel mouth lobe (CML) and of the abandoned pathway of the Posada fan channel.

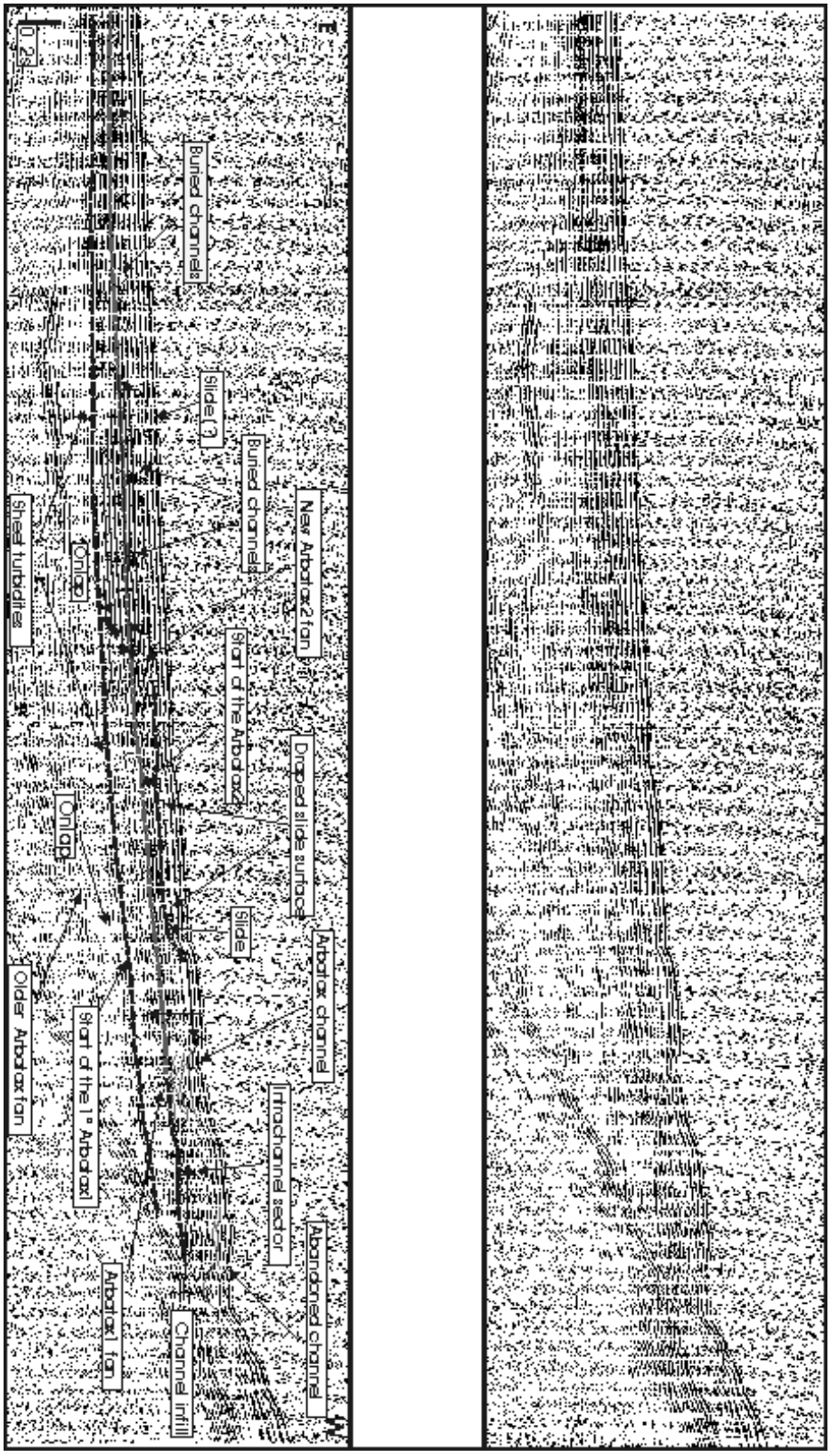

Fig. 7d Sparker seismic profile of the Southern sector of the Arbatax deep sea fan. See fig. 7 for the location of the profile.

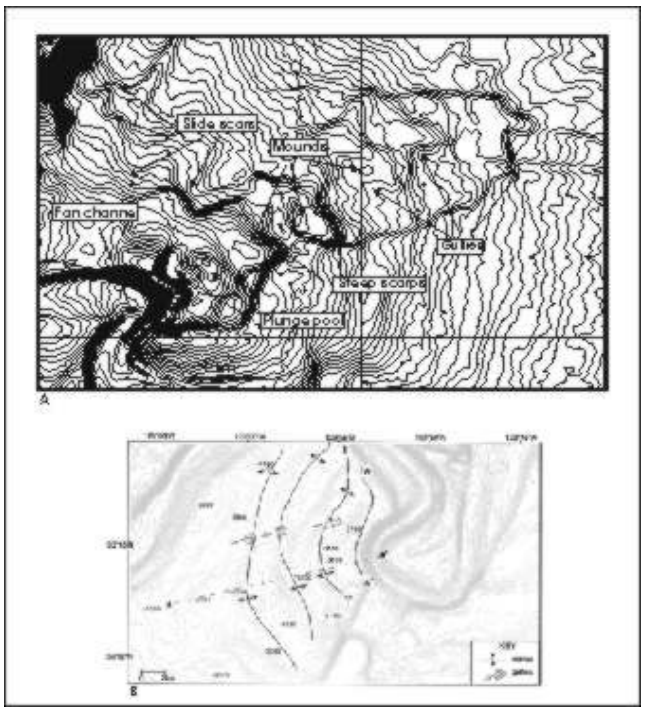

Fig. 7e A. Multibeam bathymetric map of the overbank area outside from the Posada fan channel turn.The overbank area of the "Shepard Meander" of the Monterey fan channe, used as analogue case. From: McHugh & Ryan, 2000

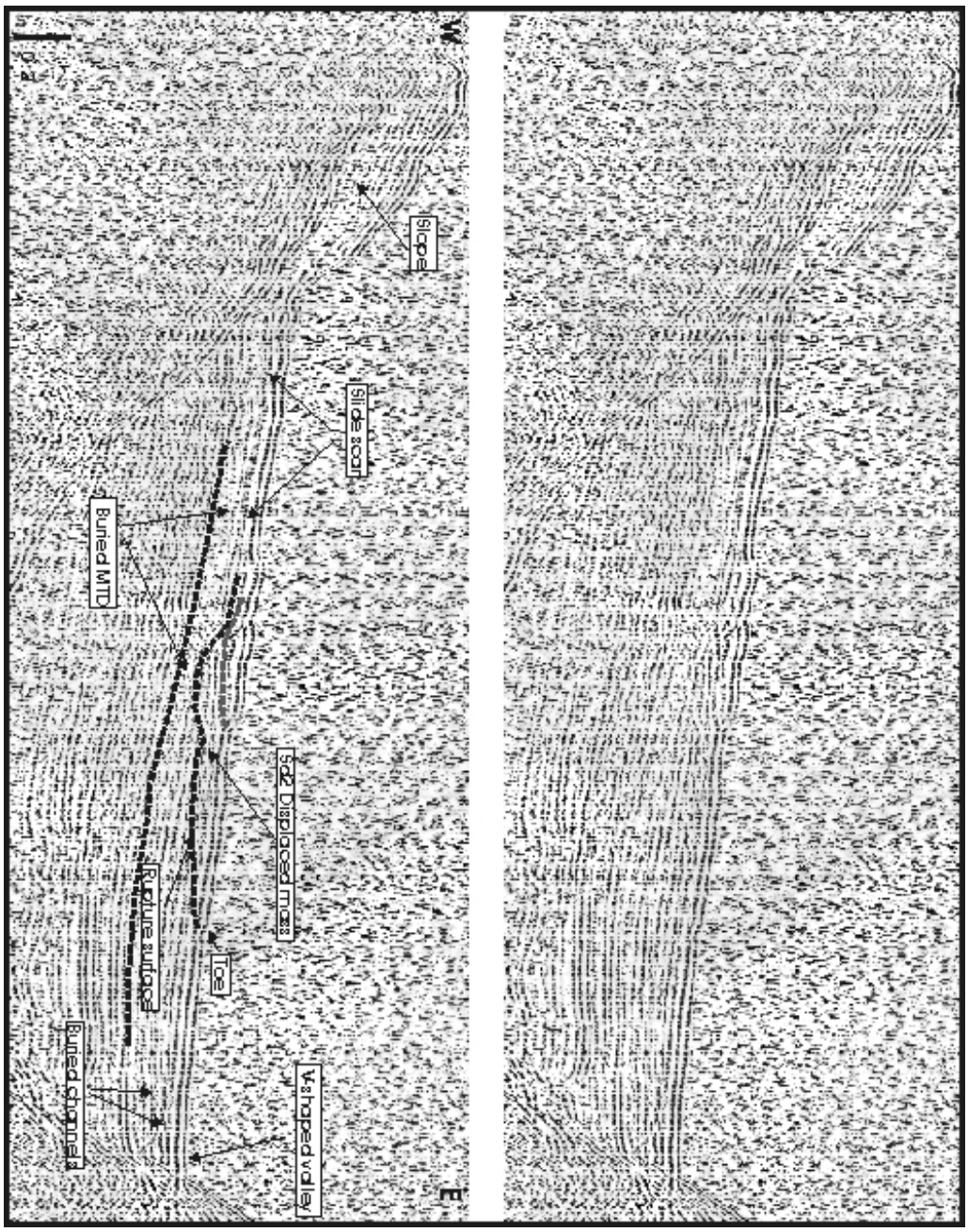

Fig. 7f Sparker seismic profile of the nothern sector of the Arbatax deep sea fan. See fig. 7 for the location of the profile.

Chapter 6

Conclusions

The analisys of the characteristic of the deep sea turbidite system of the eastern Sardiani margin has put in evidence as the combination of both external and internal controls have a strong control in the size, geometry and development on the systems of this small, young passive margin.

External factors of control on deep water system of eastern Sardinian margin

The effects of external factors such as the type of feeder system, type of sediments, shelf and continental slope setting, control the shape, size and the morphology of the deep sea fans, independently from the topogaprhy confinement effect.

i) Feeder systems

The Caprera turbidite system is the largest turbidite system of the entire eastern Sardinian margin, and has the unique tract of the eastern Sardinian margin turbidite systems of a long, wide leveed channel. The architecture of the Caprera fan could be explained by the fact that the feeder canyons face a wide shelf area, and are not directly connected with onland river systems. The wide shelf prevents sand transport to the basin that is mostly trapped in the shallow water storage areas. As soon as the base of slope is reached, the coarse-grained-depleted density currents give rise to a leveed channel, with the coarsest fraction being deposited in the channel itself and the finer one that overspill the channel building high-relief levees.

On the contrary, the Posada, the Arbatax, the Mortorio and the Tavolara turbidite systems develop small (< than 10 km in radius) radial deep sea fan, at the base of slope. This architecture could be explained by the fact that head of the corresponding canyon is located rather close to the shoreline, thus coarse grained sediments can be directly fed by the river source to the proximal part of the turbidite systems. The Posada and Arbatax deep sea fan are fed by a single-point source and

they equate with low efficency, coarse grained-dominated fans of many authors. The Posada and the Arbatax systems are characterized by deep slope-incised feeder canyons that are directly connected with small drainage-basin rivers, that presumably furnishes long duration, sustained gravity flows. On the contrary, the Mortorio and Tavolara canyons are less incised on the continental slope due to their disconnection with Sardinia river systems and face a wider shelf sector. It can be assumed that a large amount of sediments can be moved by longshore drift to the head of the Mortorio and Tavalora canyons that then deliver it to the basin (canyon-fed fan). Their base of slope deep-sea fans tend to be more localized, and of smaller size than the Arbatax and Posada fans likely owing to a lower volume of sediments available to the basin.

ii) Slope settings

-Low angle slope

The low angle slope sector of the Olbia continental slope promotes the development of meandriform canyons. The sinuosity index of the canyons is inversely correlated with the average dip of the surrounding slope. The low angle slope represent a relatively stable, low energy environment characterized by deposition mainly through emipelagic fall out and overbanking from the flows running within the slope canyons. The relative stable conditions of the low angle slope environment is also confirmed by the presence of carbonate mud mound. The presence of field of pockmarks do not affect the slope stability, but rather, the along slope alignment of these depression could lead to the development of chutes and embryonic canyons.

-High angle slope

High angle slope setting as in the case of the lower slope of the Olbia basin and the slope of the Baronie basin are areas of destructive processes and sediment bypass. Slope instability and mass wasting are the main processes that affect these sectors characterized by wide network of slide scars and canyon and chutes. Canyons and slope incision are generally short, straight, with a wide amphitheatre-like headwall

scars. In some cases the slope canyons show hybrid characters, with erosive tract alternated to depositional ones. The canyon are also characterized by several phases of activation, with erosion on the slope, followed by phases of abandonment with backfilling processes predominantly through hemipelagic fall out. They tend to be fixed in space being localized in the same slope sectors, and at the base of slope do not develops well defined deep sea fans.

Internal factors of control on deep water system of eastern Sardinian margin

The development and large scale architectural elements of the turbidite system of the eastern Sardinian margin is also controlled by internal factors as the bounding seamount topography and the shape and the setting of the receiving basins.

i) Fan channel, levees and overbanikg areas

The classical, unconfined fan models implies a base of slope fan with a semicircular shape in plianview, where the fan channel occupies a radial position. Shifting and avulsion of the fan channels are consequence of predominalty autocyclic processes of the turbidite systems: growth of depositional lobe drive the channel to shift into marginal depressions at the edge of the lobes.

In the studied cases, the seamounts related topography of the eastern Sardinian margin force the fan channels of the turbidite systems to change their pathways forming marked bend sectors and promoting avulsion processes.

This effect control also the evolution of the deep sea fans, that display sectors of sedimentary activity downfan the upper fan channel and sector of abandonment in the outside sectors of the channel turns. These area are the locus of flowstripping of the sedimentary flows confined within the fan channel, and show dismantlement features, such as scars, slide, and slumps. Headless overbanking channels are also founded in the overbaking areas, indicating that the sedimentary flows stripppe of from the main fan channels still retain an erosional behaviour.

ii) Lower fan: distributary channels and V-shaped valleys

The distal sectors of the deep sea fans are not characterized by predominant sediment deposition and by peripheral lobes development, as the classical fan models predicts. The presence of an escape pathway to lower base level lead to the creation of distributary channels, both with erosional and depositional characters also to great distance from the main fan channel mouth, and in some case not connected with it. The channels shows different sedimentary characters: erosional straight channels and straight channels with small levees. The erosional character is enhanced by the creation of the new base level that promote an acceleration of the sedimentary flows in the distal part of the turbidite system. Only the basal part of the flows remain confined in the low relief channel, and the progressive flow stripping of the finer parts could explaine the occurrence of the levees.
The distributary channels joins in wider, low relief V-shaped valleys, that are the locus of prevalent erosional processes and sediments bypass. These sediment fairways show that the sediment gravity flows have an erosional behaviour also in the distal sector of the turbidite system, and represent the upslope portions of the bypass conduits, that put in connection the upper intraslope basins with the lower basins, lying at a deeper base level.

Effects of base level variation on the turbidite system

The intraslope basin of the Olbia and of the nothern Ogliastra basin are completely filled, and the progressive downcutting of the canyon in the distal portions is the result of the estabilishment of a new base level for the sediments discharged by the main turbidite systems. The result of the progressive incision into the upper parts of the confined basin succession are representend by the V-shaped valley and the bypass canyons. This erosional scour could be interpreted as the modern equivalent of the scours founded in the southern sub-basin of Annot Sandstones. The base level create new accommodation space for the sediments of the upper basins, driving the progradation of the turbidite system to the distal part of the basins.

Processes and products at bounding slopes

The effect of the confinement of the bounding slopes control the localization of the V-shaped valley, that generally runs at the base of the flanks of the seamounts that bound seaward the intraslope basins. In addition, the bounding seamount slope promote also the erosive character of the V-shaped valley, with a lateral confinement effect of the sedimentary flows, as has been demonstrate at the laboratory-scale. This effect can be responsible of the modification of the usual systematic proximal to distal changes in the turbidite systems such as percentage sands, percentage amalgamation and bed thickness. Thus, an increase of coarse-grained sediments along these escape pathways could be expected in this kind of depositional setting.

Effects of interaction of sedimentary flows with bounding slopes toward slumping and triggers of debris flows and turbidity currents off opposing slopes.

Seafloor instability and fan evolution

Large scale mass wasting processes affecting the deep sea fans show that the reorganization of a turbidite system through mass transport complex is not only a peculiar characteristic of tectonically active basin and of thrust-front settings as generally though. A similar evolution could strongly controls also the evolution of the turbidite systems in a tectonically dormant margin ad the case of the eastern Sardinian margin. Mass wasting processes act not only through the destruction of the sedimentary pathway of the deep sea fan, but also in the creation of new accommodation space, and forcing the transition from channel confined environment to a less confined environment, that in turn change the behaviour of the sedimentary flows. It can also largely impact the distribution of sand-prone interval both in time and space.

A fan model for confined deep water systems.

References

Acosta J., Canals M., López-Martínez J., Muñoz A., Herranz P., Urgeles R., Palomo C., Casamor J.L. (2002). The Balearic Promontory geomorphology (western Mediterranean): morphostructure and active processes. Geomorphology, 49, 177–204.

Acosta J., Muñoz A., Herranz P., Palomo C., Ballesteros M., Vaquero M., Uchupi E. (2001). Pockmarks in the Ibiza Channel and western end of the Balearic Promontory (western Mediterranean) revealed by multibeam mapping. Geo-Mar. Lett., 21, 123-130.

Akhmetzhanov A.M., Kenyon N.H., O'Byrne C.J., Ivanov M. SPECULOBE, a high resolution study of a modern sand lobe at the end of a gravity flow channel. Geological Society of London (*in press*).

Alexander J. & Morris S. (1994). Observations on experimental, non-channelized, high concentration, turbidity currents and thickness variations around obstacles. J. Sed. Res., 64, 899-909.

Al-Jaidi O., McCaffrey W.D., Kneller B.C. (2004). Factors influencing the deposit geometry of experimental turbidity currents: implications for sand-body architecture in confined basins, In: Lomas S.A. & Joseph P. (eds.) Confined Turbidite Systems, Geol. Soc. London, Spec. Pub., 222, The Geological Society of London, Bath, 45-58.

Allen J.R.L. (1985). Principles of Physical Sedimentology: London, George Allen & Unwin, pp. 272.

Amy L.A., McCaffrey W.D., Kneller B.C. (2004). The influence of a lateral basin-slope on the depositional patterns of natural and experimental turbidity currents, In: Joseph P. & Lomas S. (eds.) Deep-Water Sedimentation in the Alpine Basin of SE France. New perspectives on the Grès d'Annot and related systems, Geol. Soc. London, Spec. Publ., 221, The Geological Society of London, Bath, 311-330.

Argent J.D., Stewart S.A., Underhill J.R. (2000). Controls on the Lower Cretaceous Punt Sandstone Member, a massive deep-water elastic deposystem, Inner Moray Firth, UK North Sea. Petroleum Geoscience, 6, 275-285.

Aríztegui D., Asioli A., Lowe J.J., Vigliotti L., Tamburini F., Chondrogianni C., Accorsi C.A., Bandini Mazzanti M., Mercuri A.M., Van der Kaars S., McKenzie J.A., Oldfield F. (2000). Palaeoclimate and the formation of sapropel S1: inferences from late Quaternary lacustrine and marine sequences in the central Mediterranean region. Palaeogeogr. Palaeoclimatol. Palaeoecol., 158, 215-240.

Babonneau N., Savoye B., Cremer M., Klein B. (2002). Morphology and architecture of the present canyon and channel system of the Zaire deep-sea fan. Mar. Petr. Geol., 19, 4, 445-467.

Baines P. G. (1995). Topographic Effects in Stratified Flows. Cambridge Academic Press, pp. 482.

Beauboeuf R.T. & Friedmann S.J. (2000). High-resolution seismic/sequence stratigraphic framework for the evolution of Pleistocene intra slope basins, Western Gulf of Mexico: depositional models and reservoir analogs. In: Weimer P., Slatt R.M., Coleman J., Rosen N.C., Nelson H., Bouma A.H., Styzen M.J., Lawrence D.T. (eds.) Deep-Water Reservoirs of the World: Gulf Coast Society, Soc. Econ. Paleon. Miner. Foundation, 20th Annual Research Conference, 40-60.

Biegert E. K, Steffens G.S., Sumner H.S, Bird D.. Back to basic: a comparative analysis on deepwater settings and associated fan systems. Mar. Petr. Geol. *in press.*

Booth J.R., Duvernay A.E., Pfeiffer D.S., Styzen M.J. (2000). Sequence stratigraphic framework, depositional models, and stacking patterns of ponded and slope fan systems in the Greater Auger Basin: Central Gulf of Mexico slope: In: Weimer P., Slatt R.M., Coleman J., Rosen N.C., Nelson H., Bouma A.H., Styzen M.J., Lawrence D.T. (eds.) Deep-Water Reservoirs of the World: Gulf Coast Society, Soc. Econ. Paleon. Miner. Foundation, 20th Annual Research Conference.

Bouma A.H. (2004). Key controls on the characteristics of turbidite systems. In: Lomas S.A. & Joseph P., (eds.) Confined Turbidite Systems. Geol. Soc. London, Spec. Publ. 22, The Geological Society of London, Bath, 9-22.

Bouma A.H., Normark W.R., Barnes N.E., (eds) (1985a). Submarine fans and related turbidite systems. New York, Springer-Verlag, pp. 351.

Damuth J.E., Kolla V., Flood R.D., Kowsmann R.O., Moonteiro M.C., Gorini M.A., Palma J.J.C., Belderson R.H. (1983). Distributary channel meandering and bifurcation patterns on Amazon deep-sea fan as revealed by long-range sidescan sonar (GLORIA). Geology, 11, 94-98.

Damuth J.E., Flood R.D., Kowsmann R.O., Belderson R.H., Gorini M.A. (1988). Anatomy and growth pattern of Amazon deep-sea fan as revealed by long-range side-scan sonar (GLORIA) and high-resolution seismic studies. Am. Ass. Petr. Geol. Bull., 72, 885-911.

Damuth J.E. (2002) The Amazon-HARP fan model: facies distribution in mud-rich deep sea fans based on systematic coring of architectural elements of Amazon fan. In F. Briand (Ed.) Turbidite systems and deep sea fans of the Mediterranean and the Black seas. Vol. 17, 19-22. CIESM Workshop.

Demyttenaere R., Tromp J.P., Ibrham A., Allman-Ward P., Meckel T. (2000). Brunei deep-water exploration: From sea floor images and shallow seismic analogues to depositional models in a slope turbidite setting. In: Weimer P., Slatt R.M., Coleman J., Rosen N.C., Nelson H., Bouma A.H., Stysen, M.J., Lawrence, D.T. (eds.) Deep-Water Reservoirs of the World: SEPM Foundation, Gulf Coast Section, Proceedings of 20th Annual Bob Perkins Research Conference, 304-317.

Dewey J.F., Helman M.L., Turco E., Hutton D.H.W., Knott S.D. (1989). Kinematics of the western Mediterranean. In: Coward M.P., Dietrich D., Park R.G. (eds.) Alpine tectonics, Geol. Soc. Lon., Spec. Pub., 45, The Geological Society of London, Bath, 265-283.

Diegel F.A., Schuster D.C., Karlo J.F., Schoup R.C., Tauvers P.R. (1995). Cenozoic structural evolution and tectonostratigraphic framework of the northern Gulf Coast continental margin. In: Jackson M.P.A. et al. (eds.) Salt tectonics: A global perspective, Am. Ass. Petr. Geol. Memoir, 65, 109-151.

Doglioni C., Innocenti F., Morellato C., Procaccianti D., Scrocca D. (2004). On the Tyrrhenian sea opening. Mem. Descr. Carta Geol. It., XLIV, 147-164.

Dolan J.F., Beck C., Ogawa Y. (1989). Upslope deposition of extremely distal turbidites: An example from the Tiburon Rise, west-central Atlantic. Geology, 17, 990-994.

Douglas R.G. & Heitman H.L. (1979). Slope and basin benthic foraminifera of the California Borderland. Soc. Econ. Paleont. Mineral., Spec. Pub., 27, 231-256.

Droz L., Marsset T., Ondreas H., Lopez M., Savoye B., Spy-Anderson F.L., (2003) Architecture of an active mud-rich turbidite system: The Zaire Fan (Congo–Angola margin southeast Atlantic): Results from Zaı¨Ango 1 and 2 cruises. AAPG Bull., 87, 7, 1145-1168.

Edwards D.A. (1993). Turbidity Currents: Dynamics, Deposits and Reversals: Springer- Verlag, Lecture Notes in Earth Sciences, 44, pp. 173, Berlin.

Farré J.A., McGregor B.A., Ryan W.B., Robb J.M. (1983). Breaching the shelfbreak: passage from youthful to mature phase in submarine canyon evolution. In: Stanley D.J. & Moore G.T. (eds.) The Shelfbreak: Critical Interface On Continental Margins, Soc. Eco. Paleont. Min. Sp. Publ., 33, 25–39.

Flood R.D., Manley P.L., Kowsmann R.O., Appi C.J., Pirmez C. (1991). Seismic facies and late Quaternary growth of the Amazon submarine fan. In: Weimer P. & Link M. H. (eds.) Seismic facies and sedimentary processes of modern and ancient submarine fans. Springer, 415-433, New York.

Fulthorpe C.S., Austin, S.Jr., Mountain G. (2000). Morphology and distribution of Miocene slope incisions off New Jersey: Are they diagnostic of sequence boundaries. Geol. Soc. Am. Bull., 112, 817-828.

Gervais A., Savoye B., Mulder T. (2006). Sandy modern turbidite lobes: A new insight from high resolution seismic data. Mar. Petr. Geol., 23, 485-502.

Gervais A., Savoye B., Piper, D.J.W., Mulder T., Cremer M., Pichevin L. (2004). Present morphology and depositional architecture of a sandy confined submarine system: the Golo turbidite System, eastern margin of Corsica. Spec. Publ. Geol. Soc. London, 222, 59-90.

Gladstone C., Phillips J.C., Sparks R.S.J. (1998). Experiments on bidisperse, constant-volume gravity currents: propagation and sediment deposition. Sedimentology, 45, 833-843.

Grecula M., Flint S.S., Wickens H.Dev., Johnson S.D. (2003). Upward-thickening patterns and lateral continuity of Permian sand-rich turbidite channel fills, Laingsburg-Karoo, South Africa. Sedimentology, 50, 831-853.

Hampton M.A., Lee H.J., Locat J. (1996). Submarine landslides: Rev. Geoph., 34, 33-59.

Haner B.E. (1971). Morphology and sediments of Redondo Submarine Fan, Southern California. Geol. Soc. Am. Bull., 82, 2413-2432.

Haughton P.D.W. (1994). Deposits of deflected and ponded turbidity currents, Sorbas Basin, southeastern Spain. J. Sed. Res., A64, 223-246.

Haughton P.D.W. (2000). Evolving turbidite systems on a deforming basin floor, Tabernas, SE Spain. Sedimentology, 47, 497-518.

Hay A.E. (1987). Turbidity currents and submarine channel formation in Rupert Inlet, British Columbia 2. The roles of continuous and surge type flow. J. Geophys. Res., 92, 2883-2900.

Hodgson D.M. & Flint S.S. (eds.) (2005). Submarine Slope Systems. Processes and Products. Geol. Soc., Spec. Publ. 244, The Geological Society of London, Bath, pp. 225.

Hovland M., Svenseb H., Forsberg C.F., Johansed H., Fichlere C., Fossa J.H., Jonssong R., Rueslatte H. (2005). Complex pockmarks with carbonate-ridges off mid-Norway: products of sediment degassing. Mar. Geol., 218, 191-206.

Howell D.G., Normark W.R., Scholle P.A., Spearing D. (1982). Sandstone depositional environments. Am. Ass. Petr. Geol. Memoir, 31, Tulsa.

Judd A.G. & Sim R. (1998). Shallow gas migration mechanisms in deep water sediments. In: Ardus D.A., Hobbs R., Horsnell M., Jardine R., Long D., Sommerville J. (eds.) Offshore Site Investigation and Foundation Behaviour: New Frontiers. Soc. Underwater Technol., London, 163-174.

Kallel N., Duplessy J.-C., Labeyrie L., Fontugne M., Paterne M., Montacer M. (2000). Mediterranean pluvial periods and sapropel formation over the last 200,000 years. Palaeogeogr. Palaeoclimatol. Palaeoecol., 157, 48-58.

Kastens K. & Mascle J. (1990). The geological evolution of the Tyrrhenian Sea: an introduction to the scientific results of the ODP LEG 107. In: Kastens K.A., Mascle J. et al. (eds.) Proc. Ocean Drill. Prog., Sci. Res., 107, 3-26.

Kenyon N.H. & Millington J.J. (1995a). Contrasting deep-sea depositional systems in the Bering Sea Basin. In: Pickering K.T., Hiscott R.N., Kenyon N.H., Ricci Lucchi F., Smith R.D.A. (eds.). Atlas of Deep Water Environments: Architectural Style in Turbidite Systems, Chapman & Hall, London, 196-202.

Kenyon N.H., Millington J., Droz L., Ivanov M.K. (1995b). Scour holes in a channel-lobe transition zone on the Rhone Cone. In: Pickering K.T., Hiscott R.N., Kenyon N.H., Ricci Lucchi F., Smith R.D.A. (eds.). Atlas of Deep Water Environments: Architectural Style in Turbidite Systems, Chapman & Hall, London, 212-215.

Klauda, J.B. & Sandler, S.I. (2003). Predictions of gas hydrate phase equilibria and amounts in natural sediment porous media. Mar. Petrol. Geol., 20, 459–470.

Kneller B.C. (1991). Oblique reflection of turbidity currents. Geology, 14, 250-252.

Kneller B.C. (1995). Beyond the turbidite paradigm: physical models for deposition of turbidites and their implications for reservoir prediction. In: Hartley A. & Prosser D.J. (eds.) Characterisation of Deep Marine Clastic Systems, Geol. Soc., Spec. Publ., 94, The Geological Society of London, Bath, 29-46.

Kneller B.C. & Branney M.J. (1995). Sustained high-density turbidity currents and the deposition of thick ungraded sands. Sedimentology, 42, 607-616.

Kneller B.C. & McCaffrey W. (1999). Depositional effects of flow non-uniformity and stratification within turbidity currents approaching a bounding slope: deflection, reflection and facies variation. J. Sed. Res., 69, 5, 980-991.

Kneller B.C. & Buckee C. (2000). The structure and fluid mechanics of turbidity currents: a review of some recent studies and their geological implications. Sedimentology, 47, 62-94.

Lamers E. & Carmichael S.M.M. (1999). The Paleocene deepwater sandstone play west of Shetland. In: Fleet A.J. & Boldy S.A.R. (eds.) Petroleum Geology of Northwest Europe: Proceedings of the 5th Conference. Geological Society of London, 645-659.

Lastras G., Canals M., Urgeles R., Hughes-Clarke J.E., Acosta J. (2004). Shallow slides and pockmark swarms in the Eivissa Channel, Western Mediterranean Sea. Sedimentology, 51, 837-850.

Lee S.E., Talling P., Ernst G., Hogg A.J. (2002). Occurrence and origin of submarine plunge pools at the base of the US continental slope. Mar. Geol., 185, 363-377.

Lien T., Walker R., Martines O. (2003). Turbidites in the Upper Carboniferous Ross Formation, western Ireland: reconstruction of a channel and spillover system. Sedimentology, 50, 113–148.

Link M.H., Squires R.L., Colburn I.P. (1984). Slope and deep-sea fan facies and paleogeography of the Upper Cretaceous Chatsworth Formation, Simi Hills, California. Am. Ass. Petr. Geol. Bull., 68, 850-873.

Lomas S.A. & Joseph P. (eds.) (2004). Confined turbidite systems, Geol. Soc., Spec. Publ., 222, The Geological Society of London, pp. 336.

Lowe D.R. (1988). Suspended-load fallout rate as an independent variable in the analysis of current structures. Sedimentology, 35, 765-776.

Lucchi R. & Camerlenghi A. (1993). Upslope turbiditic sedimentation on the southeastern flank of the Mediterranean Ridge. Boll. Oceanol. Teor. Appl., 11, 3-25.

Malinverno A. & Ryan W.B.F. (1986). Extension on the Tyrrhenian Sea and shortening in the Apennines as result of arc migration driven by sinking of the lithosphere. Tectonics, 5, 2, 227-243.

Marani M. & Gamberi F. (2004). Structural framework of the Tyrrhenian sea unveiled by seafloor morphology. Mem. Descr. Geol. It., XLIV, 97-108.

Marjanac T. (1990). Reflected sediment gravity flows and their deposits in flysch of Middle Dalmatia, Yugoslavia. Sedimentology, 37, 921-929.

Marr J.G., Harff P.A., Shanmugam G., Parker G. (2001). Experiments on subaqueous sandy gravity flows: The role of clay and water content in flow dynamics and depositional structures. Geol. Soc. Am. Bull., 113, 1377-1386.

Marr J.G. (1999). Experiments on subaqueous sandy gravity flows: flow dynamics and deposit structures: M.S. thesis, University of Minnesota, Minneapolis, pp. 121.

McAdoo B.G., Pratson L.F., Orange D.L. (2000). Submarine landslide geomorphology, US continental slope. Mar. Geol., 169, 103-136.

McCaffrey W.D. & Kneller B.C. (2004). Scale effects of non-uniformity on deposition from turbidity currents with reference to the Grès d'Annot of SE France. In: Joseph P. & Lomas S.A. (eds.) Deep-water sedimentation in the Alpine Basin of SE France: New perspectives on the Grès d'Annot and related systems, Geol. Soc., Spec. Publ., 221, The Geological Society of London, Bath, 301-310.

Meckel, L.D. et al. (2002). Genetic Stratigraphy Architecture and Reservoir Stacking Patterns for Upper Miocene-Lower Pliocene Greater Mars-Ursa Intraslope Basin Mississippi Canyon, Gulf of Mexico. 22nd Annual Gulf Coast Section SEPM Foundation Bob F. Perkins Research Conference, 113-146.

Mohrig D., Straub K.M., Buttles J., Pirmez C. (2006). Controls on geometry and composition of a levee built by turbidity currents in a straight laboratory channel. In: Parker G. & García M.H. (eds.) River, Coastal and Estuarine Morphodynamics. Taylor & Francis Balkena Group, London.

Moraes M.A.S., Becker M.R., Marcelo C., Monteiro, S.L. (2000). Using outcrop analogs to improve 3D heterogeneity modeling of Brazilian sandrich turbidite reservoirs. In: Weimer P., Slatt R.M., Coleman J., Rosen N.C., Nelson H., Bouma A.H., Stysen M.J., Lawrence D.T. (eds.) Deep-Water Reservoirs of the World, SEPM Foundation, Gulf Coast Section, Proceedings of 20th Annual Gulf Coast Section SEPM Foundation Bob Perkins Research Conference, 304–317.

Morris S.A., Kenyon N.H., Limonov A.F., Alexander J. (1998). Downstream changes of large-scale bedforms in turbidites around the Valencia channel mouth, north-west Mediterranean: implications for paleoflow reconstruction. Sedimentology, 45, 365-377.

Muck M.T. & Underwood M.B. (1990). Upslope flow of turbidity currents: A comparison among field observations, theory, and laboratory models. Geology, 18, 54-57.

Mulder T., Syvistski J.P.M., Skene K.I. (1998). Modeling of erosion and deposition by turbidity currents generated at river mouths. J. Sed. Res., 68, 124-137.

Mutti E., Ricci Lucchi F., Roveri M. (2002). Revisiting turbidites of the Marnoso-arenacea Formation and their basin margin equivalent: problems with classic models-Excursion Guidebook. Workshop organized by Dipartimento di Scienze della Terra, University of Parma and Eni-Divisione Agip for the 64th EAGE Conference and Exibition, Florence, Italy, 27-30 May 2002.

Mutti E. (1992a). I cicli silicoclasti/carbonati nelle facies di retropiattaforma del Capitan Reef Complex, Permiano, Guadalupe Mountains, New Mexico, USA. Mem. Soc. Geol. It., 45, 701-706.

Mutti E. (1992b). Turbidite sandstones. Agip, Milano 275p.

Mutti E. & Normark W.R. (1987). Comparing examples of modern and ancient turbidite systems: Problems and Concepts In: Legget J.K. & Zuffa G.G. (eds.) Deep waterclastic deposits: Models and Case Histories, 1-38.

Mutti E. (1979). Turbidites et cones sous-marins profonds. In: Sedimentation detritique (fluviatile, littorale et marine), Institut de Geologie de l'University de Fribourg, Short Course, Fribourg, Institut de Geologie de l'University de Fribourg, 353-419.

Mutti E. & Ricci Lucchi F. (1972). Le torbiditi dell'Appennino settentrionale: introduzione all'analisi di facies. Mem. Soc. Geol. Ital., 11, 161-199.

Nelson C.H., Karabanov E.B., Colman S., Escutia C. (1999). Tectonic and sediment supply control of deep rift lake turbidite systems: Lake Baikal, Russia. Geology, 27, 2, 163-166.

Nelson C.H. (1983). Modern submarine fans and debris aprons: an update of the first half century. In: Boardmna, S.J. (eds.) Revolution in the Earth Sciences. Kendall/Hunt, Dubuque, Iowa, 148-165.

Normark W.R. (1970). Channel piracy on Monterey deep-sea fan. Deep-Sea Res., 17, 837-846.

Normark W.R., Piper D.J.W., Hess G.R. (1979). Distributary channels, sand lobes and meso topography of Navy submarine fan, California border land, with application to ancient fan sediments. Sedimentology, 26, 749-774.

Normark W.R. & Piper D.J. (1991). Initiation processes and flow evolution of turbidity currents: implications for the depositional record. Soc. Econ. Paleont. Miner. Spec. Publ., 46, 207-230.

Normark W.R., Posamentier H., & Mutti E. (1993) Turbidite systems: state of the art and future directions. Rev. Geoph., 32 (2), 91-116.

Normark W.R., Piper D.J.W., Hiscott R.N. (1998). Sea level controls on the textural characteristics and depositional architecture of the Hueneme and associated submarine fan systems, Santa Monica Basin, California. Sedimentology, 45, 53-70.

Parker G. & Izumi N. (2000). Purely erosional cyclic and solitary steps created by flow over a cohesive bed. J. Fluid Mech., 419, 203–238.

Parsons J.D. & Garcia M.H. (1998). Similarity of gravity current fronts. Physics of Fluids, 10, 3209-3213.

Parsons J.D., Mullenbach B.L., Lamb M.P., Finlayson D.P., Nittrouer C., Orange D. Role of turbidity currents in the creation of a distributary channel on the Eel River margin, northern California. Geol. Soc. Am. Bull., in press.

Patacca E., Sartori R. & Scandone P. (1990). Tyrrhenian basin and Apenninic arcs: kinematic relations since Late Tortonian times. Mem. Soc. Geol. It., 45, 425-451.

Peakall J., McCaffrey W.D., Kneller B.C. (2000). A process model for the evolution, morphology and architecture of sinuous submarine channels. J. Sed. Res., 70, 434-448.

Pickering K.T. & Corregidor J. (2005). Mass transport complexes and tectonic control on confined basin-floor submarine fans, Middle Eocene, south Spanish Pyrenees. In: Hodgson D.M. & Flint S.S. (eds.) Submarine Slope Systems: Processes and Products, Geol. Soc., Spec. Publ., 244, The Geological Society of London, Bath, 51-74.

Pickering, K.T. & Hilton V.C. (1998). Turbidite Systems of Southeast France: Application to Hydrocarbon Prospectivity, London, Vallis Press, pp. 229.

Pickering K.T., Hiscott R.N., Kenyon N.H., Ricci Lucchi F., Smith R.D.A. (eds.) (1995). Atlas of Architectural Styles in Turbidite Systems, Architectural style in turbidite systems. Chapman & Hall, London.

Pickering K.T. & Hiscott R.N. (1985). Contained (reflected) turbidity currents from the Middle Ordovician Cloridorme Formation, Quebec, Canada: an alternative to the antidune hypothesis. Sedimentology, 32, 373-394.

Piper D.J.W., Hiscott R. N., Normark W. R. (1999). Outcrop-scale acoustic facies analysis and latest Quaternary development of Hueneme and Dume submarine fans, offshore California. Sedimentology, 46, 47-78.

Piper D.J.W. & Normark W.R. (1983). Turbidite-deposits, patterns and flow characteristics, Navy Submarine Fan, California borderland. Sedimentology, 30, 681-694.

Pirmez C. &. Flood R.D. (1995). Morphology and structure of Amazon Channel. In:. Flood R.D., Piper D.J.W., Klaus A. et al. (eds.) Proc. Ocean Drill. Prog., In. Rep., College Station, Texas (Ocean Drilling Program), 155, 23-45.

Pirmez C., Beaubouef R.T., Friedmann S.J., Mohrig, D.C. (2000). Equilibrium Profile and Baselevel in Submarine Channels: Examples from Late Pleistocene systems and Implications for the Architecture of Deep-water Reservoirs. GCSSEPM Foundation 20th Annual Research Conference on Deep-Water reservoirs of the world, December 3-6, 2000.

Posamentier H.W., Erskine R.D., Mitchum R.M. Jr. (1991). Models for submarine fan deposition within a sequence-stratigraphic framework. In: Weimer P. & Link M.H. (eds.) Seismic Facies and Sedimentary Processes of Submarine Fans and Turbidite Systems, New York, Springer-Verlag, 127-136.

Prather B.E., Booth J.R., Steffens G.S., Craig P.A. (1998). Classification, lithologic calibration, and stratigraphic succession of seismic facies of intraslope basins, deep-water Gulf of Mexico. Am. Ass. Petr. Geol. Bull., 82, 5a, 701-728.

Pratson L.F., Ryan W.B., Mountain G.S., Twichell D.C. (1994). Submarine canyon initiation by downslope-eroding sediment flows; evidence in late Cenozoic strata on the New Jersey continental slope. Geol. Soc. Am. Bull., 106, 395–412.

Reading H.G. & Richards M. (1994). Turbidite systems in deep-water basin margins classified by grain-size and feeder system. Am. Ass. Petr. Geol. Bull., 78, 792-822.

Richards M. & Bowman M. (1998) Submarine fans and related depositional systems II: variability in reservoir architecture and wireline log character. Mar. Petr. Geol., 15, 821-839.

Rothwell R.G., Pearce T.J., Weaver P.P.E. (1992). Late Quaternary evolution of the Madeira Abyssal Plain, Canary Basin, NE Atlantic. Basin Res., 4, 103–131.

Rottman J.W., Simpson J.E., Hunt J.C.R. (1985). Unsteady gravity current flows over obstacles: some observations and analysis related to the Phase II trials. J. Haz. Mat., 11, 325-340.

Sartori R. (1990). The main results of ODP Leg 107 in the frame of Neogene to Recent Geology of the peri-Tyrrhenian areas. Proc. ODP, Sci. Results, 107, 715–730.

Satterfield W.M. & Behrens E.W. (1990). A late quaternary canyon/channel system, northwest Gulf of Mexico continental slope. Mar. Geol., 92, 51-67.

Schwalbach J.R., Edwards B.E., Gorsline D.S. (1996). Contemporary channel-levee systems in active borderland basin plains, California Continental Borderland. Sediment. Geol., 104, 53-72.

Shanmugam G. & Moiola R.J. (1988). Submarine fans: characteristics, models, classification, and reservoir potential. Earth-Sci. Rev., 24, 383-428.

Shanmugam G. (2000). 50 Years of the turbidite paradigm (1950s-1990s): deep-water processes and facies models- a critical perspective. Mar. Petr. Geol., v. 17, p. 285-342.

Shor A., Piper D., Hughes Clarke J., Mayer L. (1990). Giant flute-like scour and erosional features formed by the 1929 Grand Banks turbidity current. Sedimentology, 37, 631-645.

Sinclair H.D. (1992). Turbidite sedimentation during Alpine thrusting: the Taveyannaz Sandstones of eastern Switzerland. Sedimentology, 39, 837-856.

Sinclair H.D. (2000). Delta-fed turbidite systems of the French Alpine foreland basin: A new depositional model for the Annot Sandstones. J. Sed. Res., 70, 504-519.

Sinclair H.D. & Tomasso M. (2002). Depositional evolution of confined turbidite basins J. Sed. Res., 72, 4, 451-456.

Smith (1987)

Smith R.U. (2004). Silled sub basin to connected tortuous corridors: sediment distribution system on topographically complex sub-aqueous slopes. In: Lomas S. A. & Joseph P. (eds.) Confined turbidite systems, Geol. Soc., Spec. Publ., 222, The Geological Society of London, Bath, 22-43.

Spadini G., Cloething S., Bertotti G. (1995). Thermo-mechanical modelling of the Tyrrhenian Sea: Lithospheric necking and kinematics of rifting. Tectonics, 14, 704-718.

Stevens S.H. & Moore G.F. (1985). Deformational and sedimentary processes in trench slope basins of the western Sunda Arc, Indonesia. Mar. Geol., 69, 93-112.

Stow D.A.V. (1985). Deep-sea clastics. Where are we and where are we going? In: Brenchley P.J. & Williams B.P.J. (eds.) Sedimentology, Recent Developments and Applied Aspects, Geol. Soc. London Spec. Publ., 18, The Geological Society of London, Bath, 67–93.

Torres J. et al. (1997). Deep-sea avulsion and morphosedimentary evolution of the Rhone Fan Valley and Neofan during the Late Quaternary (north western Mediterranean). Sedimentology, 44, 457-477.

Trincardi F. & Zitellini N. (1987). The rifting of the Tyrrhenian Basin, Geo-Mar. Lett., 7, 1-6.

Twichell D.C. & Roberts D.G. (1982). Morphology, distribution, and development of submarine canyons on the U.S. Atlantic Continental Slope between Hudson and Baltimore Canyons. Geology, 10, 408 -412.

Underwood M.B. & Karig D.E. (1980). Role of submarine canyons in trench and trench–slope sedimentation. Geology, 8, 432-436.

Van Andel T.H. & Komar P.D. (1969). Ponded sediments of the Mid-Atlantic ridge between 22° and 23° North latitude. Geol. Soc. of Am. Bull., 80, 1163-1190.

Walker R.G. (1978). Deep-water sandstone facies and ancient submarine fans: model for exploration for stratigraphic traps. Am. Ass. Petr. Geol. Bull., 62, 6, 932-966.

Weimer P. & Slatt R.M. (2004). The Petroleum Systems of Deep-Water Settings: SEG Distinguished Instructor Short Course Notes, pp. 488.

Weimer P.P., Varnai P., Budhijanto F.M., Acosta Z.M., Martinez R.E., Navarro A.F., Rowan M.G., McBride B.C., Villamil T., Arango C., Crews J R., Pulham A.J. (1998). Sequence stratigraphy of Pliocene and Pleistocene turbidite systems, northern Green Canyon and Ewing Bank (offshore Louisiana), northern Gulf of Mexico. Am. Ass. Petr. Geol. Bull., 82, 5b, 918-960.

Weimer P. & Link H. (eds.) (1991) Seismic facies and sedimentary processes of submarine fans and turbidite systems. Frontiers in Sedimentary geology. Springer-Verlag, New York, pp. 447.

Winker C.D. (1996). High-resolution seismic stratigraphy of a late Pleistocene submarine fan ponded by salt-withdrawal minibasins on the Gulf of Mexico continental slope. Proc. 3rd Annual Offshore Technology Conference, 28, 1, p. 619-628.

Woods A.V., Bursik M.I., Kurbatov A.V. (1998). The interaction of ash flows with ridges. Bull. Volcanol., 60, 38-51.

Wynn R.B., Kenyon N.H., Masson D.G., Stow D.A.W., Weaver P.P.E. (2002). Characterization and recognition of deep-water channel–lobe transition zones. Am. Ass. Petr. Geol. Bull., 86, 1441-1462.